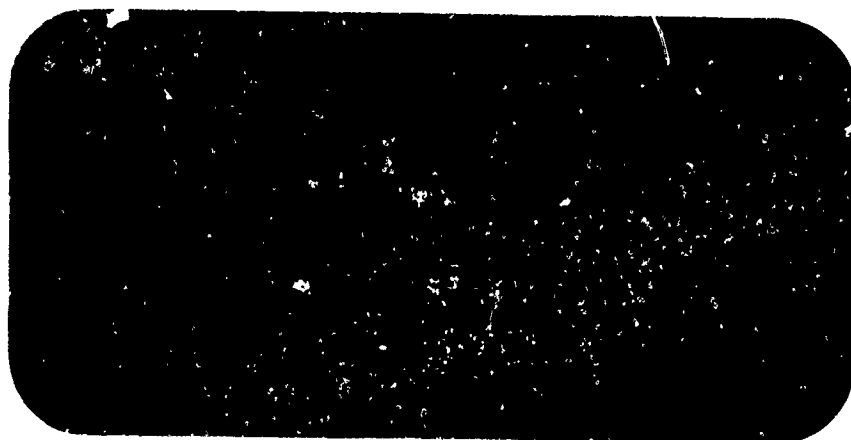
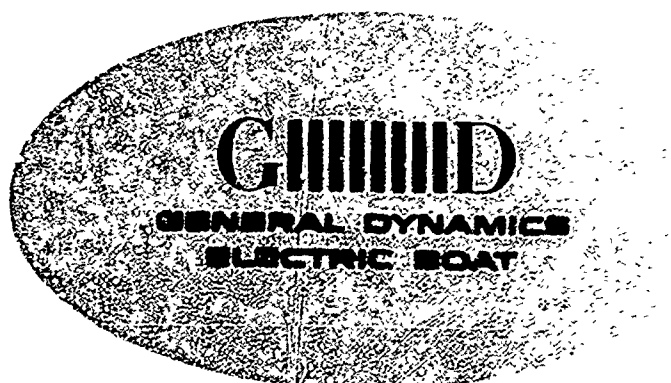


AD620144



CLEARINGHOUSE FOR FEDERAL SCIENTIFIC AND TECHNICAL INFORMATION		
Hardcopy	Microfiche	
\$3.00	\$0.75	85 ready
ARCHIVE COPY		



FINAL REPORT
THE DESIGN OF AIR CUSHION VEHICLE
AUTOMATIC AND SEMI-AUTOMATIC
CONTROLS

BuShips Code 632B

NO(bs) 92050

SS215-000 Task 10302

by

Frank J. Hannigan

Research and Development Department

GENERAL DYNAMICS CORPORATION

ELECTRIC BOAT DIVISION

Groton, Connecticut

Reviewed: R.A. Miller
R.A. Miller
Project Engineer

Reviewed: W.F. Leuze
W.F. Leuze, Chief of the
Servomechanisms Section

Approved: L.H. Chen
L.H. Chen, Manager of the
Basic Engineering Division

U411-65-032
July 1, 1965

ABSTRACT

This report presents a practical technique for designing automatic and semi-automatic (quickened) control systems for air cushion vehicles (ACV's). These systems have been designed to minimize a major problem in ACV control, vehicular sideslip. General equations of five degrees of freedom of ACV dynamic operation are included from which a mathematical model can be derived; this derivation is also included. The design technique is valid for most vehicle configurations and examples of its application are included for three different control methods. The quickened concept is explained and results of its usage are included. Analog computer data is presented for turning maneuvers at the operating conditions for which the systems were designed as well as at off-design points.

From the study that preceded this report it was concluded that an automatic, or a quickened, control system for an ACV offers distinct advantages over conventional manual control, particularly in minimizing sideslip and establishing and maintaining a command heading.

TABLE OF CONTENTS

	Page No.
ABSTRACT	1
INTRODUCTION	1
DEVELOPING A MATHEMATICAL MODEL	4
ANALOG COMPUTER STUDY	7
AUTOMATIC CONTROL SYSTEM DESIGN	9
Automatic Control of Vehicle with Two Rudders Behind the C.G.	10
Automatic Control with Propellers Fore and Aft	15
Automatic Control with Two Propellers Behind the C.G.	19
Effects of Wind on Automatic Systems	21
QUICKENED SYSTEM DISCUSSION	23
IMPLEMENTATION	30
CONCLUSIONS	34
RECOMMENDATIONS	36
REFERENCES	37
APPENDIX I	
Sign Conventions	I-1
Nomenclature Used in Equations	I-2
Vehicle Equations with Linearized Model	I-5
Examples of Linearized Equations for Yaw and Side Force	I-12
APPENDIX II	
Analog Computer Diagrams	
APPENDIX III	
Block Diagrams of Automatic and Quickened Controls	
APPENDIX IV	
Analog Computer Data	

LIST OF FIGURES

FIG. NO.	TITLE	PAGE NO.
1	Vehicle Configurations Considered in Control System Design	2
2	ACV Control Station Simulator	4
3	Flow Diagram of the Linearized Equations for Rudders Behind the C.G.	12
4	Flow Diagram of Decoupled Linearized Equations	13
5	Flow Diagram of Ideally Decoupled Equations	13
6	Flow Diagram of Linearized Equations with Automatic Control	14
7	Idealized Response for Turning Maneuver	16
8	First Control Method for Fore-Aft Configuration	18
9	Revised Control Method for Fore-Aft Configuration	18
10	Flow Diagram of Automatic Control Designed from the Linearized Equations of the Fore-Aft Configuration	19
11	Flow Diagram of Automatic Control Designed from the Linearized Equations with Two Propellers behind the C.G.	20
12	Analog Diagram for a Second Order System	23
13	Analog Diagram for a Second Order Quickened System	24
14	Quickened Scope Displays - Numbers One and Two	26
15	Display of Various Errors on Quickened Scope Display - Number One	28
16	Display of Various Errors on Quickened Scope Display - Number Two	29

LIST OF FIGURES (Cont.)

FIG. NO.	TITLE	PAGE NO.
17	Implementation Diagram	31
18	Possible Head-Up Display Symbols	33
APPENDIX I		
	Sign Conventions	I-1
	Nomenclature	I-2
	Equations of Motion	I-5
	Examples of Linearized Equations	I-12
APPENDIX II		
	Analog Computer Symbols	II-1
	Analog Computer Program of Vehicle Dynamics	II-2
	Analog Computer Program of Controls for Fore-Aft and Two-Propellers - Behind - C.G. Configurations	II-3, 4
	Circuitry for Quickened Display - Number One	II-5
	Circuitry for Quickened Display - Number Two	II-6
APPENDIX III		
	Block Diagram of Automatic Control with Rudders Behind the C.G.	III-1
	Block Diagram of First Automatic Control with Fore-Aft Propeller Configuration	III-2
	Block Diagram of Revised Automatic Control with Fore-Aft Propeller Configuration	III-3
	Block Diagram of Automatic Control with Propeller Behind the C.G.	III-4
	Block Diagram of Quickened System with Rudders Behind the C.G.	III-5

LIST OF FIGURES (Cont.)

TITLE	PAGE NO.
APPENDIX III (Cont.)	
Block Diagram of Quickened System with Fore-Aft Propeller Configuration	III-6
Block Diagram of Quickened System with Two Propellers Behind the C.G.	III-7
APPENDIX IV	
Explanation of Analog Computer Data	IV-1
Manual Control with Rudders Behind the C.G.	IV-3
Automatic Control with Idealized Forces	IV-4
Automatic System with Rudders Behind the C.G. Maneuvering at the Design Velocity	IV-5
Automatic System with Two Rudders Behind the C.G. - Maneuvering at $1/2$ the Design Velocity	IV-6
Automatic System with Rudders Behind the C.G. - Nulling an Initial Side Velocity	IV-7
Turns with Automatic Fore and Aft Configuration at the Forward Design Velocity (50 Knots)	IV-8
Turns with Automatic Fore and Aft Configuration at $1/2$ Forward Design Velocity	IV-9
Automatic Fore and Aft Propeller Configuration - Nulling an Initial Side Velocity	IV-10
Quickened System with Rudders Behind the C.G.	IV-11
Quickened System with Two Propellers Behind the C.G.	IV-12

INTRODUCTION

Maneuvering an air cushion vehicle (ACV) presents difficulties that are unique to this mode of transportation. Because the vehicle is designed to minimize surface friction and water drag, it has little resistance to side and yawing motion. Therefore, external forces must be applied simultaneously to control these variables. An analog computer investigation¹ has confirmed that manual coordination of these forces is difficult.

To give the ACV operator control of these forces the study summarized in this report, was conducted under contract N0bs 92050, Phase II. The project was to provide a method for designing automatic and semi-automatic control systems with the following capabilities: accurate course-keeping in the presence of disturbances, and accurate course-changing with a low sideslip angle. Sideslip is defined as the angle which the relative wind makes with the vehicle's bow (see Appendix I).

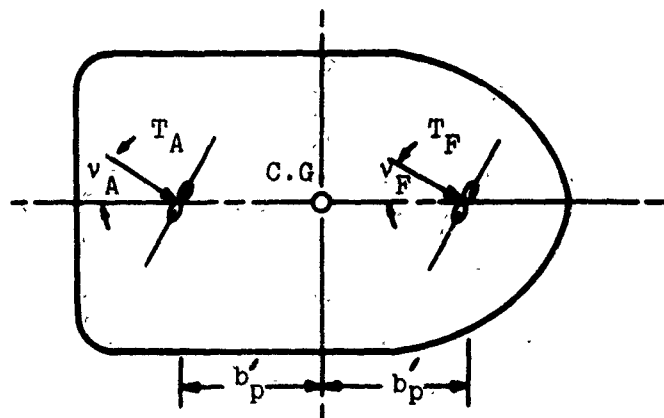
Both the automatic and semi-automatic approaches were designed for the three existing ACV configurations shown in figure 1:

- 1) propellers located fore and aft of the center of gravity (c.g.).
- 2) propellers located behind the c.g., and
- 3) rudders located behind propellers behind the c.g.

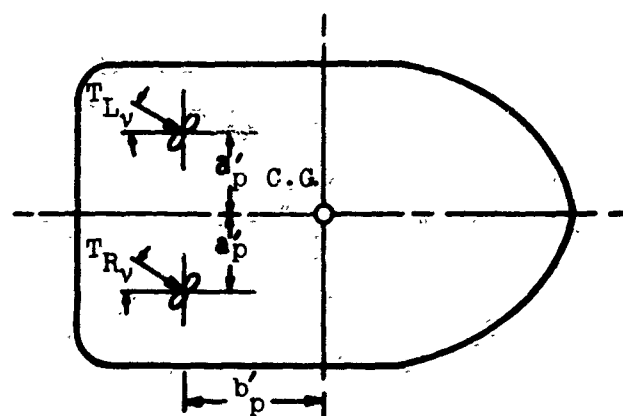
Three configurations were chosen to ensure that the design procedure is generally applicable.

Since the equations developed for the mathematical representation of the vehicle were too nonlinear and complex (Appendix I) to use for control design, they were reduced to a manageable form by assuming an operating condition and linearizing the equations about this condition (Appendix I). The response was checked for off-design conditions to see what effect this variation would produce.

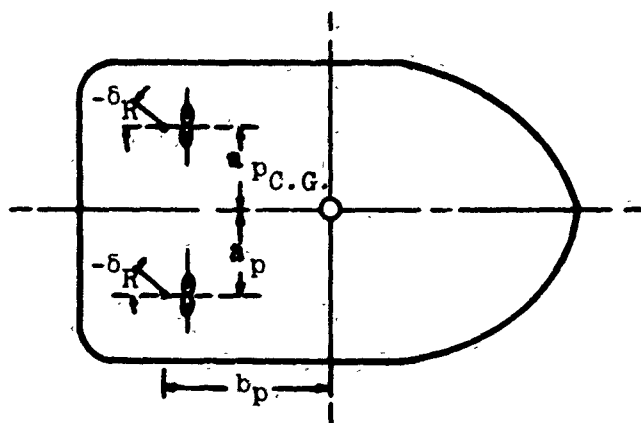
¹A superscripted number in the text refers to a publication listed on page 37.



CONFIGURATION "A" - PROPELLERS LOCATED FORE AND AFT OF THE C.G.



CONFIGURATION "B" - PROPELLERS LOCATED BEHIND C.G.



CONFIGURATION "C" - RUDDERS LOCATED BEHIND C.G.

FIGURE 1 VEHICLE CONFIGURATIONS IN CONTROL SYSTEM DESIGNS

From these linearized equations a transfer function was derived from yaw moment to vehicle heading. This transfer function combined with specifications of maximum turning rate, acceleration, and zero overshoot was used to design the vehicle controller.

The linearized equations were programmed on the analog computer and the response was compared to the predicted response after studying the analog computer simulator shown in figure 2. Variations of the feedback terms were made where it was necessary to minimize the deviation of the actual response from the predicted response. Then the exact equations of motion for the vehicle were programmed and the response was again studied and the controller modified.

For the semi-automatic (quickened) system, two different forms of display signals were used. In the first, the stick position (i.e., acceleration input) was used as one of the feedback terms; in the second, this term was zero. In this system, while the actual control is completely manual the use of the manual control is dictated by an error display presented to the operator. For the well-behaved turn there are two quantities which must be controlled: side force and yaw moment. Two methods were used to display these two controls (figures 15 and 16).

If the operator keeps the control signal in the proper position, the forces which he commands should produce the same vehicle response that would have been produced by the automatic system. Therefore, first the automatic system was modified to allow the operator to act as an error detector and an actuator within the control loop. Then the quickened system was redesigned by varying the parameters to produce a good response without too much operator effort.

This design procedure was used for three vehicle configurations: fore- and aft propellers, two propellers behind the c.g., and rudders behind two props behind the c.g. Results were obtained for each of these cases and are included in the appendices.

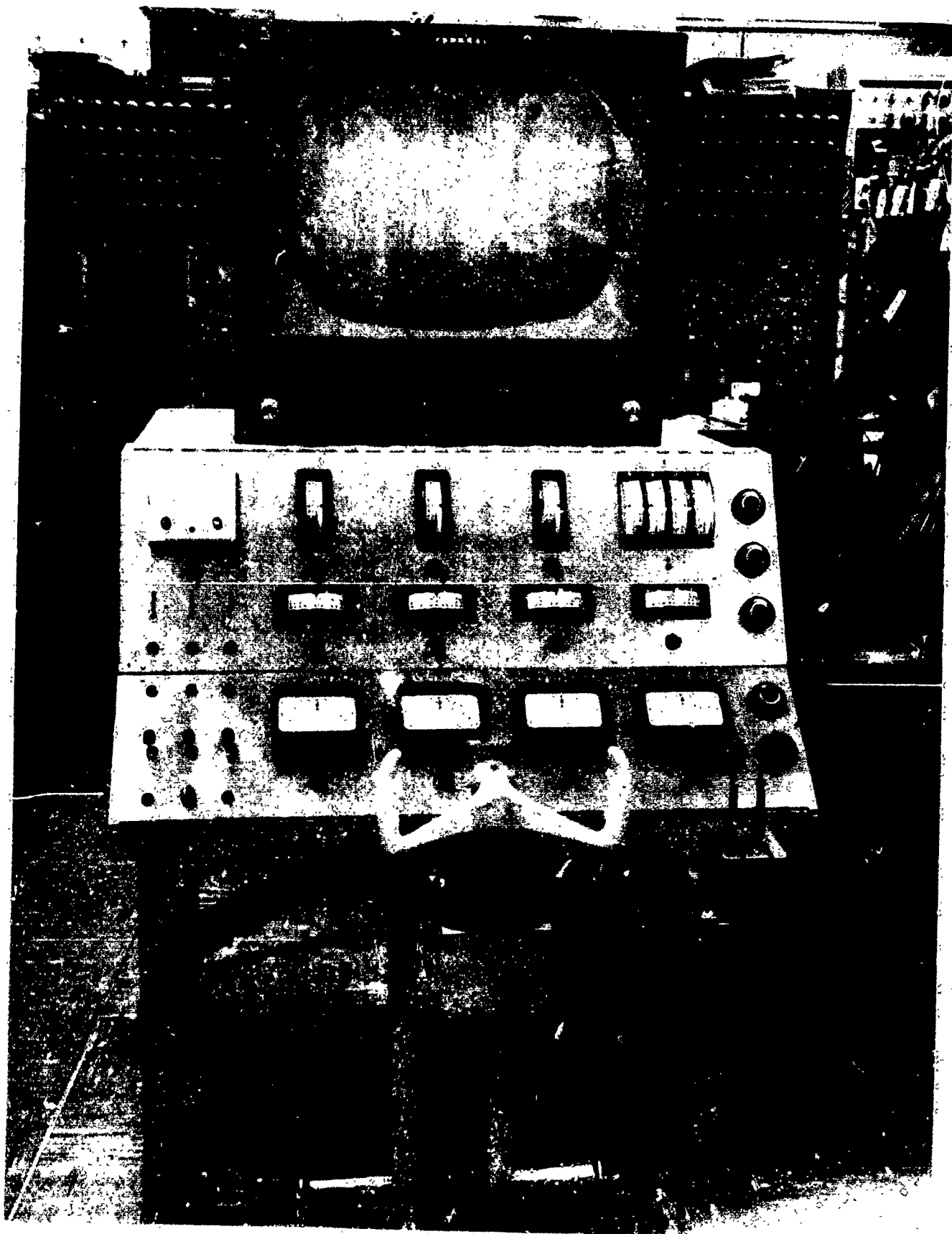


FIGURE 2 ACV CONTROL STATION SIMULATOR

DEVELOPING A MATHEMATICAL MODEL

To describe the dynamic operation of an ACV, equations of motion must be available from which a mathematical model can be developed; these equations were obtained from reference 1. Together with the data on Electric Boat's test vehicle SKIP-1, they describe all the forces that act on the vehicle in any dynamic condition. Their derivation applies to any ACV with particular emphasis on a vehicle equipped with rudders.

Five degrees of freedom are included in the equations - forward velocity, side velocity, pitch, roll and yaw, with only the heave dynamics omitted. The two dominant equations used to design a controller for the vehicle are the side force and yawing moment equations. Each of the other equations contributes terms which affect these two equations, but the complexity is reduced by a simplification technique. The method of simplification was to select an operating condition and linearize the equations about this point.

The linearization of the equations was accomplished by taking the partial derivatives of each of the acceleration terms with respect to the fundamental variables. The partial derivative was evaluated at a particular condition and this value was used as a constant slope of the acceleration with respect to the variable. For example, the yaw acceleration ($\ddot{\psi}$) is a function of the left propeller pitch angle (β_L), the right propeller pitch angle (β_R), the propeller speed, the rudder angle (δ_R), the side velocity (V), the forward velocity (U) and the yaw rate ($\dot{\psi}$). If external wind is considered, yaw acceleration is also a function of the magnitude and angle of this wind; however, for the example, wind was neglected.

With a constant propeller speed, the above statement may be written as an equation:

$$\ddot{\psi} = f(\beta_L, \beta_R, \delta_R, V, U, \dot{\psi}) \triangleq g.$$

If the linearization technique is used, regardless of the complexity of this original function, the final form is simple.

The linearized yaw moment equation is

$$\Delta \ddot{\psi} = \frac{\partial g}{\partial \beta_L} \Delta \beta_L + \frac{\partial g}{\partial \beta_R} \Delta \beta_R + \frac{\partial g}{\partial \delta_R} \Delta \delta_R + \frac{\partial g}{\partial V} \Delta V + \frac{\partial g}{\partial U} \Delta U + \frac{\partial g}{\partial \dot{\psi}} \Delta \dot{\psi}.$$

Each of these partial derivatives reduces to a constant when evaluated at the selected operating point. The symbol Δ denotes a deviation from the operating condition. If $\frac{\partial g}{\partial \beta_L}$ is defined as k_1 and $\frac{\partial g}{\partial \beta_R} \triangleq k_2$, etc.,

then in the vicinity of the operating point

$$\ddot{\psi} = k_1 \beta_L + k_2 \beta_R + k_3 \delta_R + k_4 V + k_5 U + k_6 \dot{\psi}.$$

This same technique was applied for all of the equations of the vehicle, and the result was linearized equations of a similar form.

It must be established over what magnitude of perturbation of each of the variables the equations are accurate. There are two problems which might arise in such an approximation technique. The first possible problem is that, although originally the vehicle is operated at the design condition, during a specific maneuver the linearized equations do not offer an adequate description of the motion because of prominent nonlinear contributions during the maneuver. The second problem is that a controller which is designed for one condition may perform properly in that situation, but at a slightly different operating point may react entirely differently.

To check the validity of the linearization it is necessary to either examine the linearized equations which are the result of deviations from the original operating conditions, or to study the controller action when it is used on an analog or similar simulation. If the linearized equations offer an inadequate description of the nonlinear equations, a nonlinear term can be introduced to validate the equations. In some cases, more than one nonlinear term may be necessary to produce equations which represent the exact equations of motion with sufficient accuracy over a reasonable range. If one or more nonlinear terms are introduced the equations are still much simpler than the original expressions.

To check the possibility that the controller is acceptable in one region yet not effective in another, there is a method similar to the one for checking the validity of the linearization. A nonlinear controller can be designed such that the nonlinear term is used to compensate for the variation which produces the error. For SKIP-1, after calculations were made to determine linear sets of equations, a controller was designed for selected operating points, and tests were made on the analog computer; the test results proved that the linear systems gave acceptable control response.

When the equations of the ACV were linearized, it was easier to take the partials of the acceleration terms with respect to some of the secondary variables, as well as the primary variables, and to expand these secondary variables in terms of the basic variables. The primary variables are all of the terms which cannot be expressed by other variables such as forward velocity, side velocity, and rudder angle. Secondary variables are those which can be defined in terms of the primary variables such as sideslip angle and rudder slipstream velocity. The simplification technique, as well as the final linearized equations for several situations, is shown in Appendix 1. These equations were used for the control system design.

ANALOG COMPUTER STUDY

For discussion purposes the computer facility is divided into three groups:

- 1) the simulation equipment for the vehicle dynamics,
- 2) the simulation equipment for the vehicle controls, and
- 3) the display and recording equipment.

In the first group, the simulation equipment for the vehicle dynamics, a 48 amplifier EAI Pace analog computer was combined with 48 additional Embree amplifiers to provide the analog computer representation of the equations. The exact equations of motion were used, i.e., those in Appendix I before the linearization process. The complete analog computer program for the vehicle dynamics with manual controls is shown in Appendix II, page II-2. This is the entire program, except for the display circuitry, that was used in the study of the quickened system with rudders behind the c.g. For each of the other systems that was studied with this program, modifications in the control force simulation had to be made. With the other vehicles the rudder contributions were disconnected and replaced by the appropriate forces, while the remainder of the dynamics of the vehicle were considered unchanged by this alteration. The analog program for each of the controls is presented in Appendix II, pages II-3 and II-4.

Of the simulation equipment for vehicle control, the major item is the control station, shown in figure 2. This station was fabricated specifically for ACV simulated control and was used for both the manual and the semi-automatic (quickened) studies. Hand and foot controls are provided for all the foreseeable control forces. Wheel motion is used to control the turning moment in all of the vehicle configurations. The stick on which the wheel is mounted has two degrees of freedom: fore-and-aft and side-to-side. The foot pedals provide two polarities

of the same control force: depressing the left foot pedal actuates a force in a preselected direction and depressing the right foot pedal reverses that force. The two hand levers to the right of the operator are independent and can be used for control of other input command signals.

The third group of the computer simulation is the display and recording equipment. The display consists of the meters and the 21-inch oscilloscope shown in figure 2. There are enough meters available to display all of the variables necessary for effective control, and the oscilloscope display is used for the quickened system which is explained later. Another use of the scope, which was not applied during this study, could be to give the operator a more informative representation of sideslip by displaying vehicle path and vehicle orientation during a turning maneuver.

Two oscillographic recorders were available for data recording purposes. The eight-channel recorder was used throughout the study to continuously record the pertinent variables while the four-channel recorder was used to check unrecorded variables as desired.

During the portions of the control studies involving manual control, an effort was made to minimize the number of errors which would be caused by simulation inadequacies in the display and controls. The design of the display and the location of the control forces on the simulator were determined by actual operation; various designs were tried until a satisfactory one was achieved.

However, with this simulation technique one major element was missing - the feeling of motion by the operator. In the actual vehicle the operator will have this information; therefore, actual vehicle control will be superior to simulated control.

AUTOMATIC CONTROL DESIGN

In order to design an effective automatic control system for an ACV, the desired response must be postulated and an accurate mathematical representation of the dynamic equations of motion must be available. For a vehicle with a pre-specified control configuration, the force and moment limitations must be incorporated in the determination of a desired response. If, for example, a turn is desired at a maximum rate of five degrees per second, 50 knots forward velocity, and zero sideslip, there must be sufficient side force available to counteract the resulting centrifugal force.

For the control designs described on the following pages, it was determined that the response should exhibit these traits:

- 1) In any turn, sideslip should be minimized;
- 2) The rate of the turn should be determined by the magnitude of the course change and the available side force at the operating velocity;
- 3) The vehicle should turn to the desired heading and maintain it (no overshoot).

In order to define a reasonable turning rate, it is first necessary to determine which of the controls is the limiting quantity. For conventional control of an ACV, the yaw moment is sufficiently high, but there is a scarcity of side force; therefore, the quantity of side force determines the maximum allowable yaw rate. This is true for the Electric Boat test vehicle.

Although study of the quickened system preceded that of the automatic system design, since the quickened system contains several ideas which are not commonly used in control design, the more familiar automatic control is discussed first.

Automatic Control of Vehicle with Two Rudders Behind the Center of Gravity

The vehicle with rudders behind the c.g. was considered prior to the other two configurations because a complete mathematical description, as well as the analog computer program, was available for this method of control. In this study, an operating condition was selected and the vehicle dynamics were described by the linearized equations listed in Appendix I. The operating condition chosen had a forward velocity of 50 knots and all other factors were zero, except those necessary to produce this velocity, such as propeller pitch angle and propeller speed. The pertinent linearized equations* for this condition are

$$\dot{y} = .562\phi - .1492\delta_R - .273V - 1.475\dot{\psi}$$

and

$$\ddot{\psi} = 1.7(\beta_L - \beta_R) + .562\delta_R + .133V$$

where all angular terms are in degrees and all linear terms are in feet. The small terms which are negligible have not been included in these equations: β_L , β_R and U into the side velocity equation and U and \dot{y} into the yaw equation.

From these equations a turning method can be selected. According to the side velocity equation, there are two possible sources of side force: rudder deflection and roll angle. Roll angle is not too advantageous since it cannot be depended upon in choppy water or on land with obstacles. Rudders also have disadvantages as side force controllers; since they are located well behind the c.g., they exert a moment which tends to yaw the vehicle. In fact, if the rudders are used for side force during a turn, they provide a moment against the desired turn. However, the rudders can be used effectively for side force control if, while they are being turned to the selected angle, a counter moment is applied that makes the total yaw moment zero. The source of this countermoment is the same as the moment which initiated the turn - differential propeller pitch ($\Delta\beta$).

* All the symbols for a vehicle with rudders are defined on pages II-2 through II-4.

During a turning maneuver the situation requires nullification of the yaw rate coupling in the side velocity equation and at the same time control of the yaw moment. Two decoupling problems are involved:

- 1) Decoupling the equations of motion, and
- 2) Decoupling the inherently coupled side force and yaw moment from the controls.

Both of these decoupling actions are possible with the forces available. The following paragraphs explain the decoupling process and the control system which is designed after decoupling.

The flow diagram of the linearized equations with rudders behind the c.g. is shown below:

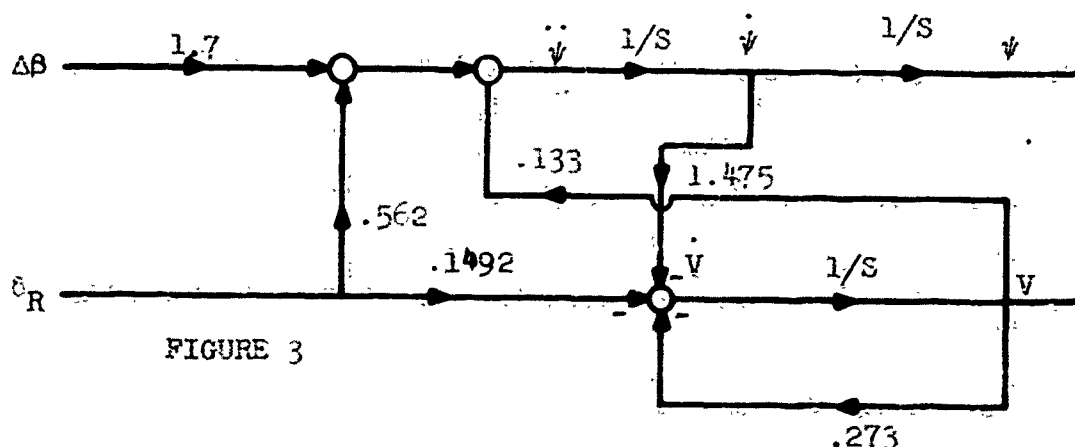


FIGURE 3

With the three apparent coupling terms (two in the vehicle dynamics and one in the controller) there are actually only two problems: decoupling the $\dot{\psi}$ into V and decoupling the rudder force into the yaw moment. If these two decouplings are successfully made, side velocity will result only from disturbances, and a pure side force can be generated to control this undesirable motion.

In the preceding discussion it was suggested that $\Delta\beta$ might be varied with δ_R so that δ_R would not cause variation in the yaw acceleration. From the flow diagram it is obvious that if $\Delta\beta$ were commanded to

equal $-\frac{.562}{1.7} \delta_R$ this would produce an effective decoupler, at least for the linearized model. To decouple yaw rate from the side velocity, an input into the rudder angle equal to $\frac{1.475}{.1492} \dot{\psi}$ is necessary.

The decoupled flow diagram appears below:

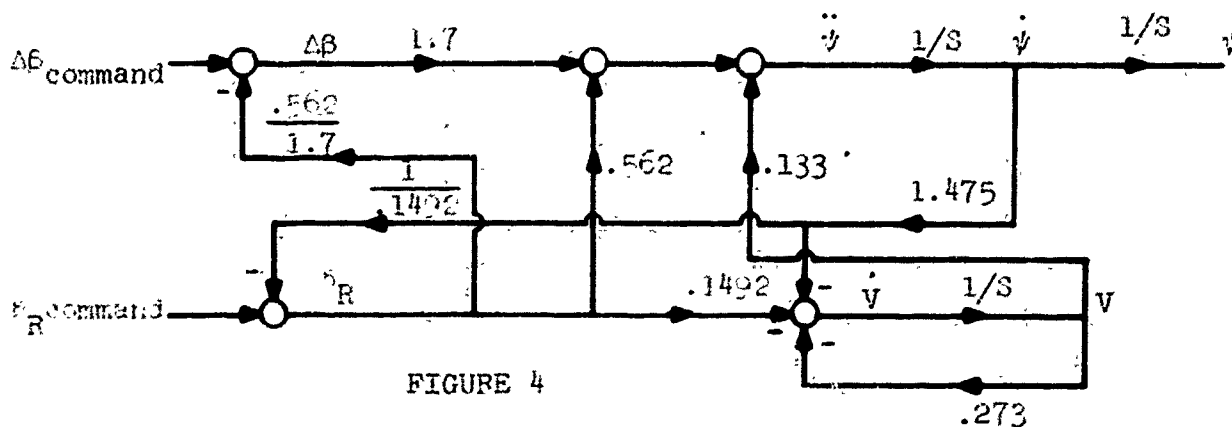


FIGURE 4

Figure 4 is equivalent to figure 5, the flow diagram of ideally decoupled equations shown below.

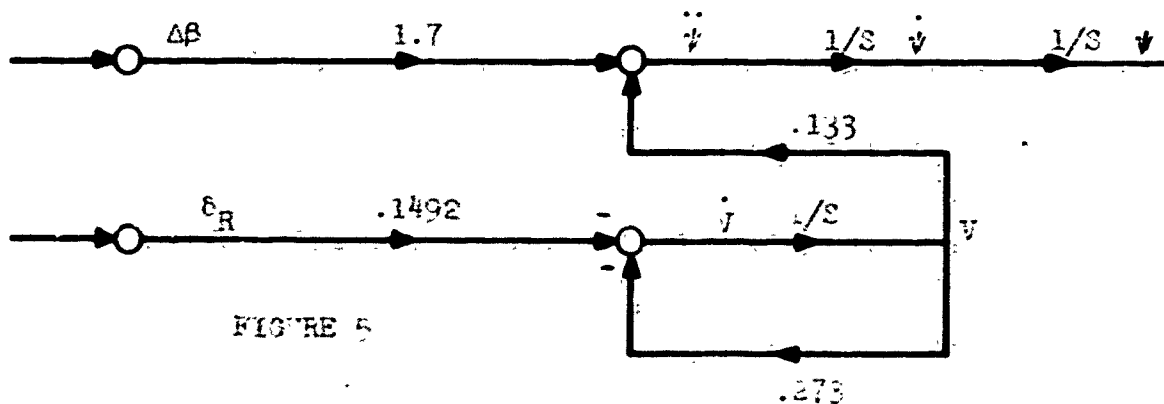


FIGURE 5

From the appearance of the above diagram, it would seem feasible to introduce another term, equal to $\frac{.133}{1.7} V$, to decouple the system completely and have independent control over two simple plants. However, this is not advisable for two reasons: 1) with separate control over

observation of the nonlinearities in the exact equations, it is unreasonable to make this assumption, therefore, a study was conducted to determine the actual response.

With the side force available at 50 knots, the maximum turning rate with no sideslip is about 3.5 degrees per second. This maximum rate was arbitrarily selected for a 20-degree turn. For any turn of greater than 20 degrees this rate will be reached, and for a turn of less than 20 degrees the maximum rate attained will be proportionally smaller. Figure 7 shows the desired turning rate and angle for a turn of less than 20 degrees. This maneuver will be the result for a new angle command if perfect decoupling is available.

Automatic Control Design with Propellers Fore and Aft

In order to design a controller for the fore and aft propeller configuration, linear versions of the equations defining this configuration must be derived. A mathematical description of the fore and aft propeller configuration was developed by subtracting the rudder terms from the equations for the vehicle with two rudders behind the c.g. and adding terms for the propellers on rotatable pylons. For a precise study of an actual fore and aft vehicle, the aerodynamic coefficients should be calculated from wind tunnel tests as in the case of the vehicle with rudders behind the c.g. However, for the study of the fore and aft vehicle simulation, the coefficients for the vehicle with rudders behind the c.g. were used. The resulting, simplified fore and aft equations are

$$\dot{V} = .562\dot{\psi} - .273V - 1.475\dot{\psi} + \frac{T_F \sin \nu_F + T_A \sin \nu_A}{m}$$

and

$$\ddot{\psi} = .133V + (T_F \sin \nu_F - T_A \sin \nu_A) \frac{57.3b^1}{I_z}$$

The variables previously undefined are

T_F - Thrust of the propeller in front of the c.g. (lbs),

T_A - Thrust of the propeller behind the c.g. (lbs),

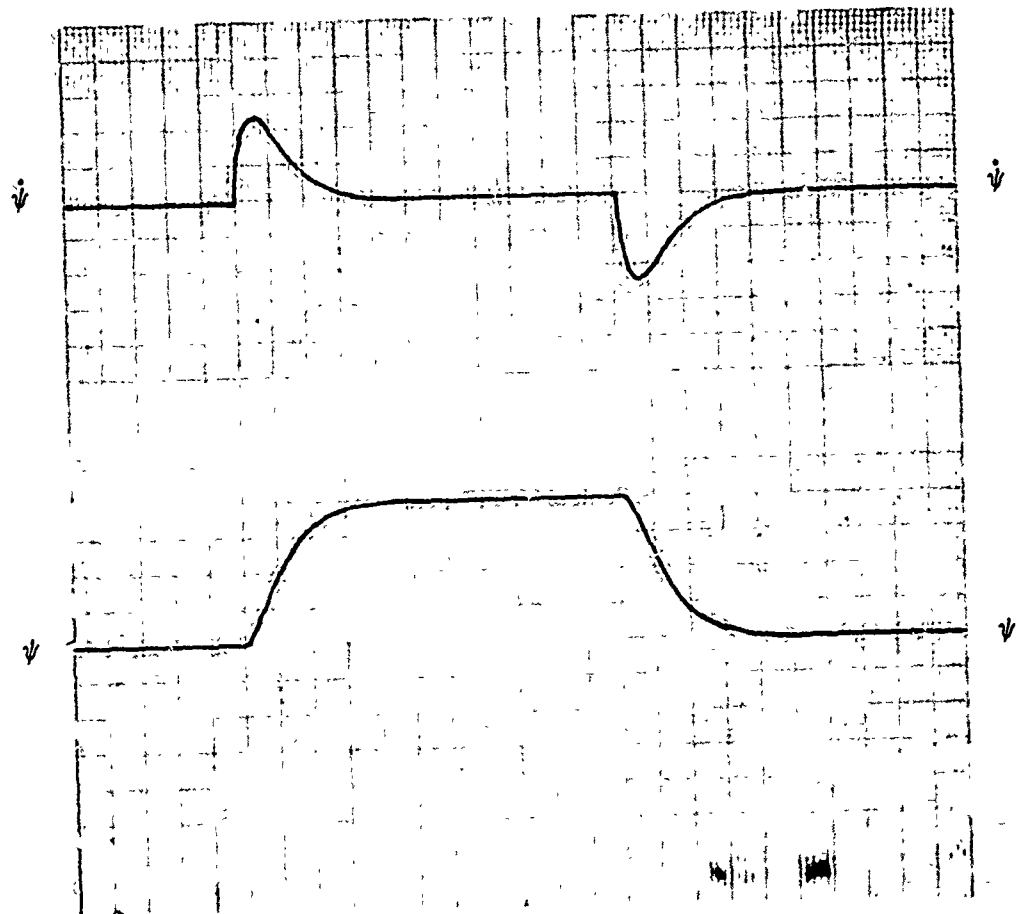


FIGURE 7
IDEALIZED VEHICLE RESPONSE

ν_F - Angle of the propeller in front of the c.g. with the centerline (degrees)

ν_A - Angle of the propeller in the back of the c.g. with the centerline (degrees)

b_p - Longitudinal distance of propellers from the c.g. (ft).

After linearizing the above equations and computing the values of the coefficients based on the dimensions of SKIP-I, the equations become:

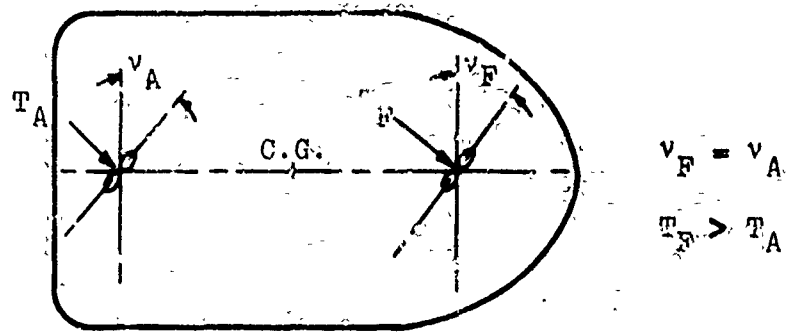
$$\dot{V} = .562\Phi - .273V - 1.475\dot{\psi} + .00848(T_F \nu_F + T_A \nu_A)$$

and

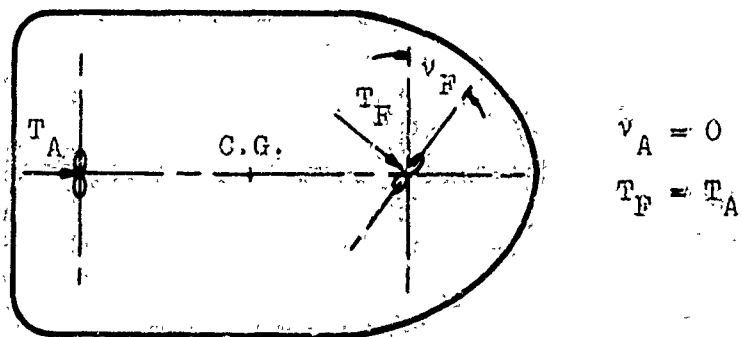
$$\ddot{\psi} = .133V + .082(T_F \nu_F - T_A \nu_A).$$

The side force for the vehicle can be obtained by turning both props to an equal angle. Roll angle is not used for the reasons cited in the previous section. The yawing moment can be obtained by one of two methods: turning one propeller pylon to a slightly different angle than the other or turning both pylons to the same angle and reducing the thrust of one prop. Originally the latter method was used and the angle to which the pylons were turned produced a beneficial side force. However, a study of this method of control on the analog computer indicated an undesirable tail in the response. The initial part of the turning maneuver was as predicted, but in the last few degrees of the turn up to 20 seconds were consumed. Analysis of the system transfer function predicts such a response, even for the linearized system. The basic problem is that any error in yaw necessarily has to actuate both a pylon angle and differential thrust.

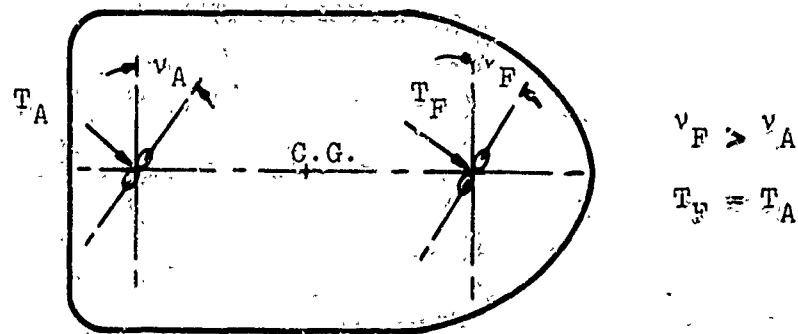
Tests of the first method, turning the props to different angles, proved it to be satisfactory. A yaw error commands the forward propeller to an angle which produces the desired turn while a side velocity error commands both pylons to an equal additional angle with the centerline. Figures 8 and 9 show the two methods of control.



POSITIVE YAW AND SIDE FORCE COMMAND FIRST CONTROL METHOD
FIGURE 8



a. POSITIVE YAW COMMAND ONLY



b. POSITIVE YAW AND SIDE FORCE COMMAND

REVISED CONTROL METHOD
FIGURE 9

The diagram illustrates a control system for a vehicle, enclosed in a dashed box labeled "VEHICLE CONTROLLER". The input is ψ_0 , which enters a summing junction with a gain K_0 and a negative sign. The output of this junction is Δv_F . This signal is fed into two parallel paths. The upper path contains a gain K_1 and a time constant $.082T_A$, followed by an integrator $1/s$. The lower path contains a gain K'_1 and a summing junction with a positive sign. The output of this junction is $v_A = v_F'$, which is then integrated by another $1/s$ block to produce \dot{v} . The output \dot{v} is fed back to the summing junction for Δv_F with a gain of $.133$ and a negative sign. Additionally, \dot{v} is fed back to the input summing junction with a gain of $.273$ and a negative sign. A feedforward path from \dot{v} goes through a gain of 1.475 and a time constant $0.01696T_F$ to a summing junction with a positive sign before the lower integrator. The output of the lower integrator is \dot{v} , which is also fed back to the input summing junction with a gain C_1 and a negative sign.

FIGURE 10

In this control loop, K_1' is used to balance the centrifugal force, C_1 determines the rate at which the side velocity decays, and K_0 and K_1 determine the response of the yaw control loop. With this control system design, all of the initial design goals were met. Typical response data obtained from the analog computer is given in Appendix IV.

The equations which describe the vehicle motion were obtained in the same manner as the vehicle with the fore and aft propeller configuration; the rudder terms are eliminated from the equations and replaced by the term due to the rotatable prop pylons. The simplified equations for this vehicle are

19

and

$$\ddot{\psi} = .133V + \frac{T_p a_p' \cos v}{I_z} - \frac{T_s a_p' \cos v}{I_z} - \frac{(T_p + T_s) b_p' \sin v}{I_z}$$

The variables not previously defined are:

- T_p - Thrust of port propeller (lbs),
- T_s - Thrust of starboard propeller (lbs),
- a_p' - Lateral distance of center of props from c.g. (ft).

The completely linearized equations are

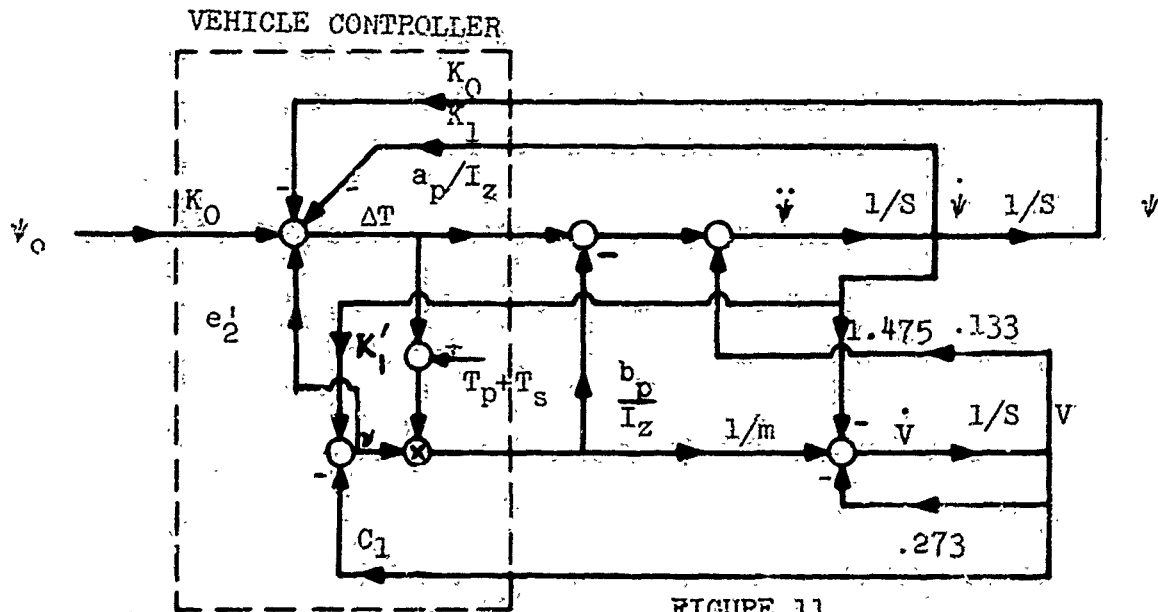
$$V = .562\psi - .273\dot{\psi} - 1.475\ddot{\psi} + .00848 (T_p + T_s)v$$

and

$$\ddot{\psi} = .123V + .082(T_p - T_s) - .00143 (T_p + T_s)v$$

The side force can be obtained by rotating the propellers to an angle which will produce the desirable side force and the unwanted moment can be canceled by applying a countermoment from differential thrust.

Figure 11 is the flow diagram of the control system design for the linearized equations with two propellers behind the c.g.



The controller is almost identical to the vehicle with rudders behind the c.g.. With this system the thrust vector is redirected by rotating the pylons, while with the vehicle with rudders the side force is generated by deflecting the air flow.

Effects of Wind on the Automatic Systems

The ability of the automatic control systems to maintain an established course against wind forces was investigated for all three configurations by inserting wind disturbance in the computer program and noting the responses. Both a constant side wind and impulses of side wind were applied. The responses of the vehicle with two props behind the c.g. and the vehicle with two rudders behind the c.g. were similar because they both exerted counter forces in a similar manner.

A constant side wind of 50 ft/sec produced a constant side velocity of 5 ft/sec and a constant yaw error of 3 degrees in each case. The transient caused by the wind was longer for the vehicles with both control forces located behind the c.g. because the vehicle with fore and aft propellers has a side force completely independent of the other forces.

For side wind impulses of 50 ft/sec, a small side velocity (2.5 ft/sec) was produced that quickly dropped to zero. For the vehicles with rudders or propellers aft of the c.g., a small excursion (about 3.5 degrees) from the command heading took place, but the vehicle promptly returned to the original course. With the fore and aft propeller configuration, the departure from the command heading was negligible (.6 degrees).

Since side acceleration is not fed back to the side force control signal, the major design variable which affects the response to wind is the velocity feedback quantity. This quantity determines the maximum side velocity which will occur for either the constant or the impulse wind input. For both types of vehicles the wind induced yaw error is proportional to this side velocity. For the vehicle with the side force located behind the c.g., a decoupling error is introduced

in the yaw equation. This error combined with the coupling of side velocity and yaw causes the yaw angle excursion. The directional stability force is the only yaw-producing term for the vehicle with pure side force.

QUICKENED SYSTEM DISCUSSION

A quickened control system is one in which an operator must respond to an error signal display to cause the generation of proportional control forces upon the vehicle. The displayed signal consists of a combination of accelerations, velocities and displacements. If the operator makes the proper control response to the error display information, he is acting as a simple gain in the control loop; therefore, he can be inserted in any control loop with a limited frequency bandwidth to act as an error detector and actuator.

The simple case described below demonstrates the concept of quickened control. For the closed loop equation a critically damped second order system was chosen with a natural frequency of .316 radians per second. This type of system was chosen to facilitate observation of any variations in the response of different operators.

The equation describing the dynamics of the system in terms of the controlled variable is

$$\ddot{X} = .1X_0 - .1X - .2\sqrt{10} \dot{X}.$$

Figure 12 is the analog computer diagram for this second order system.

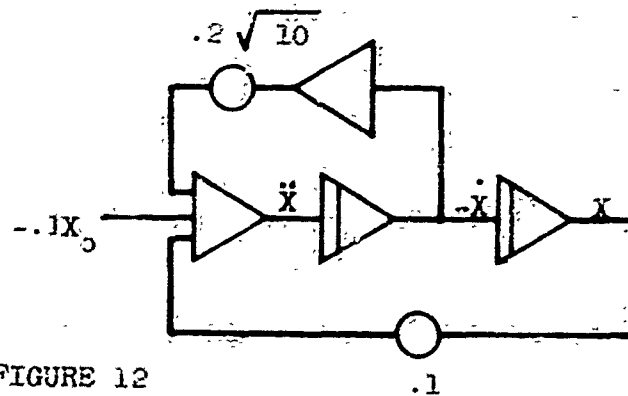
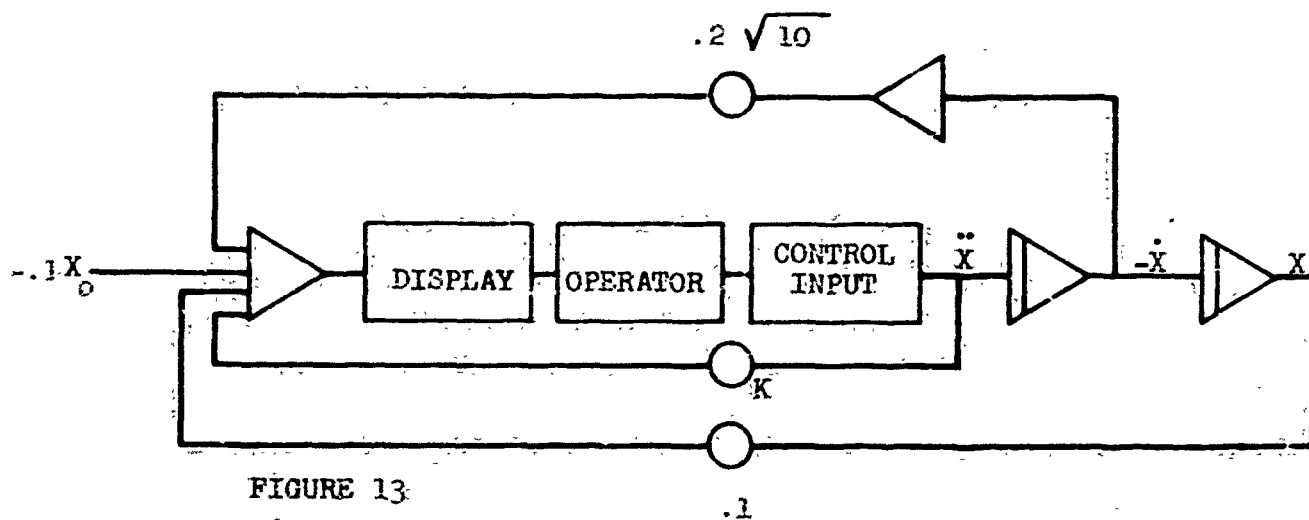


FIGURE 12

If a step input X_0 is commanded, there will be no overshoot and the variable will rise to a final value of X_0 . During its rise to X_0 , the acceleration is always equal to the sum of three components: $.1X_0$, $-.1X$ and $-.2\sqrt{10}\dot{X}$. If a displayed error signal proportional to this expression is used and if the operator maintains the error at zero, the response will be the same. The block diagram of the quickened manual control system is shown in figure 13. Although this method of operation is referred to as semi-automatic, if the operator chooses to disregard the quickened display, the control system may be operated in its simplest mode - manually.



Since the operator is instructed to maintain the display at zero, which he can do since he has direct control over \ddot{X} , the following differential equation describes the motion of the variable (X):

$$K\ddot{X} - .1X_0 + .1X + .2\sqrt{10}\dot{X} = 0.$$

If $K = 1$, then the equation can be written as

$$\ddot{X} = .1X_0 - .1X - .2\sqrt{10}\dot{X},$$

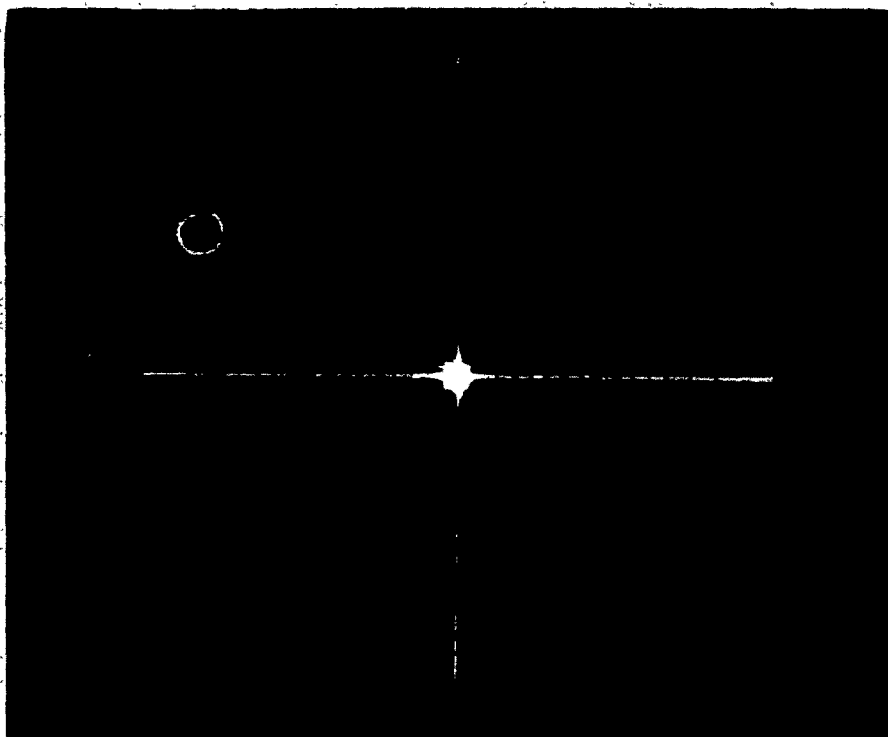
which is the same differential equation that describes the motion for the closed loop system. The operator gain can be varied simply by changing the acceleration coefficient (K). Reducing the magnitude of K increases the operator gain and increasing the magnitude of K decreases the gain. The damping ratio and natural frequency can be varied in the same manner that they are for closed loop control systems, by changing velocity and position feedback.

In the preliminary analysis, the quickened systems can be studied by replacing the operator with a simple gain. The analog computer should then be used to determine how large the variation is between the predicted and the actual response. As well as the usual errors which can arise in the design of automatic systems, other errors can occur when using the quickened control systems: the display may be slightly in error, some system motions may be too fast for the human to respond to, and the operator may have moments of inattention.

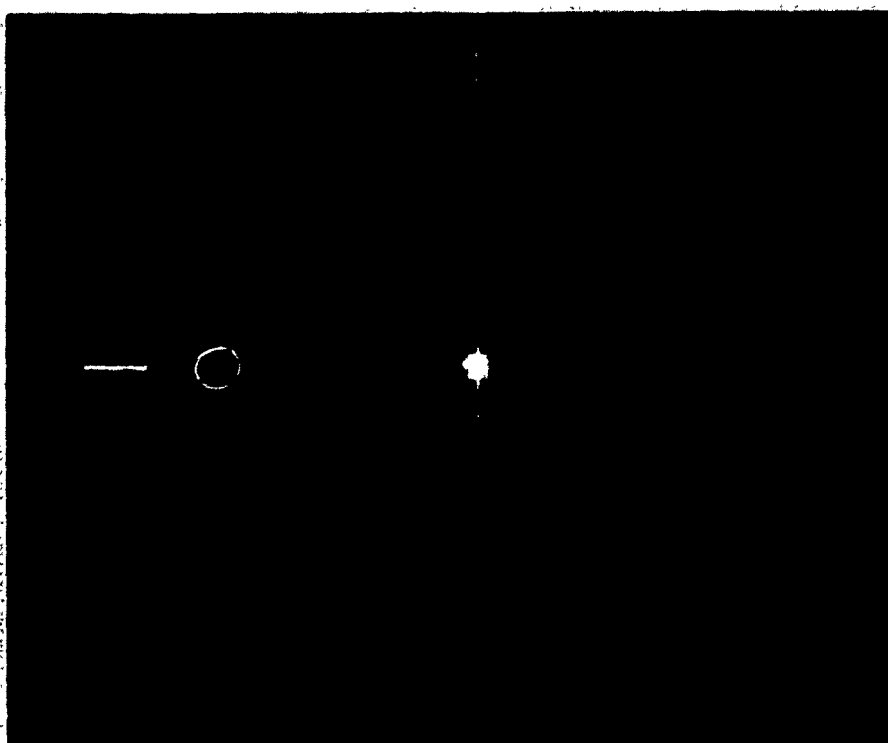
The first two of these possible errors must be minimized by the system designer; the third will probably cause more problems with a simulator than on an actual vehicle. In actual flight the operator will "feel" the motion of his craft and, therefore, sense as well as see the need for quickened assistance.

The first display tested was a one-dimensional (one control) voltmeter and the indicator on this meter had to be positioned at zero. This display soon fatigued the operator so that he could not operate effectively. Because of this difficulty a new, two-control display was devised for two-dimensional systems.

This display has two forms both using the 21-inch oscilloscope. In the first form, shown in figure 14a, the circle which can move in two dimensions must be kept at the origin. In the second form, shown in figure 14b, the operator must keep the horizontal line centered on the circle, which must be kept on the vertical reference line. With the controls set up on the simulator, the second display method is less tiring for the operator.



a) Quickened Scope Display - Number One

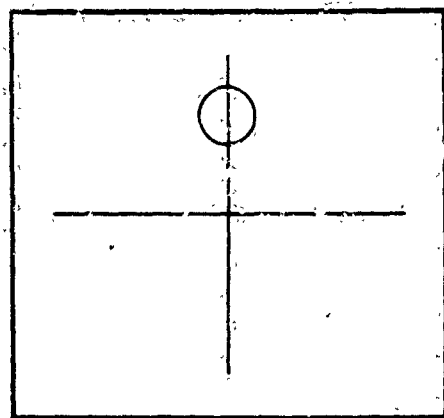


b) Quickened Scope Display - Number Two

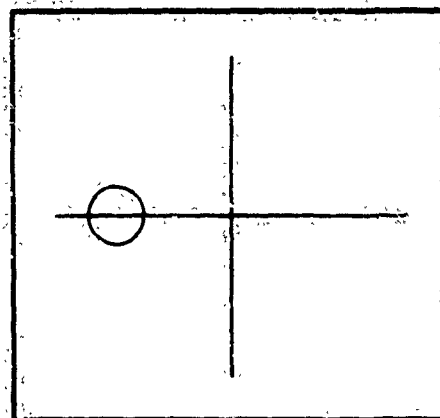
FIGURE 14 QUICKENED SCOPE DISPLAY NUMBERS ONE AND TWO

In the first display, a horizontal displacement of the circle symbol from the origin is proportional to the yaw error signal and a vertical displacement indicates a side velocity error signal. If the symbol is to the left of the origin, the control must be turned to the right to bring it over the origin. If the symbol is above the vertical reference line, the stick must be pulled back to cancel this error. When this display is used, the yaw motion is generated by turning the wheel, and the side force control is generated by moving the stick forward and back. While this would not be a desirable motion for an actual vehicle, the simulator operator has the feeling of having direct control over the symbol position since the error signal moves in the direction of stick motion.

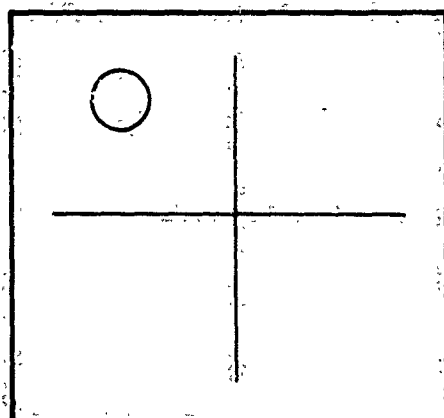
The second display will be more useful to the actual vehicle than the first display and will also be easier to control on the simulator. In this display the distance from the center of the line to the center of the circle represents the side velocity error. Motion of the stick to the right moves the line to the right and motion of the stick to the left moves the line to the left. The yaw error is represented and controlled as in the first display. In the control station simulation for SKIP-I, the foot pedals control the rudder side force. Hence the foot pedals are used to control the distance of the line from the circle center and the wheel controls the position of the circle. Figures 15 and 16 show the two displays in various conditions of operation.



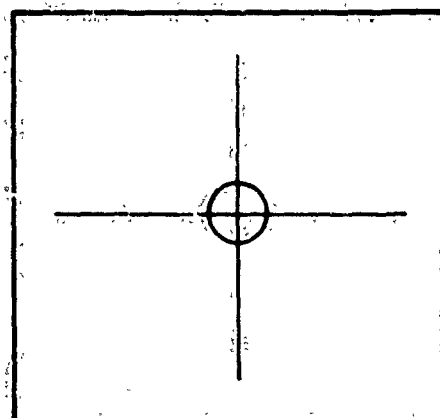
a) Side Velocity Error -
Command Is To Pull
Stick Back



b) Yaw Control Error -
Command Is To Turn
Wheel Right

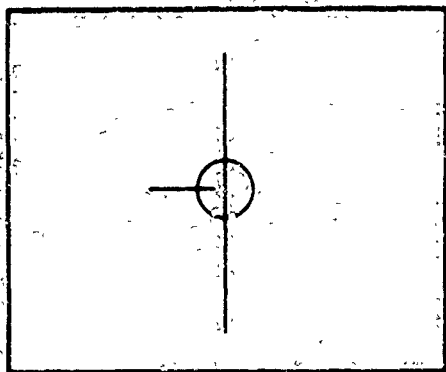


c) Both Yaw And Side Velocity
Error - Command Is To Pull
Stick Back While Turning
Wheel Right

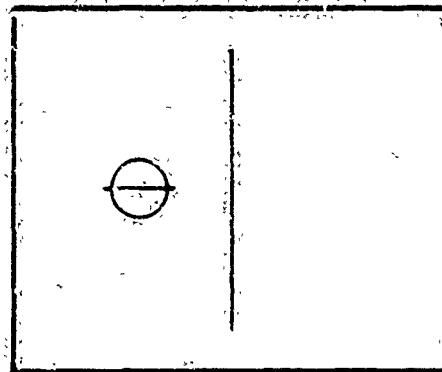


d) Controls Properly Used

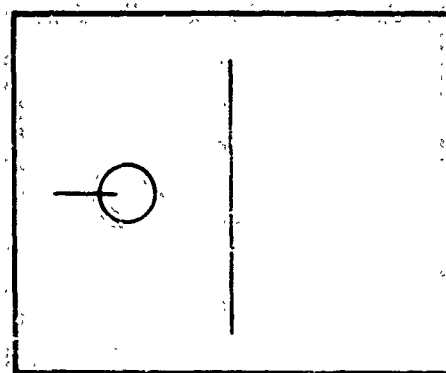
FIGURE 15 QUICKENED SCOPE DISPLAY - NUMBER ONE



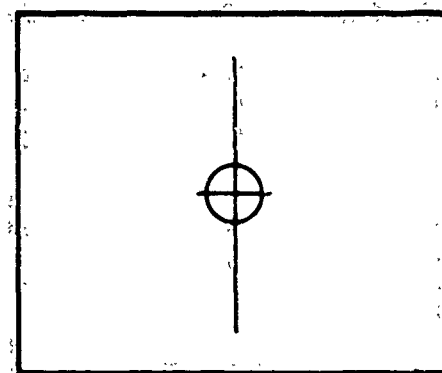
a) Side Force Error - Command Is To Push In Right Pedal



b) Yaw Control Error - Command Is To Turn Wheel Right



c) Both Yaw and Side Force Error - Command Is To Push Right Pedal While Turning Wheel Right



d) Controls Properly Used

FIGURE 16 QUICKENED SCOPE DISPLAY - NUMBER TWO

IMPLEMENTATION

This section describes an approach to implementation of the automatic system and possible displays for the quickened control signal.

Figure 17 shows the implementation of the automatic control system with two rudders behind the c.g. Each of the components represented is a common item. Electrical signals which are proportional to the variables, and combine to produce the actuating signal, must be obtained. These variables are yaw angle, yaw command, yaw rate, rudder angle, and side velocity.

The difference between the actual yaw angle and the command yaw angle is generated by a synchro control transformer after a directional gyro senses the yaw angle. The range of the directional gyro must be zero to 360 degrees. The proper scaling of this term is achieved by adjusting the gain on an a-c amplifier.

The yaw rate signal is generated by a rate gyro aligned along the yaw axis. This sensor must be accurate from zero to 15 degrees per second and must be able to withstand rates of up to 45 degrees per second. The signal produced contributes to both the rudder angle and differential propeller pitch angle.

The electrical signal which is proportional to the rudder deflection angle is acquired by using a potentiometer with the wiper driven by the rudder shaft. This voltage feeds back to the δ_R power amplifier and also into the $\Delta\beta$ power amplifier as part of the actuator signal. The typical sensor range would be -45 to +45 degrees.

Side velocity is the only quantity which is not directly measured. An accelerometer is mounted to detect side acceleration and this output is integrated to obtain a signal proportional to the side velocity. The upper limit of the side velocity is approximately 40 knots. A side-looking doppler radar could also be used for overland operation as long as the operator remembers that when operating over water he must correct for the water motion sensed by the doppler.

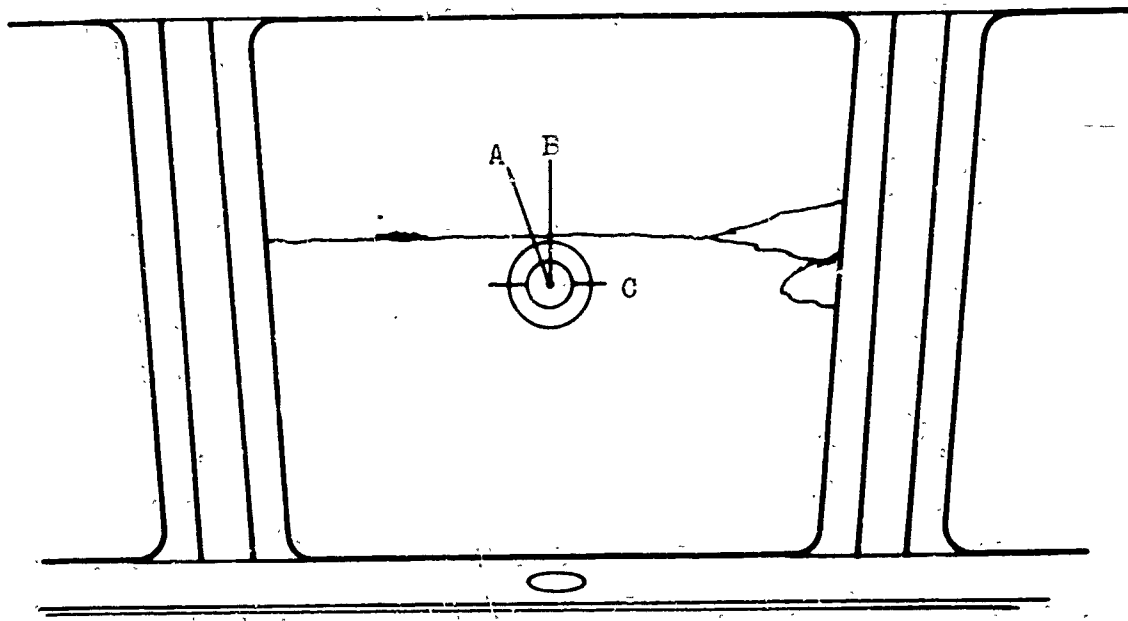
The yaw rate limit is obtained by using logic circuitry. When the rate reaches the maximum allowable value, the $\Delta\beta$ command from the yaw error signal is grounded; and when the yaw angle approaches the command heading, the error signal again actuates the $\Delta\beta$ command.

All of the above signals are in terms of a-c voltages except rudder deflection. These a-c signals must be demodulated to produce the d-c signals which actuate the controls. To allow manual operation, a switch should be provided to remove the outputs of the demodulators.

The quickened system display presents a more novel implementation problem. During the operation on the analog computer, the operator's complete attention was on the quickened control signal with only an occasional glance at the meter displays. In the actual ACV, he will not be able to give complete attention to an oscilloscope display since he will also be watching the ground track and any potential flight hazards. Therefore, it is advisable to use a display that will project this information into his line of vision without interfering with his normal flight vision. The "Head-up" display system developed for aircraft flight offers such a solution.

The head-up display, shown in figure 18, is a group of symbols projected from a cathode ray tube on the windshield in the pilot's line of sight. To eliminate the need for the operator to refocus his eyes from the ground track to the display, it is focused at infinity. In an airplane the main use for this system is to give the pilot information for manual control of the vehicle. The advantages of this system to the pilot are less eye fatigue and uninterrupted attention to the flight path. Each of these display symbols usually shows one of the operating variables. In the quickened application, the symbol positions would be governed in the same manner as the symbols on the scope display during the computer study, which is a combination of these variables.

The symbols in figure 18 represent only two of many possibilities for a head-up display. To require the operator to maintain line A on line



POSSIBLE HEAD-UP DISPLAY SYMEOLS

FIGURE 18

B would be an effective way to present the quickened yaw display since the required rotation of line A would be analogous to the wheel motions.. Another possible representation of the quickened errors could be derived from these symbols. The yaw error could be represented by the distance of one circle from the origin. Lateral motion of either the other circle or the horizontal line C could indicate side velocity error.

Several possibilities exist for displaying the required symbols. The selection of the best symbols requires more work in human factors, which is beyond the scope of this study.

CONCLUSIONS

After designing automatic and semi-automatic controls for three general vehicle configurations, the following conclusions were made:

- 1) The quickened, or semi-automatic, system has advantages over manual control for all three vehicle configurations. With quickened aid the operator can eliminate overshoot, coordinate the two forces that control yaw and sideslip, and perform these operations with less effort.
- 2) The controls, such as rudder angle, propeller pitch, and pylon angle, can be combined effectively to control sideslip and yaw in all three vehicle configurations and can be designed to make prescribed maneuvers within the limits of the available forces. Of the two methods devised for manipulating the fore and aft propellers to control yaw, the one that uses the differential prop angle is the most effective for the automatic and quickened operations. The other involves turning both pylons to the same angle and reducing the thrust of one propeller.
- 3) Automatic systems that provide effective course-changing and course-keeping operation can be designed for all three configurations. The course-changing method can minimize sideslip during maneuvers.
- 4) The automatic systems can be implemented with conventional sensing and actuating devices.
- 5) For the conventional, two-propeller ACV, an automatic system can be used either entirely with control components within the loop or with an operator replacing the error sensors and actuating devices.

- 6) For the conventional, two-propeller ACV with or without rudders, the automatic and semi-automatic (quickened) systems are comparable in effectiveness. Either control system can predetermine maneuvers and either system can be designed to make optimum use of the available forces.

A general conclusion is that the same design procedure can be used for vehicles with more than two propellers as was used for the three configurations selected for this study. This information is based on the knowledge that all of the forces of at least one of the two-propeller configurations are available for any vehicle with three propellers or more.

RECOMMENDATIONS

As a result of these studies of the automatic systems it has been concluded that they are ready for implementation. No major problems were found that require further study. Therefore, it is recommended that the next course of action should be to apply the automatic systems to actual vehicles in order to test the controls under more realistic conditions. The automatic designs can be applied directly to any vehicle for which an adequate mathematical description of its dynamic operation is available. From the study conducted on the implementation, the application of these automatic designs should offer no major difficulties. The automatic system for the vehicle with two rudders behind the c.g. is ready to be applied to the actual vehicle. It remains only to select the particular components, which are readily available.

The quickened display, however, needs some additional development before it is usable. It is recommended that a head-up display be devised for an actual quickened system and this study include developing the controls using human factors engineering until they can be used with a minimum of operator effort. After this study is complete the total quickened system design should be installed and tested on a vehicle to evaluate its performance under realistic conditions and compare this to that of the vehicle operated without the benefit of quickened aid.

REFERENCES

1. Analog Computer Study of Ground Effect Machine Controllability;
Richard A. Miller, General Dynamics/Electric Boat Report
U411-63-024, July, 1963.
2. The Dynamics of Air Cushion Vehicles - Progress Report #1;
John H. Leighton, Jr., General Dynamics/Electric Boat Report
U411-64-028, October, 1964.
3. Cockpit Displays and the Possible Applications of Head-up Display;
J. M. Walsh, Symposium on Aircraft Takeoff and Landing Problems,
R.A.E., December, 1962.

APPENDIX I

- 1) NOMENCLATURE USED IN EQUATIONS
- 2) VEHICLE EQUATIONS WITH LINEARIZED MODEL
- 3) EXAMPLES OF LINEARIZED EQUATIONS FOR
YAW AND SIDE FORCE

SIGN CONVENTIONS

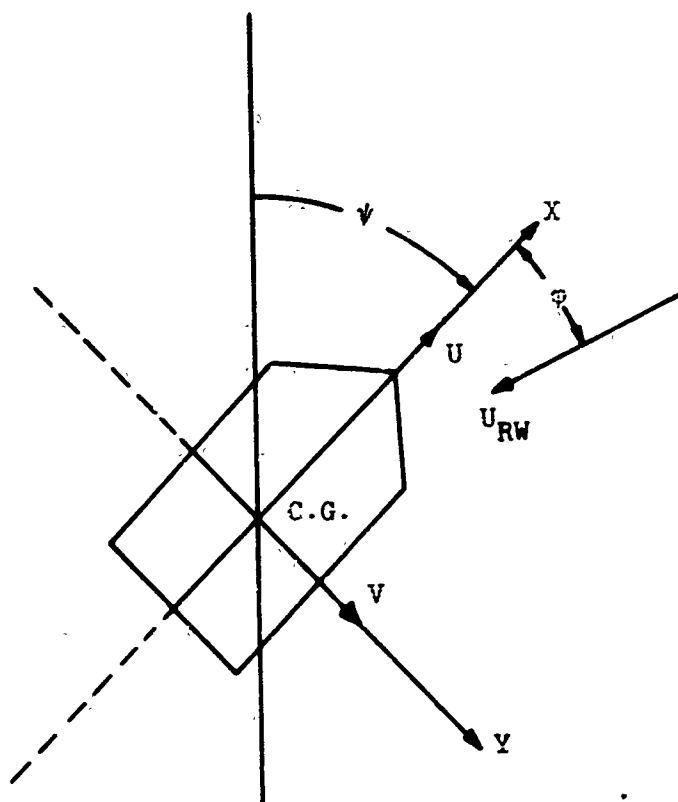
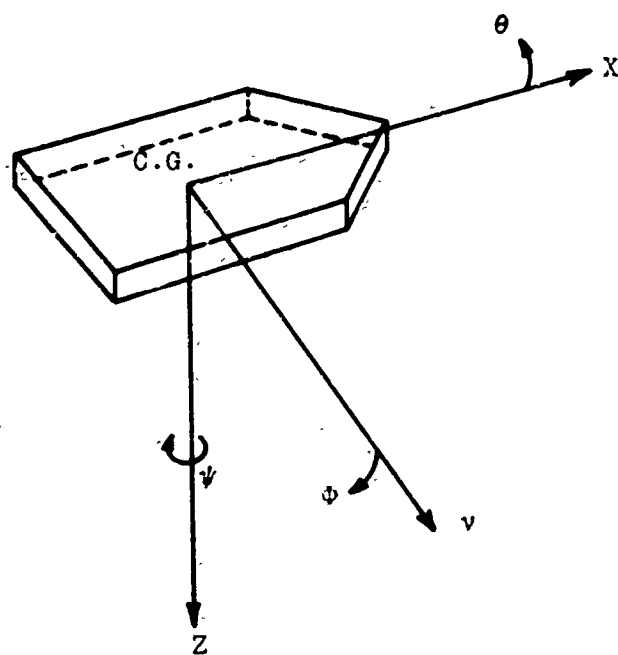


FIGURE I-1

A_B	Area of the base enclosed by the peripheral jet centerline - ft^2
A_D	Area of the disc generated by each rotating propeller - ft^2
a_p	Horizontal distance in the y direction between the CG and the thrust line of one propeller - ft
a_t	Horizontal distance in the y direction between the CG and the Center of Pressure (CP) of one fin - ft
CG	The center of gravity of the vehicle
C_{DR}	The drag coefficient of each fin based on the fin area immersed in the propeller slipstream
C_L	The lift coefficient based on the area, A_B ,
C_{LR}	The lift coefficient in a horizontal plane of each fin based on the fin area immersed in the propeller slipstream
C_{Nf}	The yawing moment coefficient of the fuselage based on the base area, A_B , and the length of the base, L_B
C_{xf}	The force coefficient of the fuselage along its x-axis based on the area, A_B
C_{yf}	The force coefficient of the fuselage along its y-axis based on the area, A_B
D	The propeller diameter - ft
g	The acceleration due to gravity - 32.2 ft/sec^2
h_f	Height of the lift fan inlet above the CG - ft
h_p	Height of each propeller thrust line above the CG - ft

h_t	Height of each fin CP above CG - ft
I_x, I_y, I_z	Moments of inertia about the x, y, and z axes respectively - slug - ft ²
l_B	Length of the cushion - ft
l_p	Distance of each propeller plane behind the CG - ft
l_{L_1}	Distance ahead of the CG of the lift acting on the fuselage - ft
l_t	Distance of each fin CP behind the CG - ft
m	Mass of the vehicle - slugs
Q_f	Volume flow rate of air through the lift fan - ft ³ /sec
S_R	Area of each fin which is immersed in the propeller slipstream - ft ²
T	Thrust - lb
T_L	Thrust of the left propeller - lb
T_R	Thrust of the right propeller - lb
U, V, W	Inertial velocities of the vehicle in the x, y, and z axes respectively - ft/sec
U_{ss}	Velocity of the propeller slipstream - ft/sec
U_{RW}	Velocity of the relative wind - ft/sec
U_{RWR}	Velocity of the relative wind over each fin - ft/sec
U_w	Velocity of the wind which is independent of the vehicle motion - ft/sec
v_1	Induced velocity of each propeller - ft/sec
W_t	Gross weight of the vehicle - lb

X, Y, Z	Earth - fixed axis system
x, y, z	Body - fixed axis system
ϵ_R	Angle between the fin chord and U_{RW_R} - rad
δ_R	Rudder deflection - rad
ρ	Mass density of air - slugs/ft ³
ψ	Angle of yaw; positive nose right - rad
θ	Angle of pitch; positive nose up - rad
ϕ	Angle of roll; positive right side down - rad
φ	Angle between the X-axis and the relative wind in a horizontal plane, sometimes called the sideslip angle - rad
α	Angle between the X-axis and the relative wind in a vertical plane, sometimes called the angle of attack; positive nose up in relation to the wind vector - rad

Other notation

$$\dot{(\quad)} = \frac{d(\quad)}{dt}$$

$$\ddot{(\quad)} = \frac{d^2(\quad)}{dt^2}$$

EQUATIONS OF MOTION

1) Forward Force -

$$\begin{aligned} \dot{U} = & -g\theta + V\dot{\psi} + \frac{T_L + T_R}{m} - \frac{Q_f \rho}{m} (U + U_{WN} \cos \psi + U_{WE} \sin \psi) \\ & + \frac{\rho S_R}{2m} \left[(U_{SSL}^2 + V_{RN}^2) C_{DRL} \cos \epsilon_{RL} + (U_{SSL}^2 + V_{RN}^2) C_{LRL} \sin \epsilon_{RL} \right. \\ & + (U_{SSR}^2 + V_{RN}^2) C_{DRR} \cos \epsilon_{RR} + (U_{SSR}^2 + V_{RN}^2) C_{LRR} \sin \epsilon_{RR} \left. \right] \\ & - \frac{\rho C_{xf} A_B}{2m} U_{RW} |U_{RW}| \end{aligned}$$

1a) Linearized Forward Force Equation -

$$\begin{aligned} \Delta \dot{U} = & -g\Delta\theta + \dot{\psi}\Delta V + V\Delta\dot{\psi} - \frac{Q_f \rho}{m} (\Delta U - U_{WN} \sin \psi \Delta \psi + \cos \psi \Delta U_{WN} \\ & + U_{WE} \cos \psi \Delta \psi + \sin \psi \Delta U_{WE}) + \frac{\rho S_R}{2m} \left[- (U_{SSL}^2 + V_{RN}^2) C_{DRL} \sin \epsilon_{RL} \Delta \epsilon_{RL} \right. \\ & + (U_{SSL}^2 + V_{RN}^2) \cos \epsilon_{RL} \left(\frac{\partial C_{DRL}}{\partial \epsilon_{RL}} \Delta \epsilon_{RL} + \frac{\partial C_{DRL}}{\partial \delta_R} \Delta \delta_R \right) + C_{DRL} \cos \epsilon_{RL} \\ & (2U_{SSL} \Delta U_{SSL} + 2V_{RN} \Delta V_{RN}) + (U_{SSL}^2 + V_{RN}^2) C_{LRL} \cos \epsilon_{RL} \Delta \epsilon_{RL} \\ & + (U_{SSL}^2 + V_{RN}^2) \sin \epsilon_{RL} \left(\frac{\partial C_{LRL}}{\partial \epsilon_{RL}} \Delta \epsilon_{RL} + \frac{\partial C_{LRL}}{\partial \delta_R} \Delta \delta_R \right) + C_{LRL} \sin \epsilon_{RL} \\ & (2U_{SSL} \Delta U_{SSL} + 2V_{RN} \Delta V_{RN}) - (U_{SSR}^2 + V_{RN}^2) C_{DRR} \sin \epsilon_{RR} \Delta \epsilon_{RR} \\ & + (U_{SSR}^2 + V_{RN}^2) \sin \epsilon_{RR} \left(\frac{\partial C_{LRR}}{\partial \epsilon_{RR}} \Delta \epsilon_{RR} + \frac{\partial C_{LRR}}{\partial \delta_R} \Delta \delta_R \right) + C_{DRR} \cos \epsilon_{RR} \\ & (2U_{SSR} \Delta U_{SSR} + 2V_{RN} \Delta V_{RN}) + (U_{SSR}^2 + V_{RN}^2) C_{LRR} \cos \epsilon_{RR} \Delta \epsilon_{RR} \\ & + (U_{SSR}^2 + V_{RN}^2) \sin \epsilon_{RR} \left(\frac{\partial C_{LRR}}{\partial \epsilon_{RR}} \Delta \epsilon_{RR} + \frac{\partial C_{LRR}}{\partial \delta_R} \Delta \delta_R \right) + C_{LRR} \sin \epsilon_{RR} \\ & (2U_{SSR} \Delta U_{SSR} + 2V_{RN} \Delta V_{RN}) \left. \right] - \frac{\rho A_B}{2m} U_{RW}^2 \left[\left(\frac{\partial C_{xf}}{\partial \phi} \Delta \phi \right) + 2C_{xf} U_{RW} \Delta U_{RW} \right] \\ & + \frac{\Delta T_L + \Delta T_R}{m} \end{aligned}$$

2) Side Force -

$$\begin{aligned} \dot{V} &= g\dot{\phi} - U\dot{\psi} - \frac{\rho Q_f}{m} (V + U_{WE} \cos \psi - U_{WN} \sin \psi) \\ &- \frac{\rho S_R}{2m} \left[(U_{SSL}^2 + V_{RN}^2) C_{DRL} \sin \epsilon_{RL} + (U_{SSL}^2 + V_{RN}^2) C_{LRL} \cos \epsilon_{RL} \right. \\ &+ (U_{SSR}^2 + V_{RN}^2) C_{DRR} \sin \epsilon_{RR} + (U_{SSR}^2 + V_{RN}^2) C_{LRR} \cos \epsilon_{RR} \left. \right] \\ &- \frac{\rho \pi D^2}{8m} \phi U_{RW}^2 (C_{y' \phi_L} + C_{y' \phi_R}) + \frac{\rho A_B}{2m} C_{y' \phi} U_{RW} |U_{RW}| \end{aligned}$$

2a) Linearized Side Force Equation -

$$\begin{aligned} \Delta \dot{V} &= g \Delta \phi - U \Delta \psi - \dot{\psi} \Delta U - \frac{\rho Q_f}{m} (V - U_{WE} \sin \psi \Delta \psi - U_{WN} \cos \psi \Delta \psi \\ &- \sin \psi \Delta U_{WN}) - \frac{\rho S_R}{2m} \left[(U_{SSL}^2 + V_{RN}^2) C_{DRL} \cos \epsilon_{RL} \Delta \epsilon_{RL} + (U_{SSL}^2 + V_{RN}^2) \sin \epsilon_{RL} \left(\frac{\partial C_{DRL}}{\partial \epsilon_{RL}} \Delta \epsilon_{RL} + \frac{\partial C_{DRL}}{\partial \delta_R} \Delta \delta_R \right) + C_{DRL} \sin \epsilon_{RL} (2U_{SSL} \Delta U_{SSL} \right. \\ &+ 2V_{RN} \Delta V_{RN}) - (U_{SSL}^2 + V_{RN}^2) C_{LRL} \sin \epsilon_{RL} \Delta \epsilon_{RL} + (U_{SSL}^2 + V_{RN}^2) \cos \epsilon_{RL} \left(\frac{\partial C_{LRL}}{\partial \epsilon_{RL}} \Delta \epsilon_{RL} + \frac{\partial C_{LRL}}{\partial \delta_R} \Delta \delta_R \right) + C_{LRL} \cos \epsilon_{RL} (2U_{SSL} \Delta U_{SSL} + 2V_{RN} \Delta V_{RN}) \\ &+ (U_{SSR}^2 + V_{RN}^2) C_{DRR} \cos \epsilon_{RR} \Delta \epsilon_{RR} + (U_{SSR}^2 + V_{RN}^2) \sin \epsilon_{RR} \left(\frac{\partial C_{DRR}}{\partial \epsilon_{RR}} \Delta \epsilon_{RR} + \frac{\partial C_{DRR}}{\partial \delta_R} \Delta \delta_R \right) + C_{DRR} \sin \epsilon_{RR} (2U_{SSR} \Delta U_{SSR} + 2V_{RN} \Delta V_{RN}) - (U_{SSR}^2 + V_{RN}^2) C_{LRR} \sin \epsilon_{RR} \Delta \epsilon_{RR} + (U_{SSR}^2 + V_{RN}^2) \cos \epsilon_{RR} \left(\frac{\partial C_{LRR}}{\partial \epsilon_{RR}} \Delta \epsilon_{RR} + \frac{\partial C_{LRR}}{\partial \delta_R} \Delta \delta_R \right) + C_{LRR} \cos \epsilon_{RR} (2U_{SSR} \Delta U_{SSR} + 2V_{RN} \Delta V_{RN}) \left. \right] \\ &- \frac{\rho \pi D^2}{8m} \left[\phi U_{RW}^2 \left(\frac{\partial C_{y' \phi_L}}{\partial T_L} \Delta T_L + \frac{\partial C_{y' \phi_L}}{\partial \beta_L} \Delta \beta_L + \frac{\partial C_{y' \phi_R}}{\partial T_R} \Delta T_R + \frac{\partial C_{y' \phi_R}}{\partial \beta_R} \Delta \beta_R \right) \right. \\ &+ 2\psi' (C_{y' \phi_L} + C_{y' \phi_R}) U_{RW} \Delta U_{RW} + U_{RW}^2 (C_{y' \phi_L} + C_{y' \phi_R}) \Delta \phi \left. \right] \end{aligned}$$

3) Yaw Moment -

$$\begin{aligned} \ddot{\psi} = & \frac{a_P}{I_Z} (T_L - T_R) + \frac{\rho A_B l_B}{2I_Z} U_{RW}^2 C_{Nf} + \frac{\rho S_R l_t}{2I_Z} \left[(U_{SSL}^2 + V_{RN}^2) C_{LRL} \cos \epsilon_{RL} \right. \\ & + (U_{SSL}^2 + V_{RN}^2) C_{DRL} \sin \epsilon_{RL} + (U_{SSR}^2 + V_{RN}^2) C_{LRR} \cos \epsilon_{RR} + (U_{SSR}^2 \\ & + V_{RN}^2) C_{DRR} \sin \epsilon_{RR} \left. \right] + \frac{\rho S_R a_t}{2I_Z} \left[(U_{SSL}^2 + V_{RN}^2) C_{LRL} \sin \epsilon_{RL} - (U_{SSL}^2 \right. \\ & + V_{RN}^2) C_{DRL} \cos \epsilon_{RL} + (U_{SSR}^2 + V_{RN}^2) C_{DRR} \cos \epsilon_{RR} - (U_{SSR}^2 + V_{RN}^2) C_{LRR} \sin \epsilon_{RR} \left. \right] \\ & + \frac{\rho \pi D^2 l_P}{8I_Z} \phi (C_y \phi_L + C_y \phi_R) U_{RW} |U_{RW}| \end{aligned}$$

3a) Linearized Yaw Moment Equation -

$$\begin{aligned} \Delta \ddot{\psi} = & \frac{a_P}{I_Z} (\Delta T_L - \Delta T_R) + \frac{\rho A_B l_B}{2I_Z} (U_{RW}^2 \frac{\partial C_{Nf}}{\partial \phi} \Delta \phi + C_{Nf} 2U_{RW} \Delta U_{RW}) \\ & + \frac{\rho S_R l_t}{2I_Z} \left[- (U_{SSR}^2 + V_{RN}^2) C_{LRL} \sin \epsilon_{RL} \Delta \epsilon_{RL} + (U_{SSL}^2 + V_{RN}^2) \cos \epsilon_{RL} \right. \\ & \left(\frac{\partial C_{LRL}}{\partial \epsilon_{RR}} \Delta \epsilon_{RR} + \frac{\partial C_{LRL}}{\partial \delta_R} \Delta \delta_R \right) + C_{LRL} \cos \epsilon_{RL} (2U_{SSL} \Delta U_{SSL} + 2V_{RN} \Delta V_{RN}) \\ & + (U_{SSL}^2 + V_{RN}^2) C_{DRL} \cos \epsilon_{RR} \Delta \epsilon_{RR} + (U_{SSL}^2 + V_{RN}^2) \sin \epsilon_{RL} \left(\frac{\partial C_{DRR}}{\partial \epsilon_{RL}} \Delta \epsilon_{RL} \right. \\ & + \frac{\partial C_{DRL}}{\partial \delta_R} \Delta \delta_R \left. \right) + C_{DRL} \sin \epsilon_{RL} (2U_{SSL} \Delta U_{SSL} + 2V_{RN} \Delta V_{RN}) - (U_{SSR}^2 \\ & + V_{RN}^2) C_{LRR} \sin \epsilon_{RR} \Delta \epsilon_{RR} + (U_{SSR}^2 + V_{RN}^2) \cos \epsilon_{RR} \left(\frac{\partial C_{LRR}}{\partial \epsilon_{RR}} \Delta \epsilon_{RR} \right. \\ & + \frac{\partial C_{LRR}}{\partial \delta_R} \Delta \delta_R \left. \right) + C_{LRR} \cos \epsilon_{RR} (2U_{SSR} \Delta U_{SSR} + 2V_{RN} \Delta V_{RN}) + (U_{SSR}^2 \\ & + V_{RN}^2) C_{DRR} \cos \epsilon_{RR} \Delta \epsilon_{RR} + (U_{SSR}^2 + V_{RN}^2) \sin \epsilon_{RR} \left(\frac{\partial C_{DRR}}{\partial \epsilon_{RR}} \Delta \epsilon_{RR} \right. \\ & + \frac{\partial C_{DRR}}{\partial \delta_R} \Delta \delta_R \left. \right) + C_{DRR} \sin \epsilon_{RR} (2U_{SSR} \Delta U_{SSR} + 2V_{RN} \Delta V_{RN}) \left. \right] + \frac{\rho S_R a_t}{2I_Z} \left[(U_{SSL}^2 \right. \\ & + V_{RN}^2) C_{LRL} \cos \epsilon_{RR} \Delta \epsilon_{RR} + (U_{SSL}^2 + V_{RN}^2) \sin \epsilon_{RR} \left(\frac{\partial C_{LRL}}{\partial \epsilon_{RL}} \Delta \epsilon_{RL} + \frac{\partial C_{LRL}}{\partial \delta_R} \Delta \delta_R \right) \\ & + C_{LRL} \sin \epsilon_{RR} (2U_{SSL} \Delta U_{SSL} + 2V_{RN} \Delta V_{RN}) + (U_{SSL}^2 + V_{RN}^2) C_{DRL} \sin \epsilon_{RL} \Delta \epsilon_{RL} \end{aligned}$$

$$\begin{aligned}
& - (U_{SSL}^2 + V_{RN}^2) \cos \epsilon_{RL} \left(\frac{\partial C_{DRL}}{\partial \epsilon_{RL}} \Delta \epsilon_{RL} + \frac{\partial C_{DRL}}{\partial \delta_R} \Delta \delta_R \right) - C_{DRL} \cos \epsilon_{RL} (2U_{SSL} \Delta U_{SSL} \\
& + 2V_{RN} \Delta V_{RN}) - (U_{SSR}^2 + V_{RN}^2) C_{DRR} \sin \epsilon_{RR} \Delta \epsilon_{RR} + (U_{SSR}^2 + V_{RN}^2) \cos \epsilon_{RR} \\
& \left(\frac{\partial C_{DRR}}{\partial \epsilon_{RR}} \Delta \epsilon_{RR} + \frac{\partial C_{DRR}}{\partial \delta_R} \Delta \delta_R \right) + C_{DRR} \cos \epsilon_{RR} (2U_{SSR} \Delta U_{SSR} + 2V_{RN} \Delta V_{RN}) \\
& - (U_{SSR}^2 + V_{RN}^2) C_{LRR} \cos \epsilon_{RR} \Delta \epsilon_{RR} - (U_{SSR}^2 + V_{RN}^2) \sin \epsilon_{RR} \left(\frac{\partial C_{LRR}}{\partial \epsilon_{RR}} \Delta \epsilon_{RR} \right. \\
& \left. + \frac{\partial C_{LRR}}{\partial \delta_R} \Delta \delta_R - C_{LRR} \sin \epsilon_{RR} (2U_{SSR} \Delta U_{SSR} + 2V_{RN} \Delta V_{RN}) \right] \\
& + \frac{\rho \pi D^2 l_P}{8 I_Z} \left[\phi U_{RW}^2 \left(\frac{\partial C_{Y' \phi_L}}{\partial T_L} \Delta T_L + \frac{\partial C_{Y' \phi_L}}{\partial \beta_L} \Delta \beta_L + \frac{\partial C_{Y' \phi_R}}{\partial T_R} \Delta T_R + \frac{\partial C_{Y' \phi_R}}{\partial \beta_R} \Delta \beta_R \right) \right. \\
& \left. + \phi (C_{Y' \phi_L} + C_{Y' \phi_R}) (2U_{RW} \Delta U_{RW}) + U_{RW}^2 (C_{Y' \phi_L} + C_{Y' \phi_R}) \Delta \phi \right]
\end{aligned}$$

4) Roll Moment -

$$\begin{aligned}
\ddot{\phi} &= -2\zeta_{\phi} \omega_{\phi} \dot{\phi} - \omega_{\phi}^2 \phi - \frac{\rho Q_f h_f}{m} \left[V + U_{WE} \cos \psi - U_{WN} \sin \psi \right] \\
& - \frac{\rho S_R h_t}{2m} \left[(U_{SSL}^2 + V_{RN}^2) C_{LRL} \cos \epsilon_{RL} + (U_{SSL}^2 + V_{RN}^2) C_{DRL} \sin \epsilon_{RL} \right. \\
& \left. + (U_{SSR}^2 + V_{RN}^2) C_{LRR} \cos \epsilon_{RR} + (U_{SSR}^2 + V_{RN}^2) C_{DRR} \sin \epsilon_{RR} \right] \\
& - \frac{\rho \pi D^2 h_P}{8 I_X} \phi (C_{Y' \phi_L} + C_{Y' \phi_R}) U_{RW} |U_{RW}|
\end{aligned}$$

4a) Linearized Roll Moment Equation -

$$\begin{aligned}
\ddot{\Delta \phi} &= -2\zeta_{\phi} \omega_{\phi} \Delta \dot{\phi} - \omega_{\phi}^2 \Delta \phi - \frac{\rho Q_f h_f}{m} \left[\Delta V - U_{WE} \sin \psi \Delta \psi + \cos \psi \Delta U_{WE} \right. \\
& \left. - U_{WN} \cos \psi \Delta \psi - \sin \psi \Delta U_{WN} \right] - \frac{\rho S_R h_t}{2m} \left[- (U_{SSL}^2 + V_{RN}^2) C_{LRL} \sin \epsilon_{RL} \Delta \epsilon_{RL} \right. \\
& + (U_{SSL}^2 + V_{RN}^2) \cos \epsilon_{RL} \left(\frac{\partial C_{LRL}}{\partial \epsilon_{RL}} \Delta \epsilon_{RL} + \frac{\partial C_{LRL}}{\partial \delta_R} \Delta \delta_R \right) + C_{LRL} \cos \epsilon_{RL} (2U_{SSL} \Delta U_{SSL} \\
& + 2V_{RN} \Delta V_{RN}) + (U_{SSL}^2 + V_{RN}^2) C_{DRL} \cos \epsilon_{RL} \Delta \epsilon_{RL} + (U_{SSL}^2 + V_{RN}^2) \sin \epsilon_{RL} \left(\frac{\partial C_{DRL}}{\partial \epsilon_{RL}} \Delta \epsilon_{RL} \right. \\
& \left. + \frac{\partial C_{DRL}}{\partial \delta_R} \Delta \delta_R \right) + C_{DRL} \sin \epsilon_{RL} (2U_{SSL} \Delta U_{SSL} + 2V_{RN} \Delta V_{RN}) - (U_{SSR}^2
\end{aligned}$$

$$\begin{aligned}
& + V_{RN}^2) C_{LRR} \sin \epsilon_{RR} \Delta \epsilon_{RR} + (U_{SSR}^2 + V_{RN}^2) \cos \epsilon_{RR} \left(\frac{\partial C_{LRR}}{\partial \epsilon_{RR}} \Delta \epsilon_{RR} + \frac{\partial C_{LRR}}{\partial \delta_R} \Delta \delta_R \right) \\
& + C_{LRR} \cos \epsilon_{RR} (2U_{SSR} \Delta U_{SSR} + 2V_{RN} \Delta V_{RN}) + (U_{SSR}^2 + V_{RN}^2) C_{DRR} \cos \epsilon_{RR} \Delta \epsilon_{RR} \\
& + (U_{SSR}^2 + V_{RN}^2) \sin \epsilon_{RR} \left(\frac{\partial C_{DRR}}{\partial \epsilon_{RR}} \Delta \epsilon_{RR} + \frac{\partial C_{DRR}}{\partial \delta_R} \Delta \delta_R \right) + C_{DRR} \sin \epsilon_{RR} (2U_{SSR} \Delta U_{SSR} \\
& + 2V_{RN} \Delta V_{RN}) - \frac{\rho \pi D^2 h_P}{8 I_x} \left[\phi (C_{y'} \phi_L + C_{y'} \phi_R) 2U_{RW} \Delta U_{RW} + \phi U_{RW}^2 \left(\frac{\partial C_{y'} \phi_L}{\partial T_L} \Delta T_L \right. \right. \\
& \left. \left. + \frac{\partial C_{y'} \phi_L}{\partial \beta_L} \Delta \beta_L + \frac{\partial C_{y'} \phi_R}{\partial \beta_R} \Delta \beta_R \right) + (C_{y'} \phi_L + C_{y'} \phi_R) U_{RW}^2 \Delta \phi \right]
\end{aligned}$$

5) Pitch Moment -

$$\begin{aligned}
\ddot{\theta} = & -2\zeta_{\theta} \omega_{\theta} \dot{\theta} - \omega_{\theta}^2 \theta - \frac{h_P}{I_y} (T_L + T_R) + \frac{Q_f \rho h_f}{I_y} (U + U_{WN} \cos \psi \\
& + U_{WE} \sin \psi) + \frac{\rho A_B L}{2 I_y} U_{RW} |U_{RW}| C_L
\end{aligned}$$

5a) Linearized Pitch Moment Equation -

$$\begin{aligned}
\ddot{\Delta \theta} = & -2\zeta_{\theta} \omega_{\theta} \dot{\Delta \theta} - \omega_{\theta}^2 \Delta \theta - \frac{h_P}{I_y} (\Delta T_L + \Delta T_R) + \frac{Q_f \rho h_f}{I_y} \left[\Delta U - U_{WN} \sin \psi \Delta \psi \right. \\
& \left. + \cos \psi \Delta U_{WN} + U_{WE} \cos \psi \Delta \psi + \sin \psi \Delta U_{WE} \right] + \frac{\rho A_B L}{2 I_y} \left[U_{RW}^2 \left(\frac{\partial C_L}{\partial \phi} \Delta \phi \right) + 2C_L U_{RW} \Delta U_{RW} \right]
\end{aligned}$$

6) Heave Equation -

The heave equation has not yet been derived due to the complexity of the base flow.

Relationships Between Independent Variables and Dependent Variables
Used in the Equation of Motion

$$1) \quad \underline{U_{SSL}^2} = \frac{8T_L}{\rho\pi D^2} + (U + U_{WN}\cos\psi + U_{WE}\sin\psi)^2$$

$$1a) \quad 2U_{SSL}\Delta U_{SSL} = \frac{8\Delta T_L}{\rho\pi D^2} + 2(U + U_{WN}\cos\psi + U_{WE}\sin\psi)(\Delta U + \cos\psi\Delta U_{WN} \\ + \sin\psi\Delta U_{WE} - U_{WN}\sin\psi\Delta\psi + U_{WE}\cos\psi\Delta\psi)$$

$$2) \quad \underline{U_{SSR}^2} = \frac{8T_R}{\rho\pi D^2} + (U + U_{WN}\cos\psi + U_{WE}\sin\psi)^2$$

$$2a) \quad 2U_{SSR}\Delta U_{SSR} = \frac{8\Delta T_R}{\rho\pi D^2} + 2(U + U_{WN}\cos\psi + U_{WE}\sin\psi)(\Delta U + \cos\psi\Delta U_{WN} \\ + \sin\psi\Delta U_{WE} - U_{WN}\sin\psi\Delta\psi + U_{WE}\cos\psi\Delta\psi)$$

$$3) \quad \underline{V_{RN}} = V + U_{WE}\cos\psi - U_{WN}\sin\psi + h_t\dot{\phi} - l_t\dot{\psi}$$

$$3a) \quad \Delta V_{RN} = \Delta V + U_{WE}\sin\psi\Delta\psi + \cos\psi\Delta U_{WE} - U_{WN}\cos\psi\Delta\psi - \sin\psi\Delta U_{WN} \\ + h_t\Delta\dot{\phi} - l_t\Delta\dot{\psi}$$

$$4) \quad \underline{U_{RW}^2} = (U + U_{WN}\cos\psi + U_{WE}\sin\psi)^2 + (V + U_{WE}\cos\psi - U_{WN}\sin\psi)^2$$

$$4a) \quad 2U_{RW}\Delta U_{RW} = 2(U + U_{WN}\cos\psi + U_{WE}\sin\psi)(\Delta U - U_{WN}\sin\psi\Delta\psi + \cos\psi\Delta U_{WN} \\ + U_{WE}\cos\psi\Delta\psi + \sin\psi\Delta U_{WE}) + 2(V + U_{WE}\cos\psi - U_{WN}\sin\psi)(\Delta V \\ - U_{WE}\sin\psi\Delta\psi + \cos\psi\Delta U_{WE} - U_{WN}\cos\psi\Delta\psi - \sin\psi\Delta U_{WN})$$

$$5) \quad \varphi = \tan^{-1} \frac{V + U_{WE} \cos \psi - U_{WN} \sin \psi}{U + U_{WE} \sin \psi + U_{WN} \cos \psi} = \tan^{-1} \frac{V_{RN}}{U + U_{WE} \sin \psi + U_{WN} \cos \psi}$$

$$5a) \quad \Delta \varphi \approx \frac{\Delta V_{RN}}{(U + U_{WE} \sin \psi + U_{WN} \cos \psi)} - \frac{V_{RN}}{(U + U_{WE} \sin \psi + U_{WN} \cos \psi)^2} (\Delta U + \sin \psi \Delta U_{WE} + U_{WE} \cos \psi \Delta \psi + \cos \psi \Delta U_{WN} - U_{WN} \sin \psi \Delta \psi)$$

$$6) \quad \epsilon_{RL} = \tan^{-1} \frac{V_{RN}}{U_{SSL}} \approx \frac{V_{RN}}{U_{SSL}}$$

$$6a) \quad \Delta \epsilon_{RL} = \frac{\Delta V_{RN}}{U_{SSL}} - \frac{V_{RN}}{(U_{SSL})^2} \Delta U_{SSL}$$

$$7) \quad \epsilon_{RR} = \tan^{-1} \frac{V_{RN}}{U_{SSR}} \approx \frac{V_{RN}}{U_{SSR}}$$

$$7a) \quad \Delta \epsilon_{RR} = \frac{\Delta V_{RN}}{U_{SSR}} - \frac{V_{RN}}{(U_{SSR})^2} \Delta U_{SSR}$$

$$8) \quad \underline{C_{yf}} = f(\varphi)$$

$$9) \quad C_{LRR} = f(\epsilon_{RR}, \delta_R)$$

$$10) \quad C_{DRR} = f(\epsilon_{RR}, \delta_R)$$

$$11) \quad C_{Nf} = f(\varphi)$$

$$12) \quad C_y' \phi_L = f(T_L, \beta_L)$$

$$13) \quad C_y' \phi_R = f(T_R, \beta_R)$$

Examples Of Linearized Equations For Yaw And Side Force

1) 50 Knot Forward Velocity

$$\dot{V} = .562\dot{\Phi} - 1.492\delta_R - .273V - 1.475\dot{\psi}$$

$$\ddot{\psi} = 1.7(\beta_L - \beta_R) + .562\delta_R + .133V$$

2) 25 Knot Forward Velocity

$$\dot{V} = .562\dot{\Phi} - .092\delta_R - .154V - .737\dot{\psi}$$

$$\ddot{\psi} = 1.1(\beta_L - \beta_R) + .346\delta_R + .093V$$

3) 50 Knot Forward Velocity - 12 Knot Side Velocity

$$\dot{V} = .562\dot{\Phi} - .160\delta_R - .262V - 1.475\dot{\psi}$$

$$\ddot{\psi} = 1.7(\beta_L - \beta_R) + .604\delta_R + .143V$$

4) 25 Knot Forward Velocity - 6 Knot Side Velocity

$$\dot{V} = .562\dot{\Phi} - .107\delta_R - .137V - .737\dot{\psi}$$


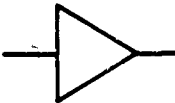
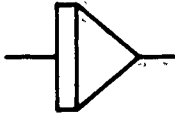


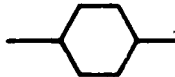

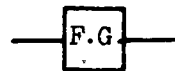
$$\ddot{\psi} = 1.1(\beta_L - \beta_R) + .402\delta_R + .101V$$

All angles are in degrees and velocities are in ft./sec.

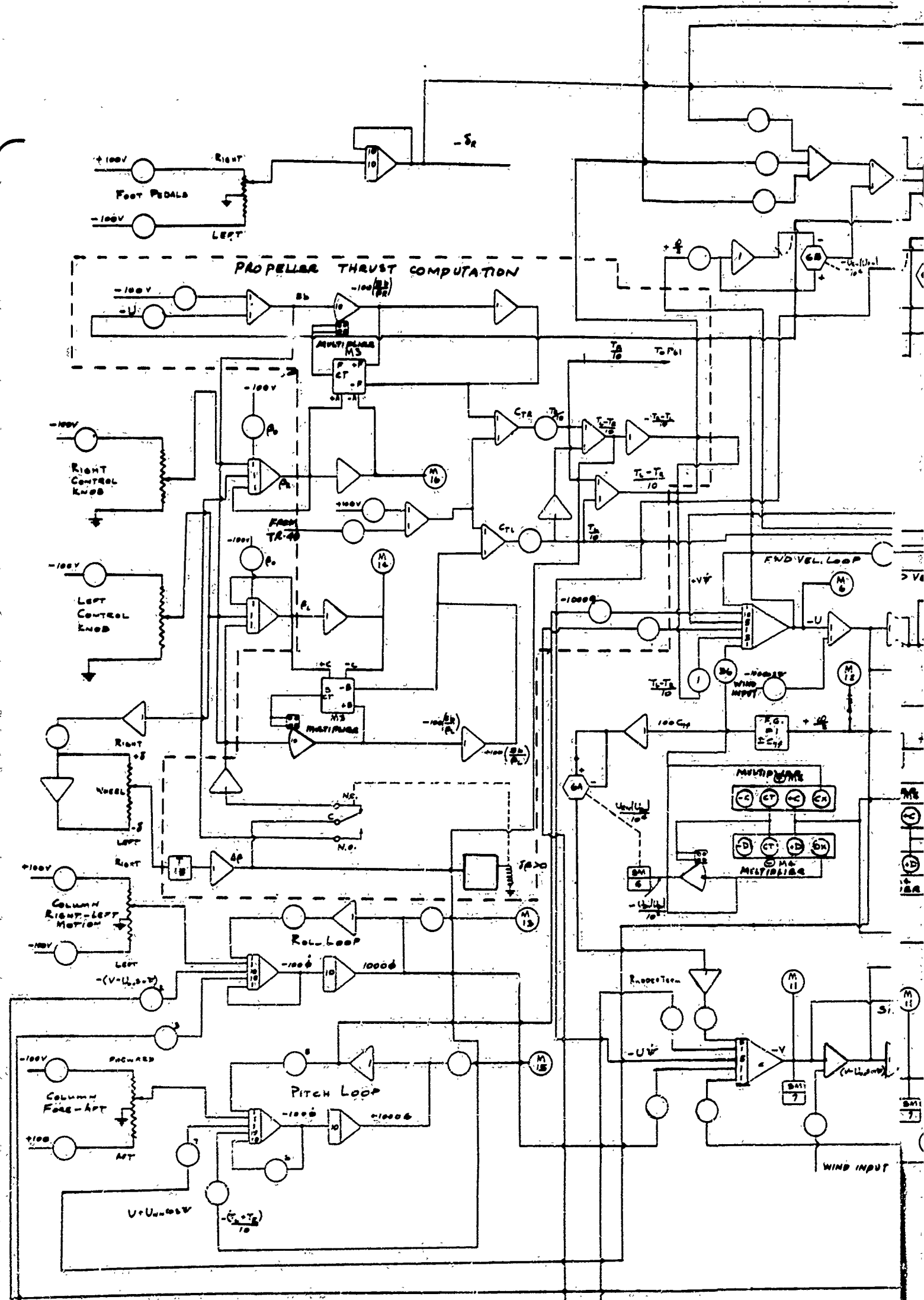
APPENDIX II

ANALOG COMPUTER DIAGRAMS

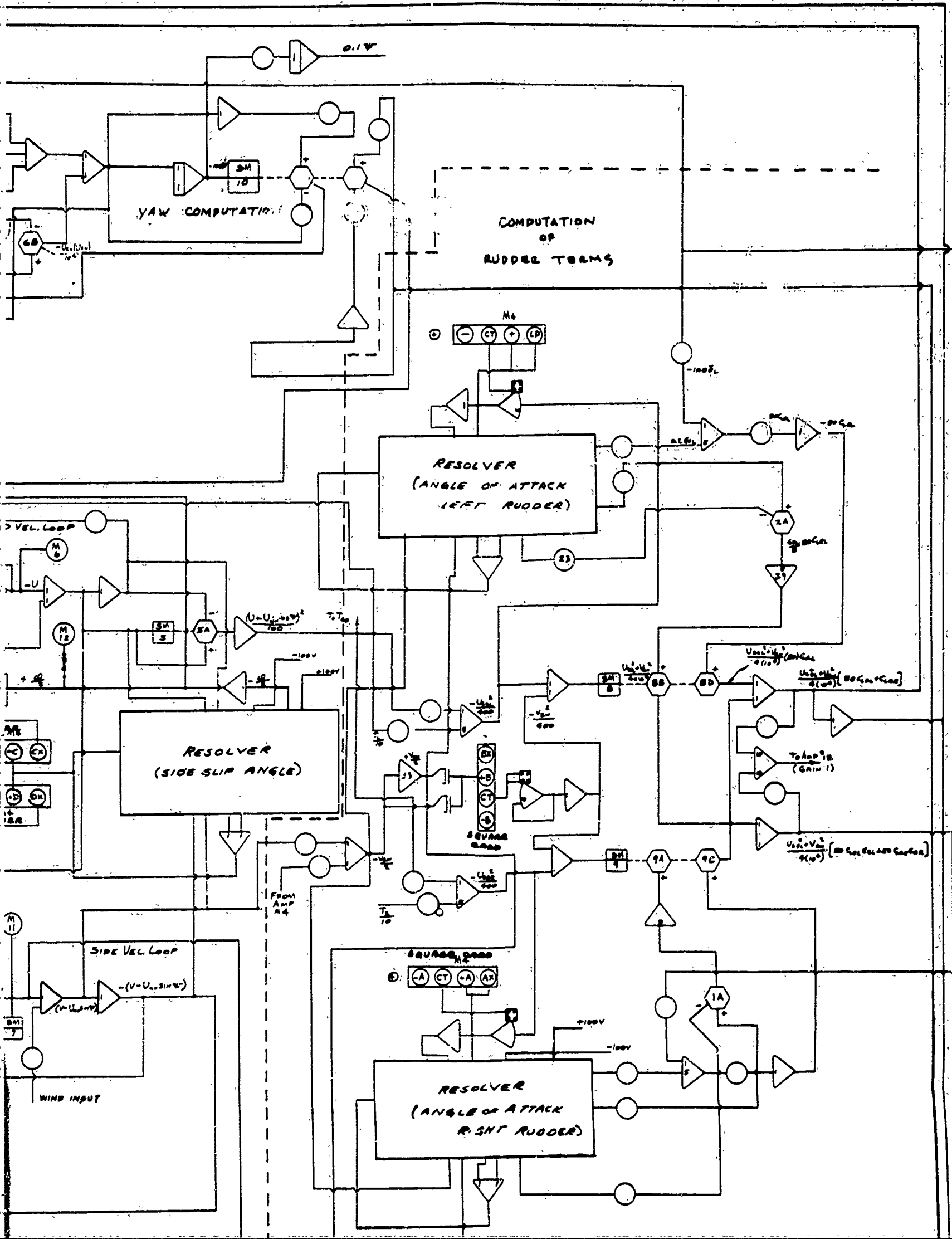
ANALOG COMPUTER SYMBOLS

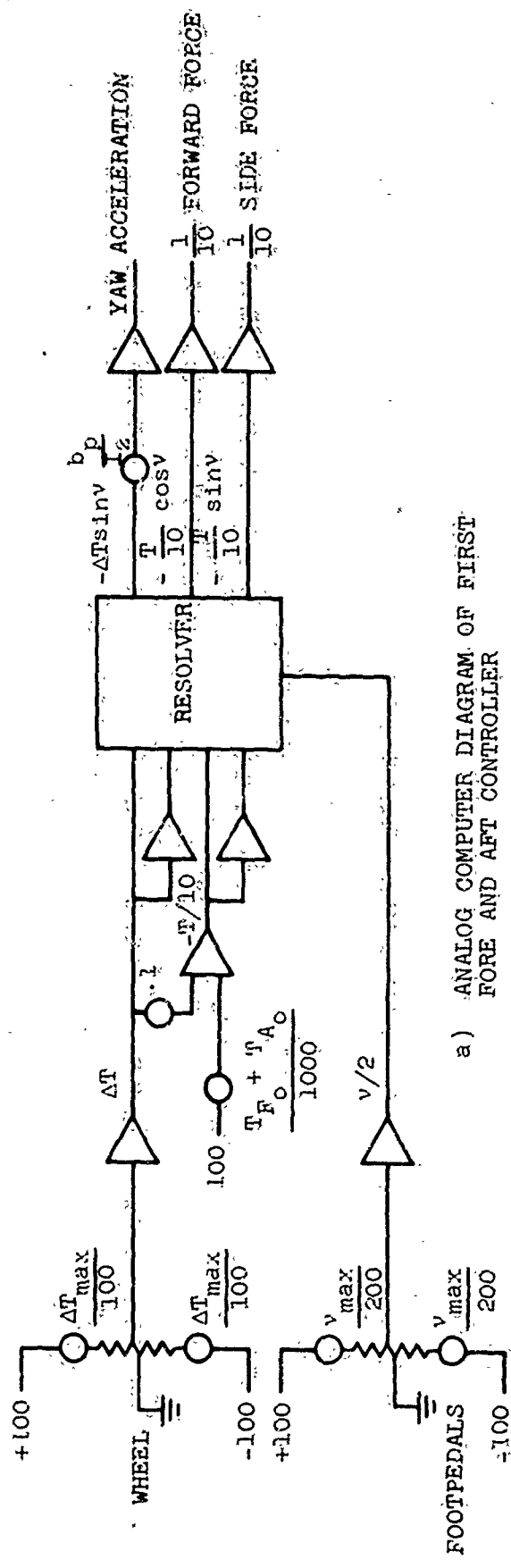
<u>SYMBOL</u>	<u>COMPONENT</u>
	Potentiometer
	Summing Amplifier
	Integrating Amplifier
	High-Gain Amplifier
	Servo-Multiplier Drive
	Servo-Multiplier Potentiometer
	Meter
	Nonlinear-Function Generator

Control Inputs



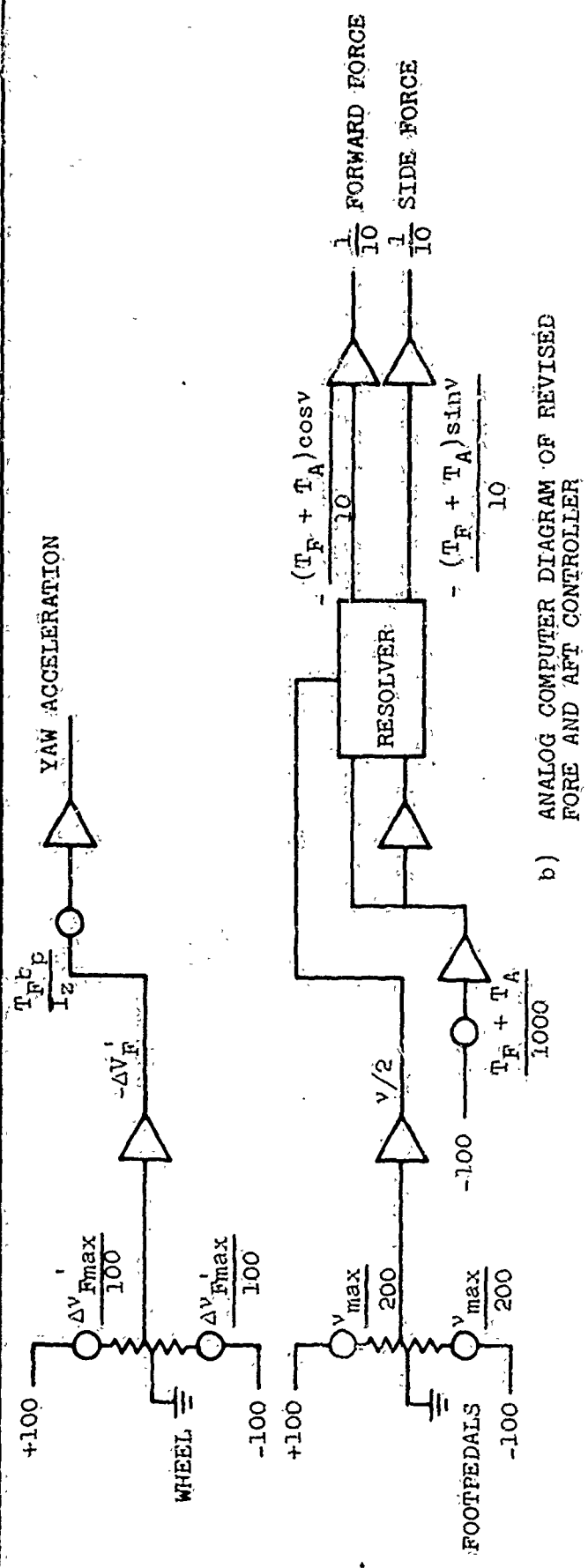
ACV COMPUTER PROGRAM (SKIP-1 CONFIGURATION)



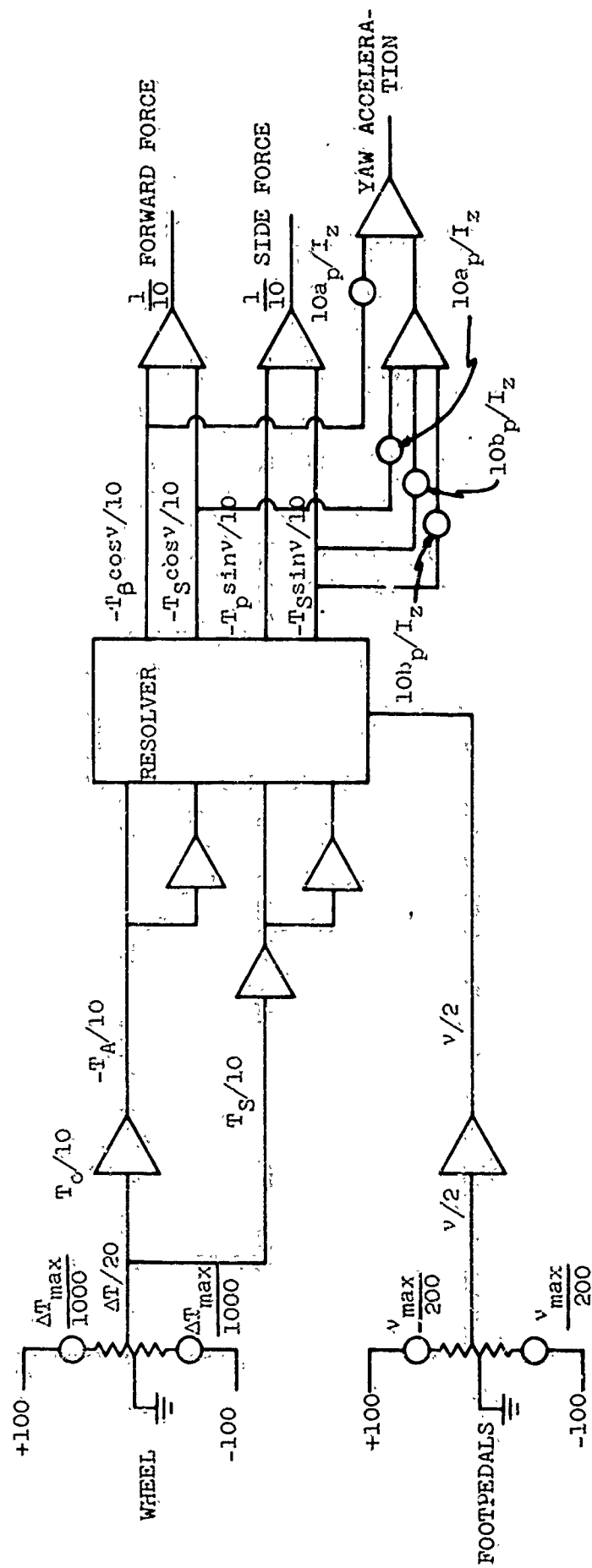


a) ANALOG COMPUTER DIAGRAM OF FIRST FORE AND AFT CONTROLLER

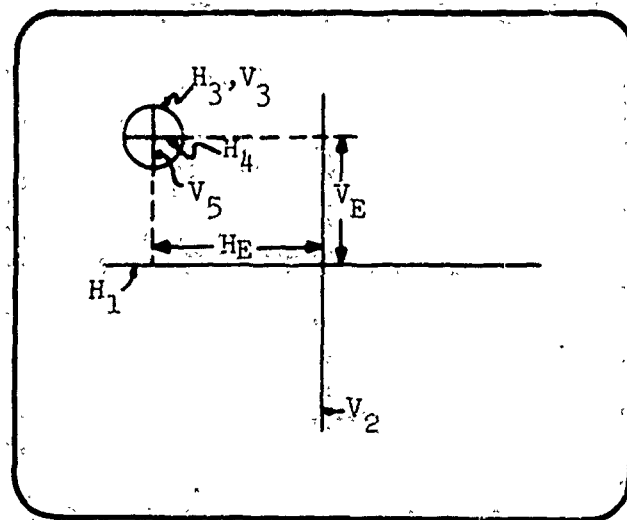
II-3



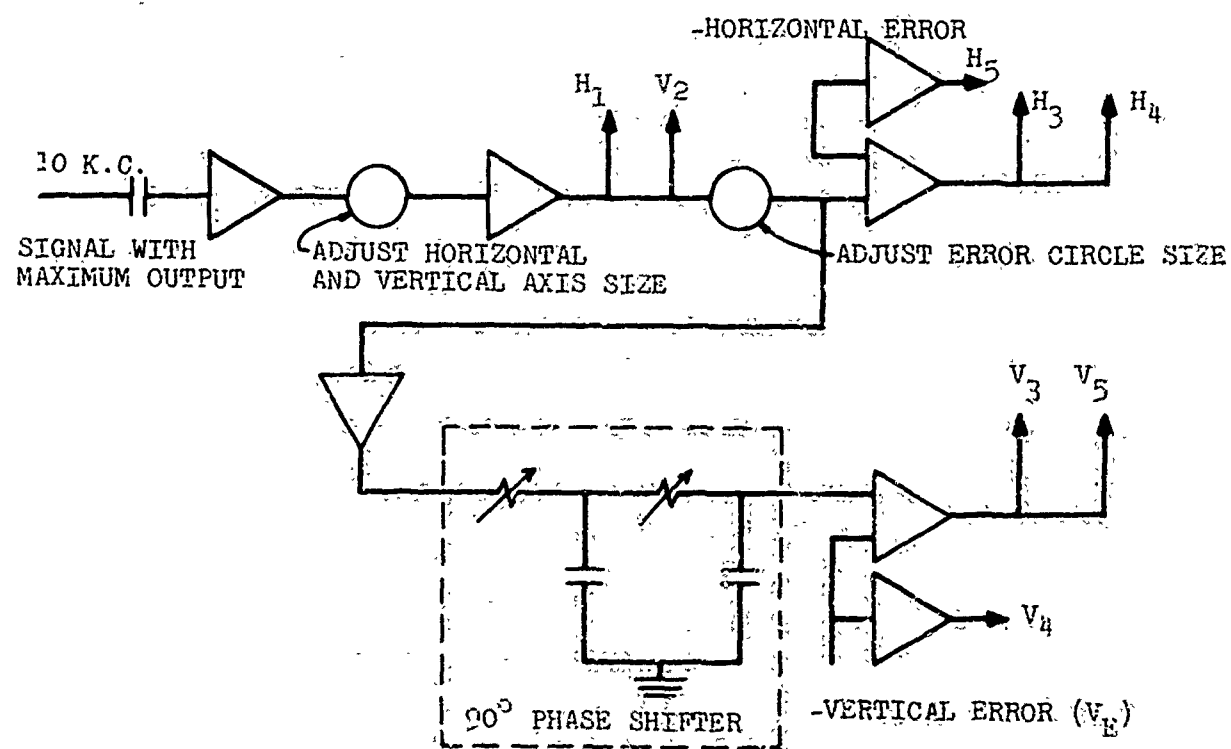
b) ANALOG COMPUTER DIAGRAM OF REVISED FORE AND AFT CONTROLLER



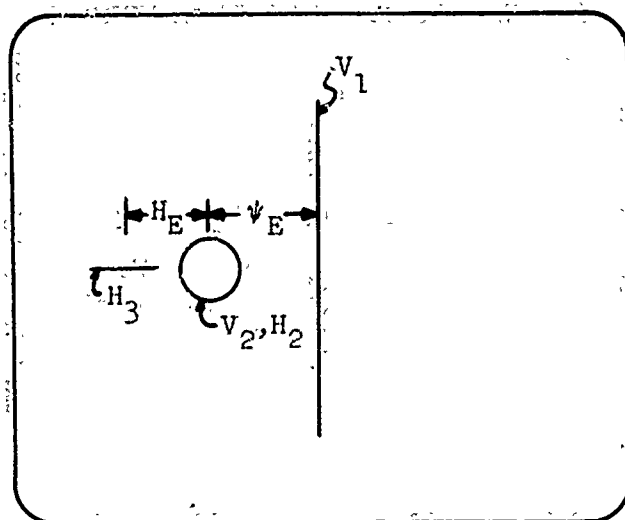
c.) ANALOG COMPUTER DIAGRAM OF CONTROLLER WITH TWO PROPELLERS BEHIND THE C.G.



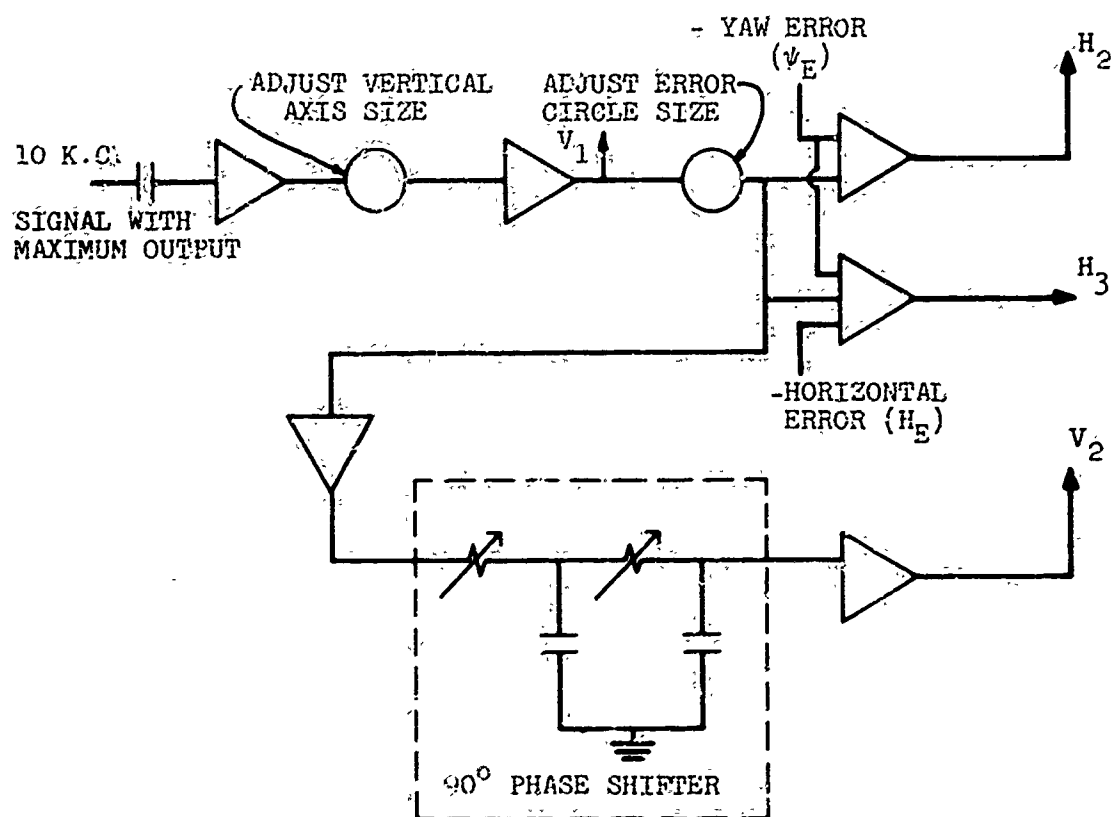
OSCILLOSCOPE DISPLAY



CIRCUITRY FOR QUICKENED DISPLAY NUMBER ONE



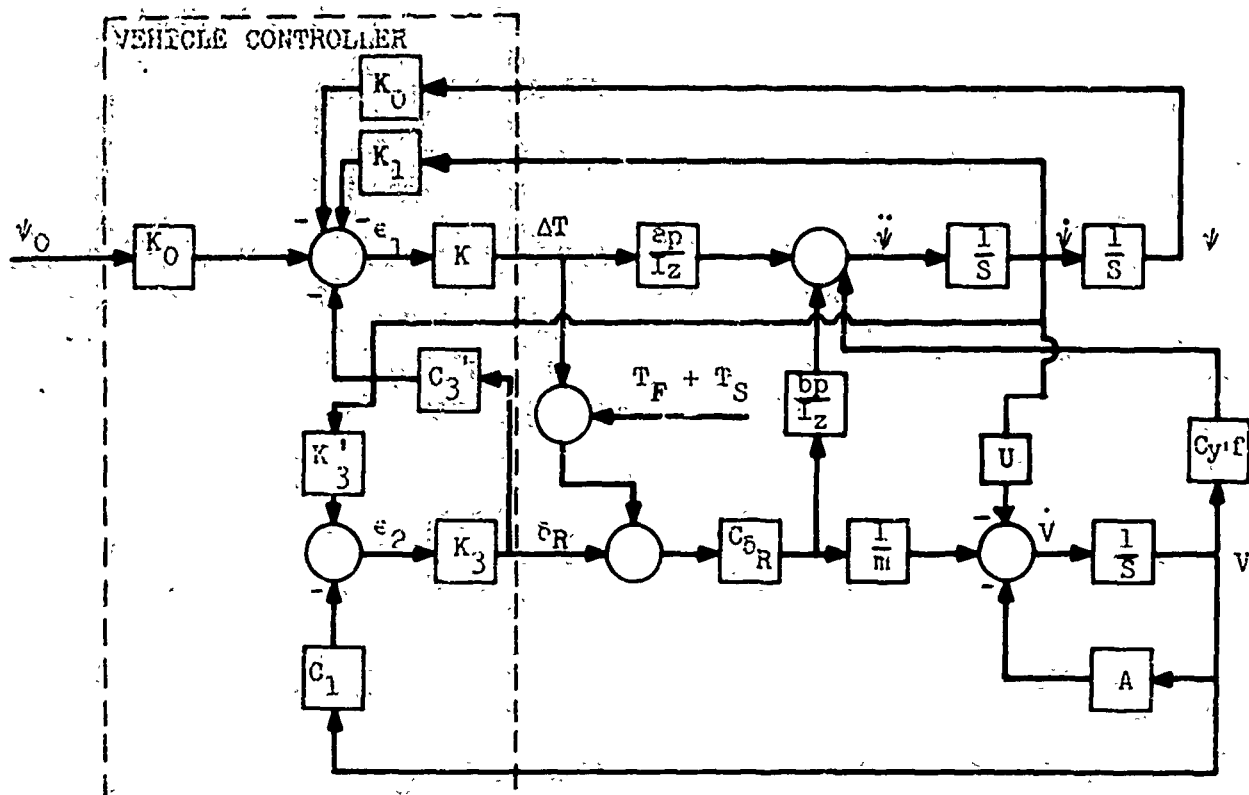
OSCILLOSCOPE DISPLAY



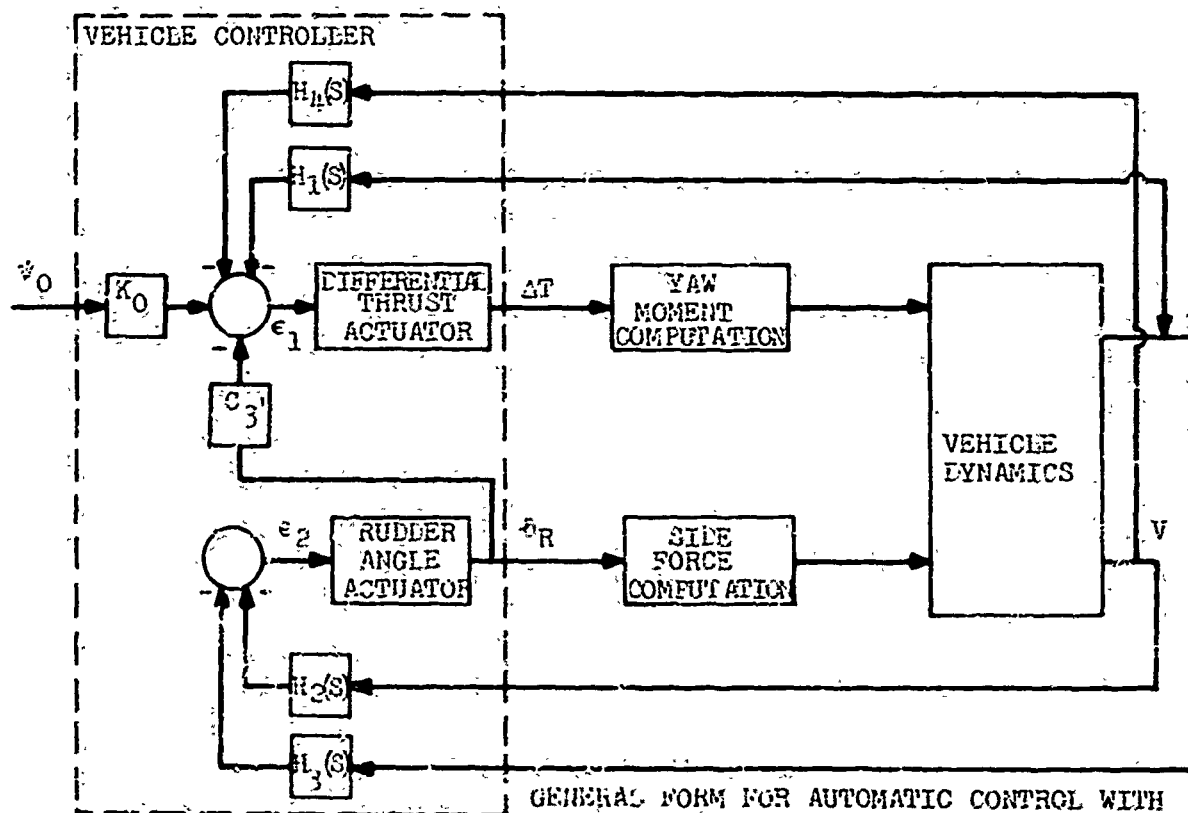
CIRCUITRY FOR QUICKENED DISPLAY NUMBER TWO

APPENDIX III

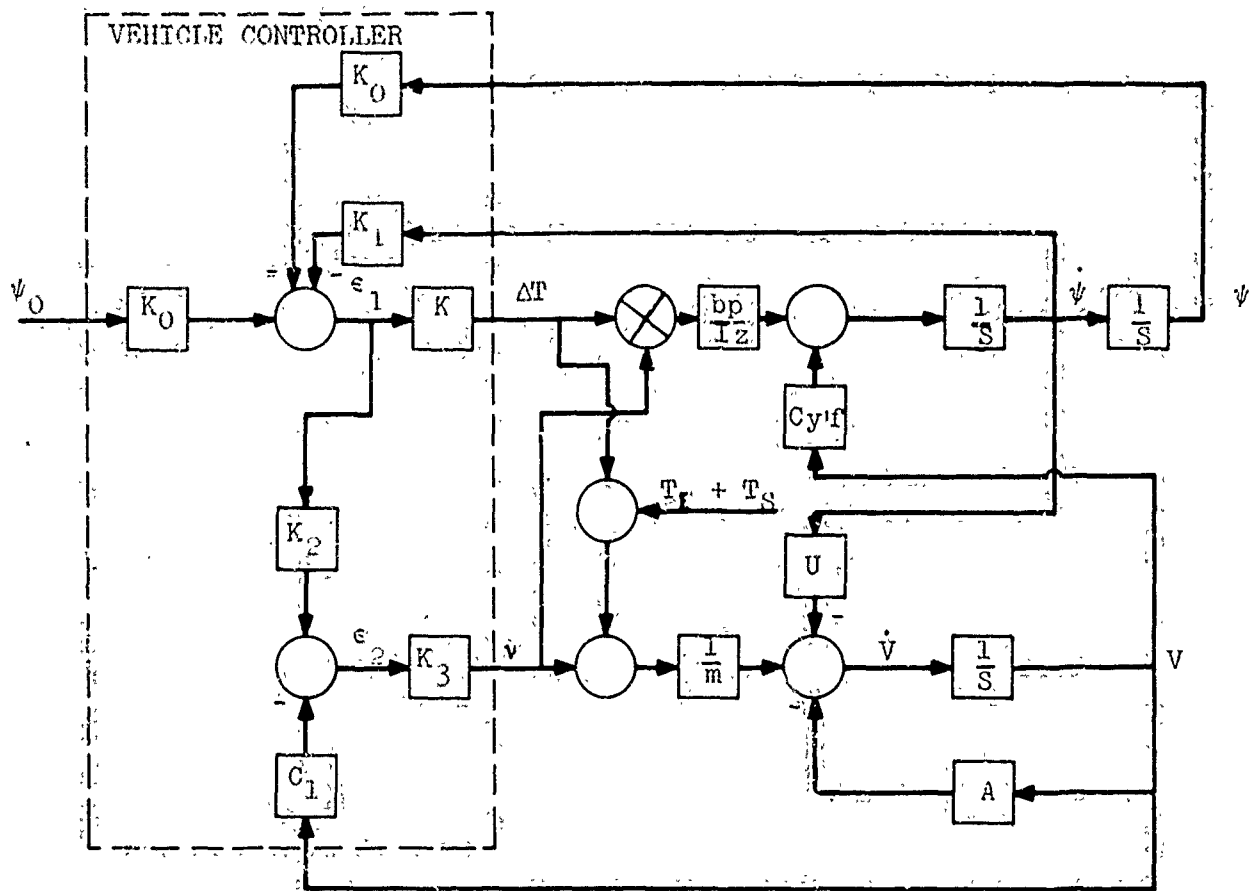
BLOCK DIAGRA , OF AUTOMATIC AND
QUICKENED CONTROLS



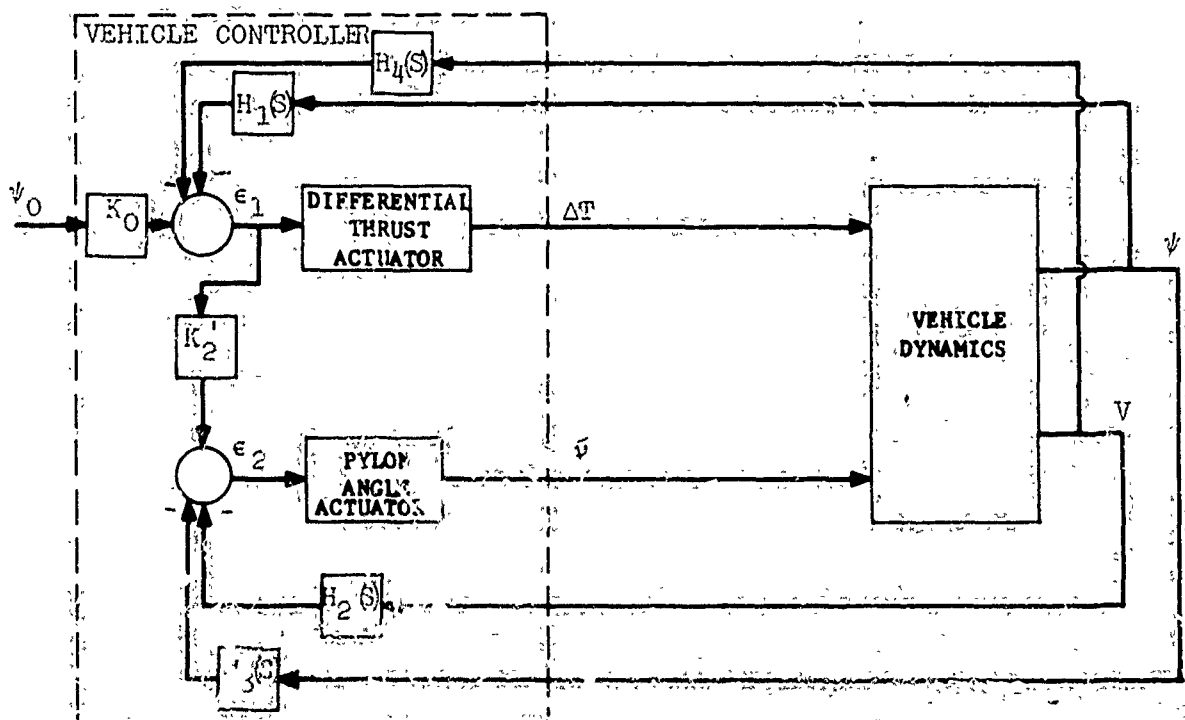
AUTOMATIC CONFIGURATION WITH RUDDERS BEHIND C.G.



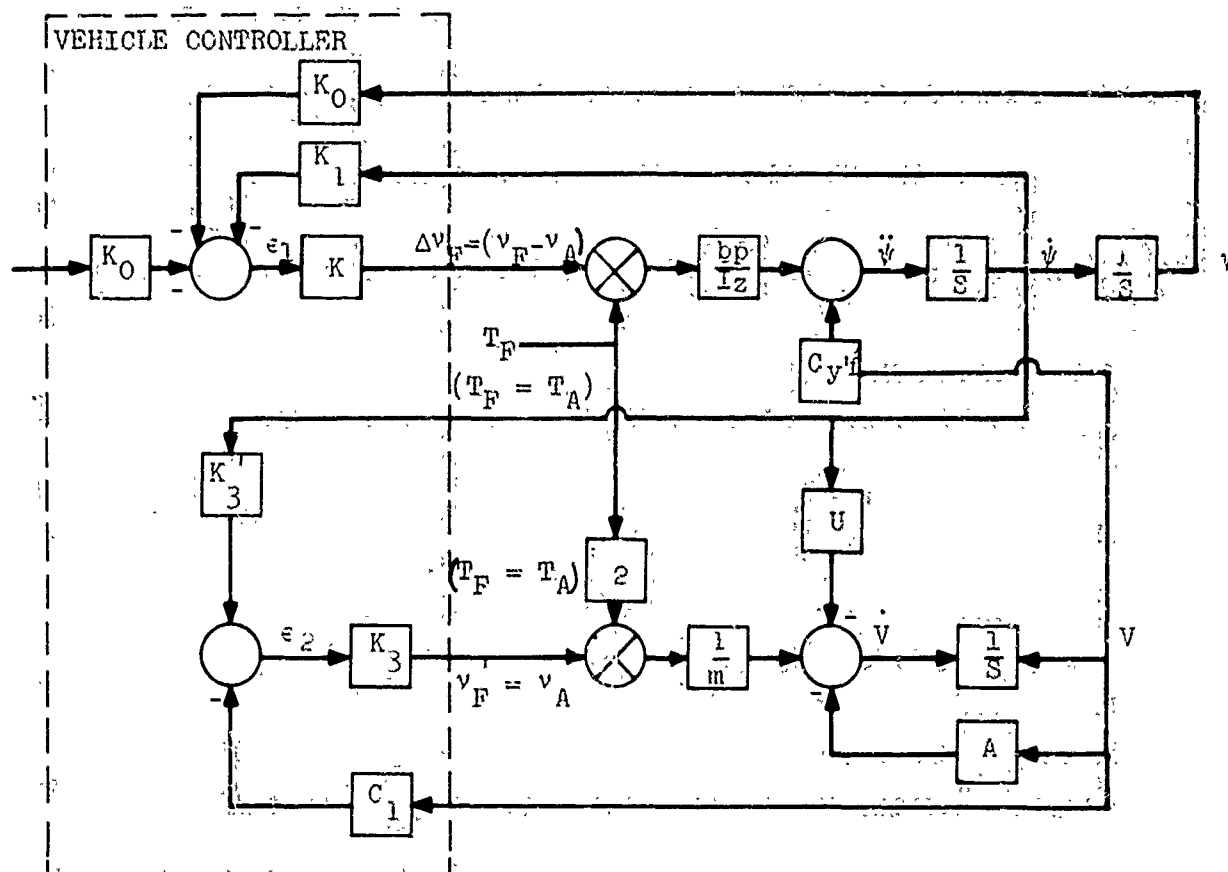
GENERAL FORM FOR AUTOMATIC CONTROL WITH RUDDER BEHIND THE C.G.



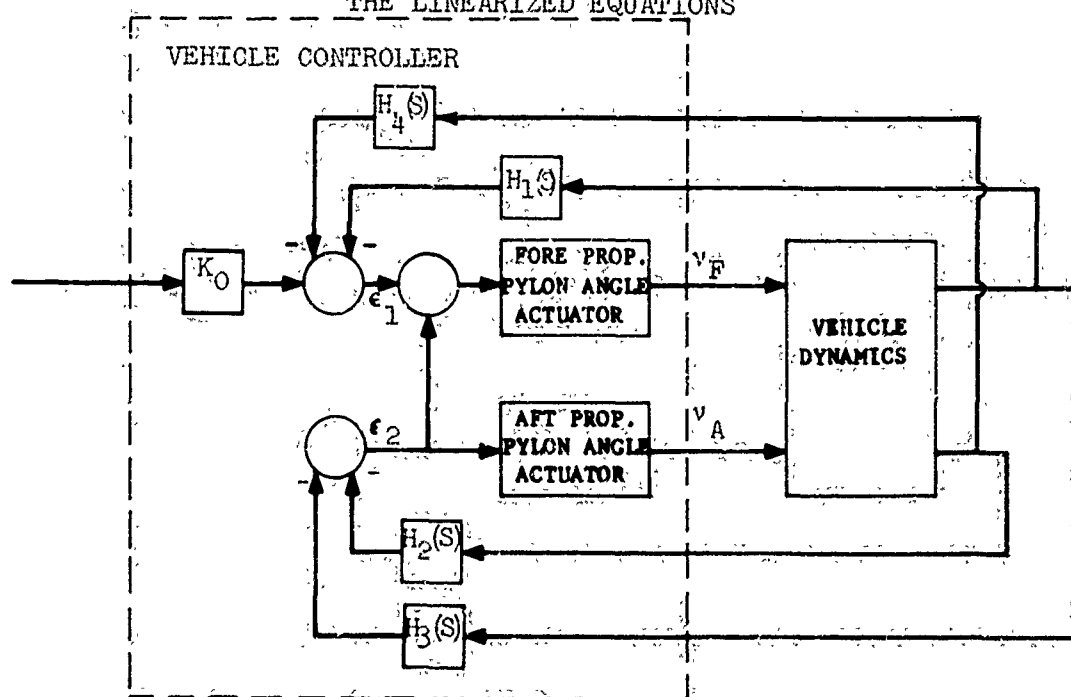
FORE AND AFT PROPELLER CONFIGURATION AUTOMATIC SYSTEM WITH THE LINEARIZED EQUATIONS



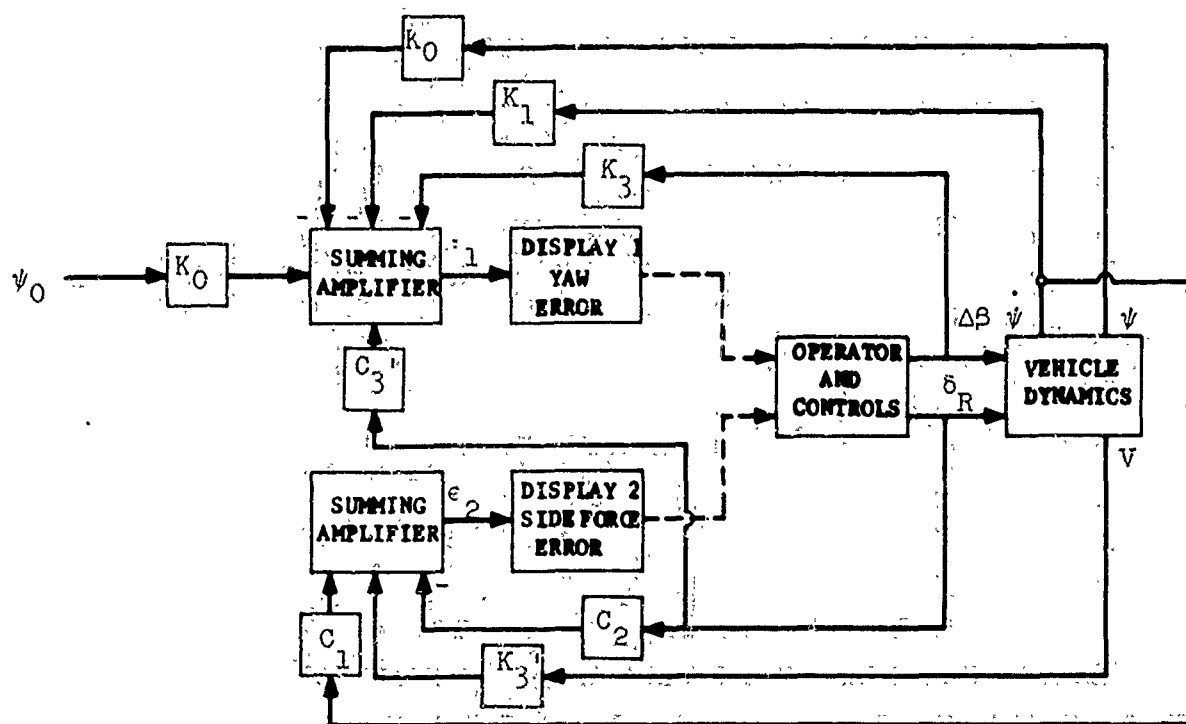
GENERAL BLOCK DIAGRAM FOR AUTOMATIC SYSTEM WITH FORE AND AFT PROPELLER CONFIGURATION



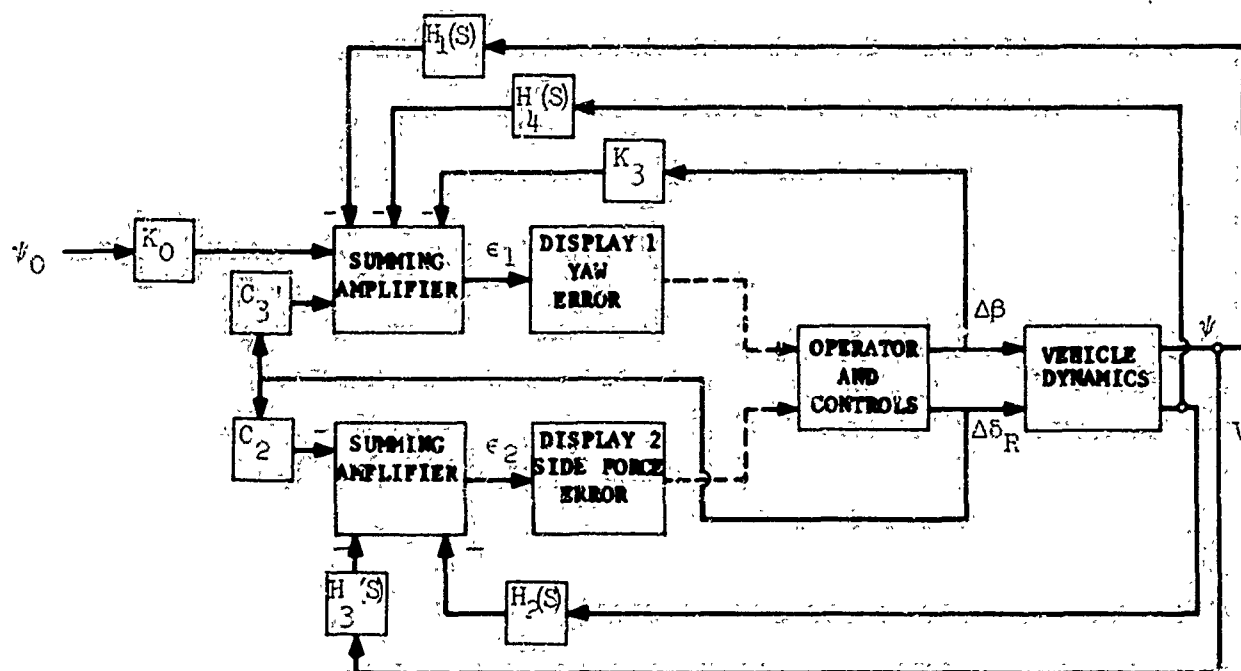
SECOND FORE AND AFT PROPELLER CONFIGURATION AUTOMATIC SYSTEM WITH THE LINEARIZED EQUATIONS



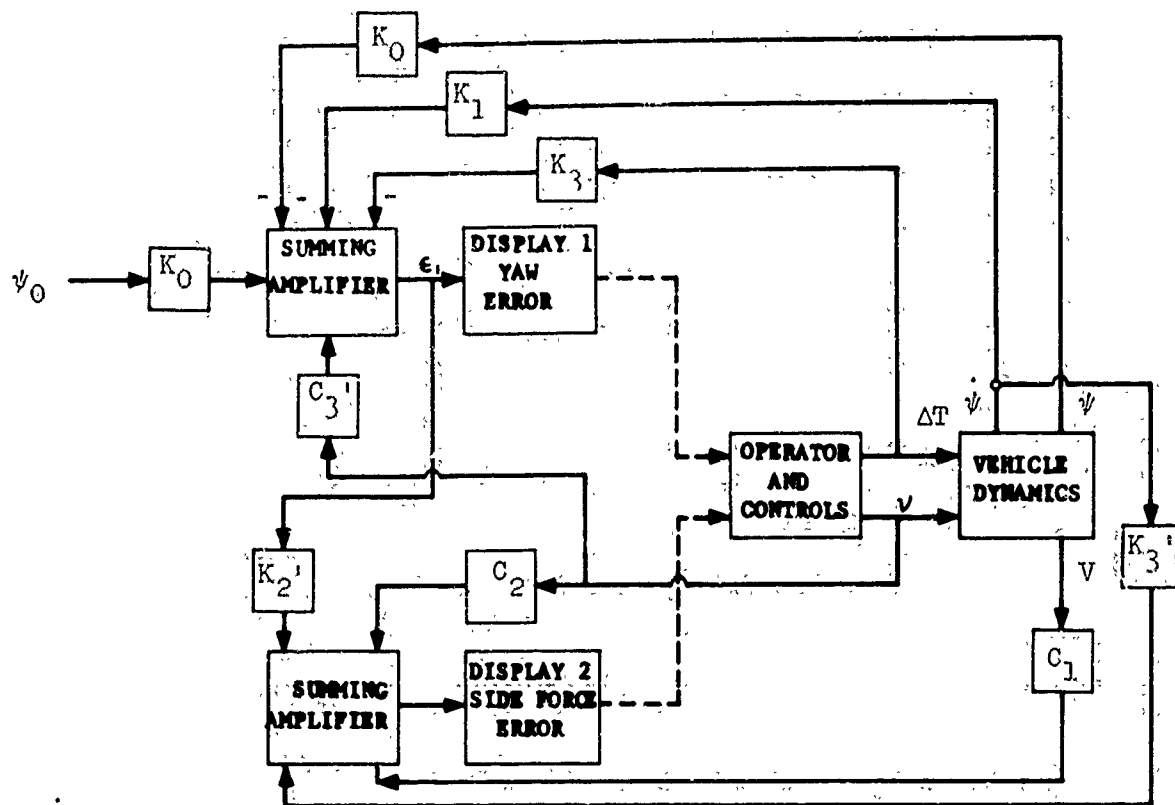
GENERAL FORM FOR REVISED AUTOMATIC SYSTEM WITH FORE AND AFT PROPELLER CONFIGURATION



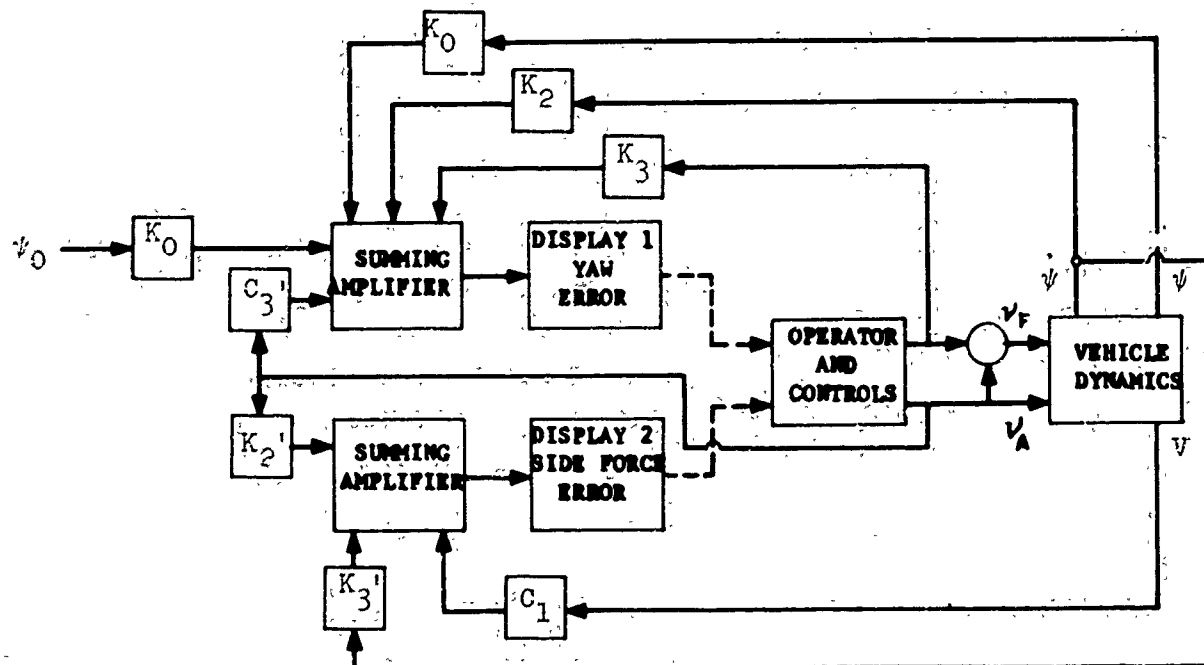
QUICKENED SYSTEM WITH TWO RUDDERS BEHIND THE C.G. DEVELOPED FROM THE LINEARIZED EQUATIONS



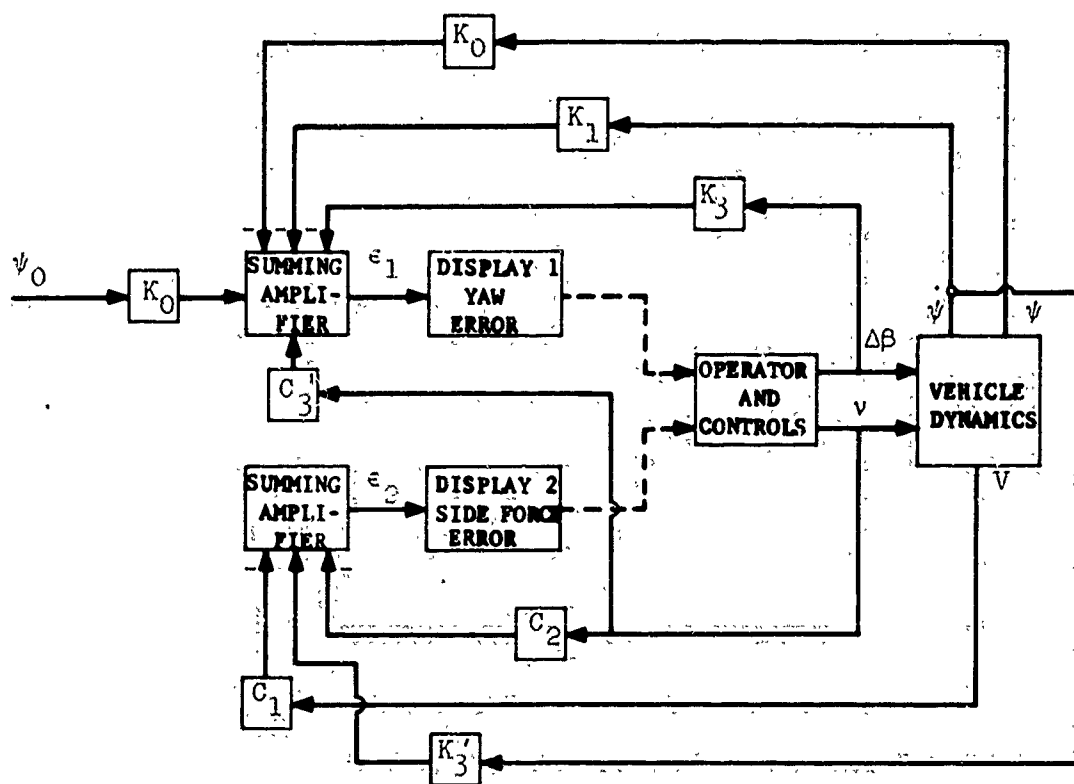
GENERAL FORM FOR QUICKENED SYSTEM WITH TWO RUDDERS BEHIND THE C.G.



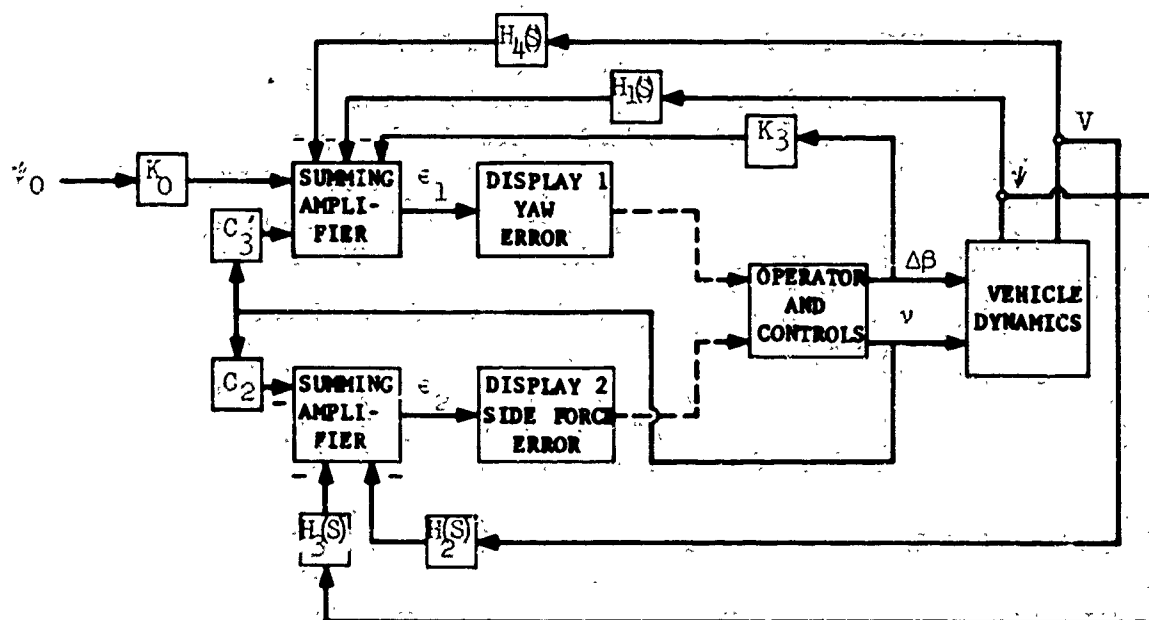
FIRST FORE AND AFT PROPELLER QUICKENED SYSTEM



REVISED FORE AND AFT PROPELLER QUICKENED SYSTEM



QUICKENED SYSTEM WITH TWO PROPELLERS BEHIND THE C.G.



GENERAL FORM FOR QUICKENED SYSTEM WITH TWO PROPELLERS BEHIND THE C.G.

APPENDIX IV
ANALOG COMPUTER DATA

EXPLANATION OF ANALOG COMPUTER DATA

This section contains the oscillographic recordings of the pertinent variables during the vehicle simulation on the analog computer. The variables of primary interest are the yaw angle and sideslip angle (or side velocity).

The manual control (page IV-3) illustrates the major problems in the vehicle control. The side velocity rises as high as 13 ft/sec and it is difficult to hold the vehicle exactly on course. The acceleration ($\ddot{\psi}$) changes signs many times as the operator tries to guess the proper yaw rate to reach the desired yaw angle. The yaw rate ($\dot{\psi}$) reflects the problems.

Page IV-4 shows the automatic control response which results from the use of idealized forces, i.e. pure side force and pure yaw moment. The $\ddot{\psi}$ term is significantly different from that resulting from the manual control. The low side velocity during the maneuver at one-half of the design velocity indicated that it is possible to generate good control responses without a nonlinear side force term proportional to $\dot{\psi}U$ (the centrifugal acceleration.)

Pages IV-5, IV-6, and IV-7 show automatic responses with the rudder behind the c.g. Page IV-5 shows that at the design velocity the sideslip is negligible - about two degrees. A sideslip of the same magnitude, but in the opposite direction, is observed while turning at one-half the design velocity. The apparent damping in yaw is also reduced at this velocity, but the overshoot is still zero. Page IV-7 shows that nullifying an initial side velocity of 10 feet per second at 50 knots forward velocity causes a 3.5 degree excursion in yaw angle. This angle returns to the command heading.

Pages IV-8, IV-9 and IV-10 show similar maneuvers for the fore and aft vehicle configuration. The response in this case is smoother than the vehicle with two rudders behind the c.g. Even at one-half

of the original design velocity the sideslip rises to only about one degree. When nullifying a side velocity, since pure side force is available, no excursion from the vehicle's commanded heading occurs.

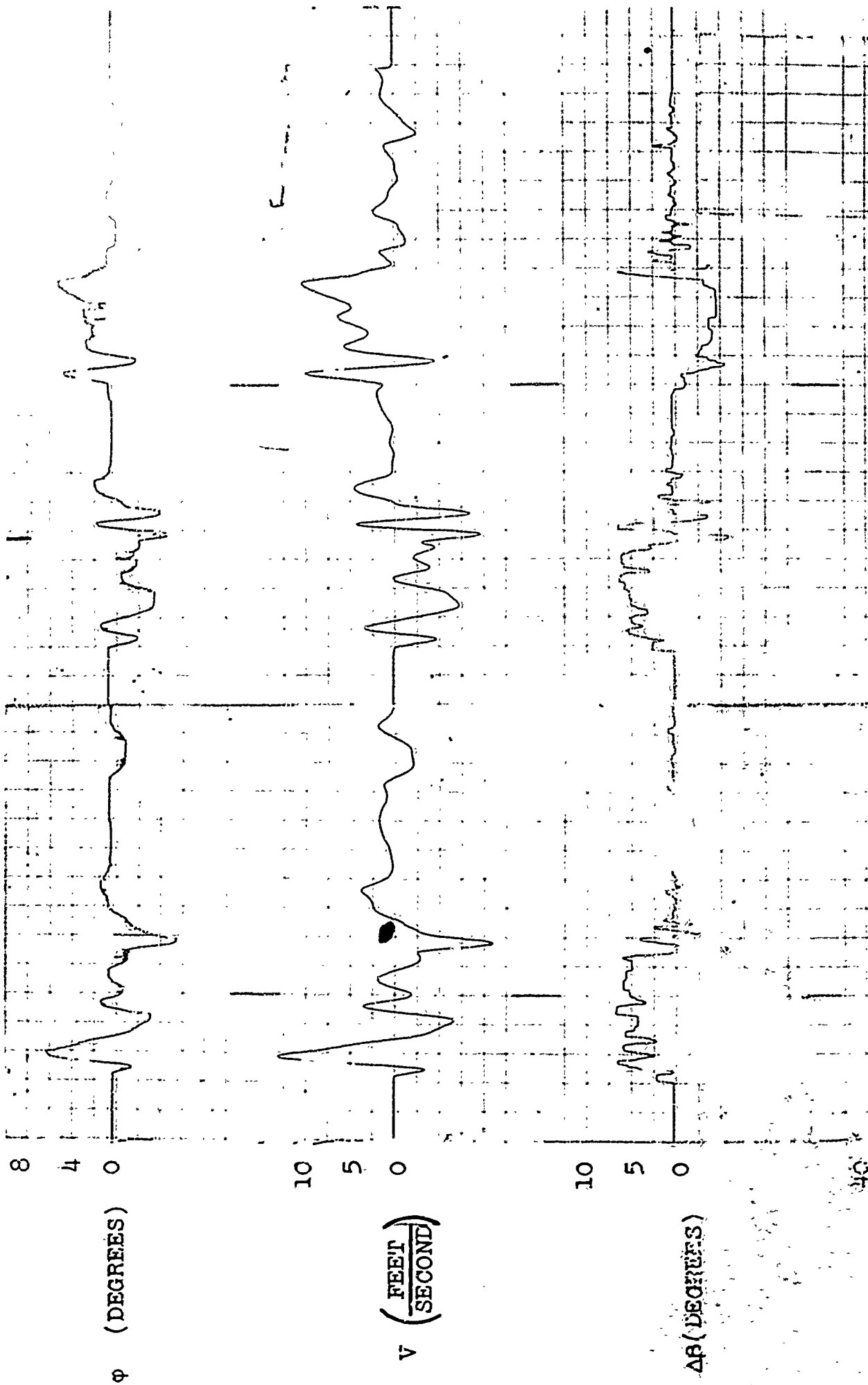
Pages IV-11 and IV-12 demonstrate the feasibility in closing a control loop with an operator inserted in it. Page IV-11 shows that the system is repeatable with the same operator and with different operators. Comparison of each of the variables with the manual system on page IV-3 indicates its ability to produce a smoother response. This characteristic is particularly evident in yaw rate ($\dot{\psi}$).

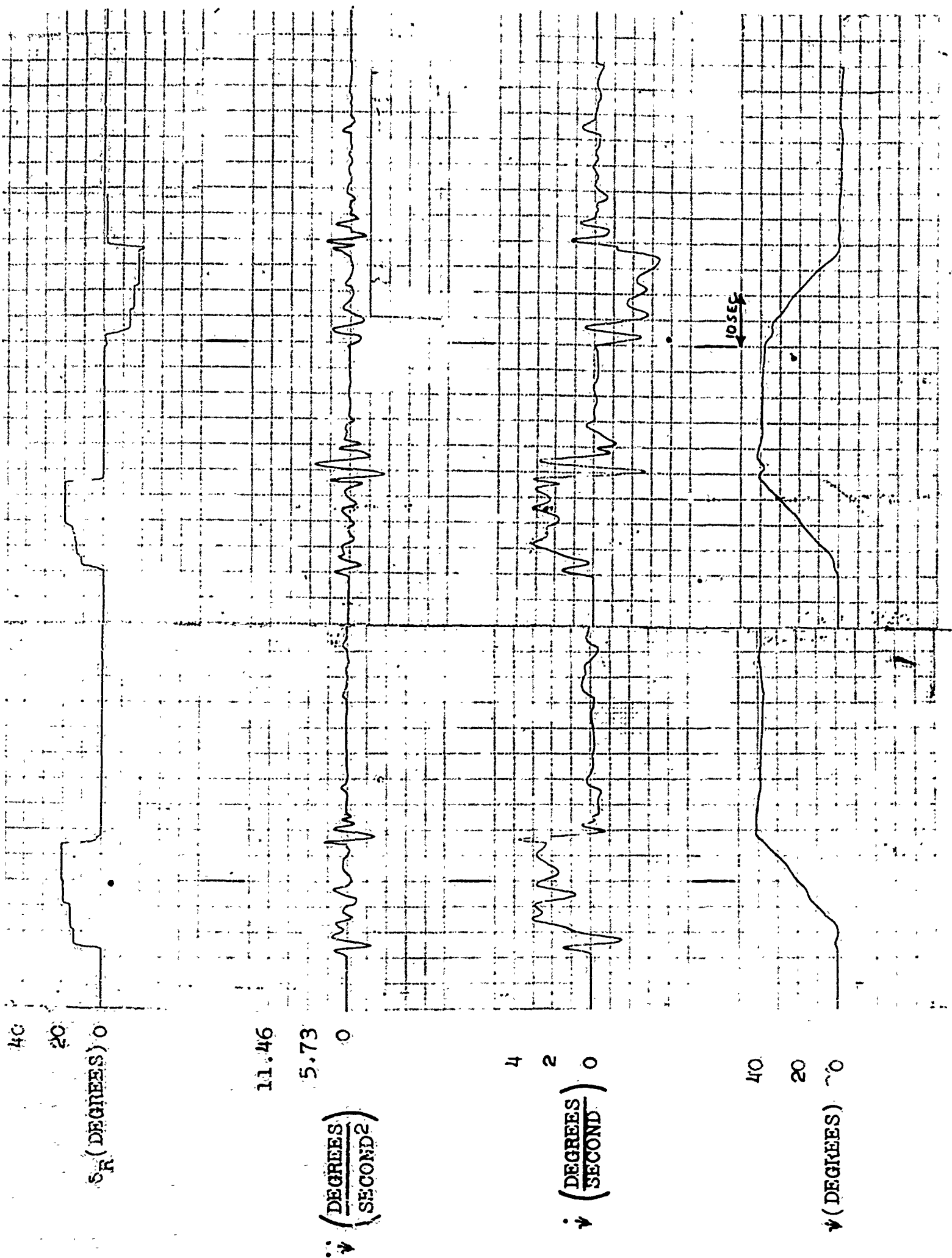
Page IV-12 shows the similarity of the response of the vehicle with two propellers behind the c.g. to the rudder - equipped vehicle.

MANUAL CONTROL WITH RUDDERS BEHIND THE C. G.

RUN 1

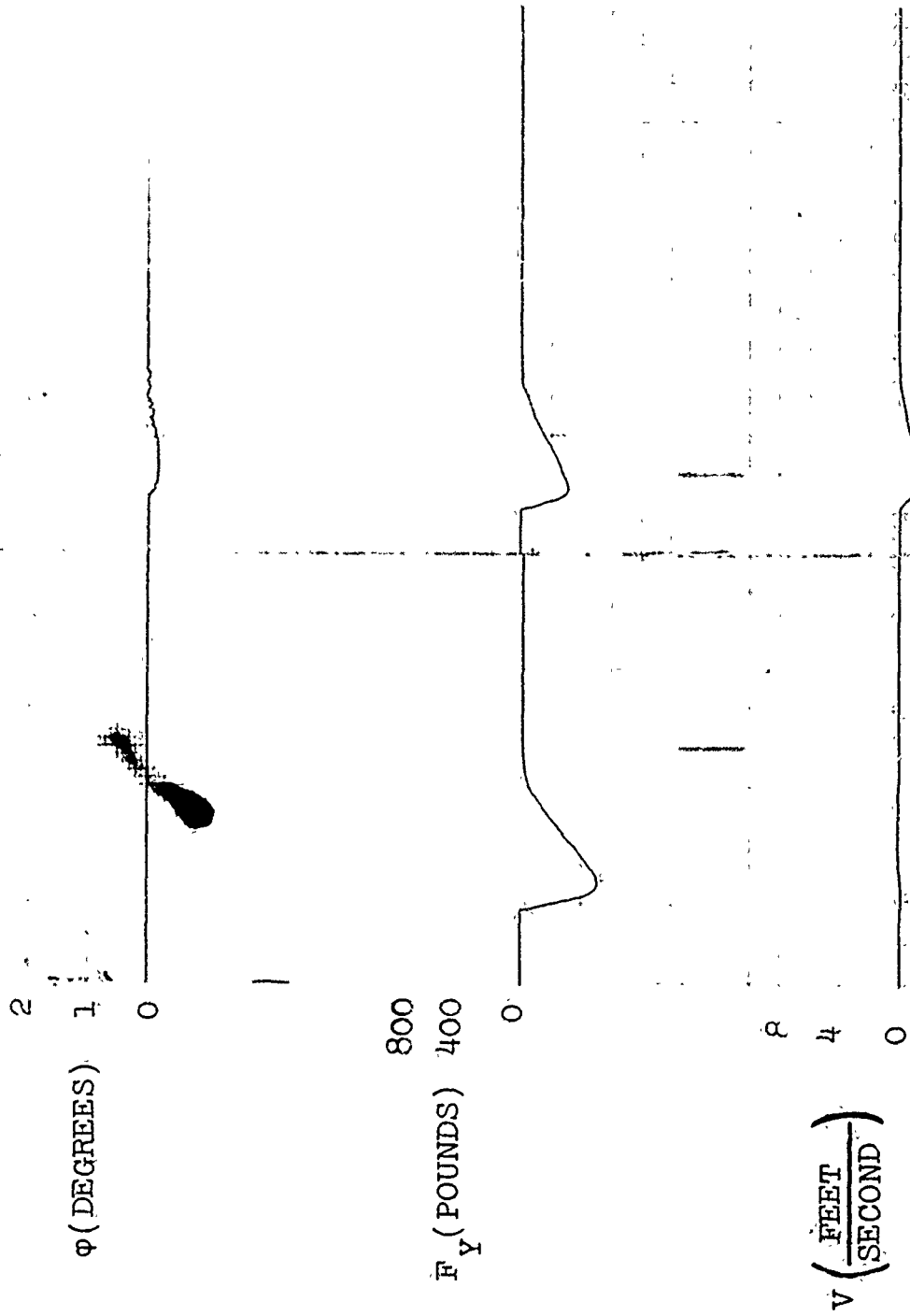
RUN 2





AUTOMATIC CONTROL WITH IDEALIZED FORCES

At the Design Velocity (50 knots) At 1/2 the Design Velocity



A

M_z (FOOT POUNDS) 70

0

4.72

2.30

0

$\ddot{\psi} \left(\frac{\text{DEGREES}}{\text{SECOND}^2} \right)$

4

2

0

$\dot{\psi} \left(\frac{\text{DEGREES}}{\text{SECOND}} \right)$

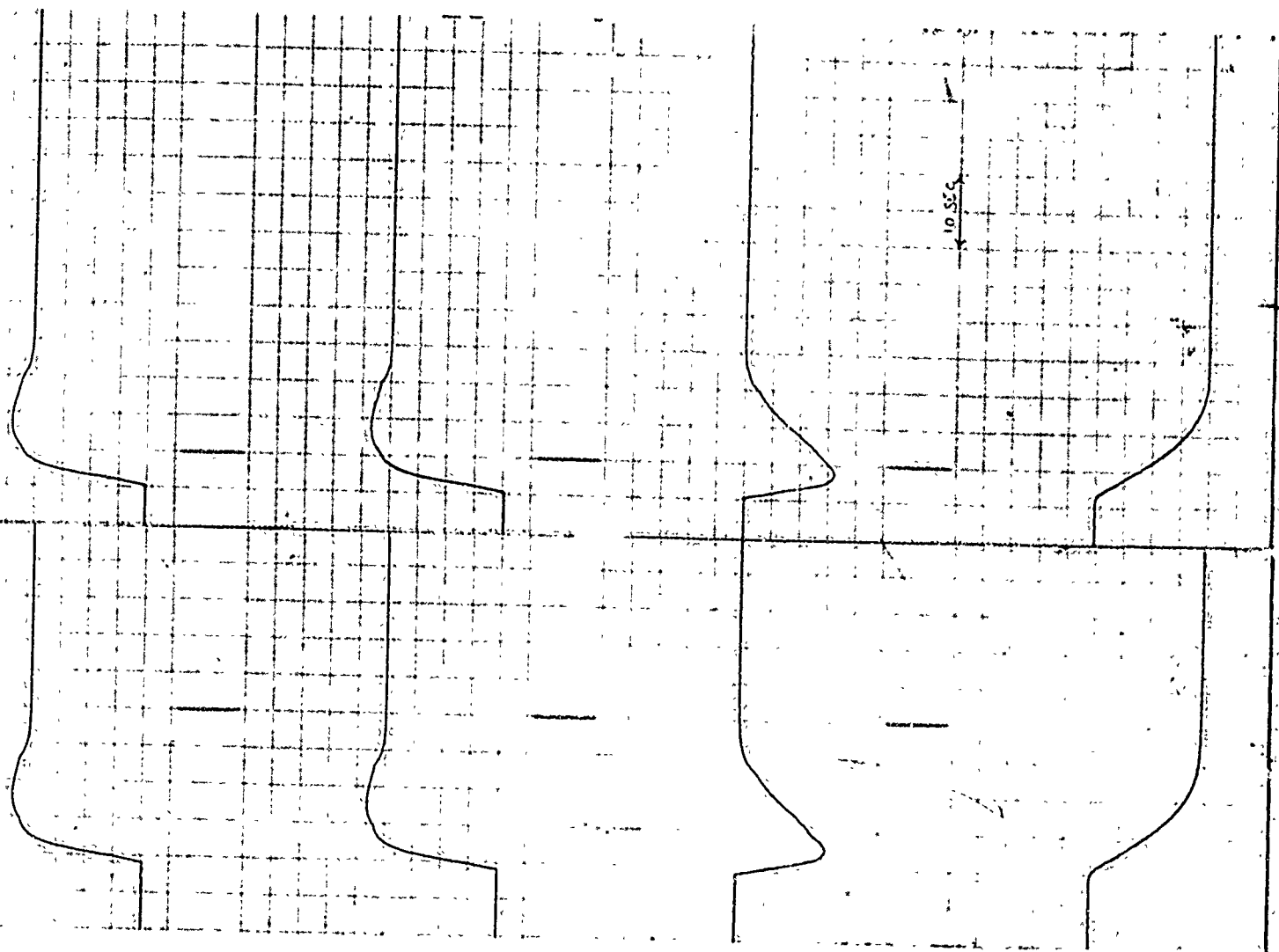
20

10

0

ψ (DEGREES)

B



AUTOMATIC SYSTEM WITH RUDDERS BEHIND THE C.G. - MANEUVERING AT THE DESIGN VELOCITY

RUN 2

RUN 1

ϕ (DEGREES)

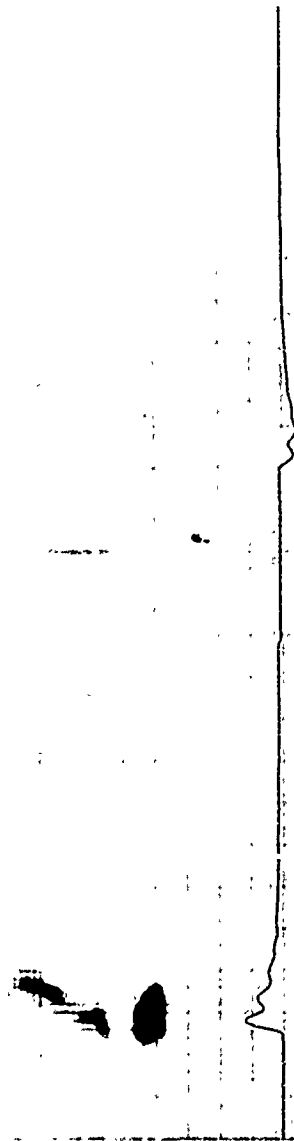


10

V $\left(\frac{\text{FEET}}{\text{SECONDS}} \right)$

5

0



10

5

0

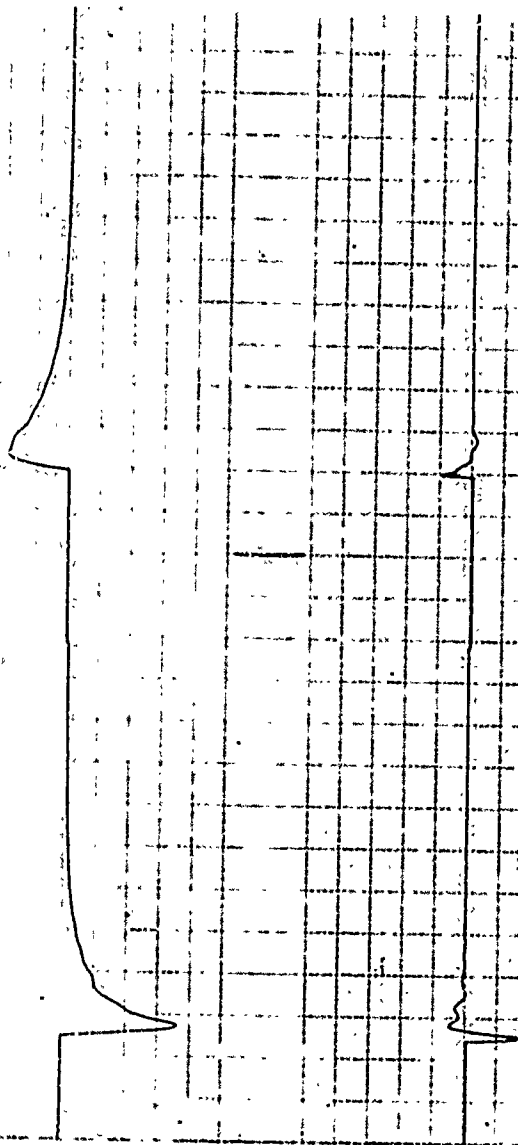
$\Delta\beta$ (DEGREES)



40

 δ_R (DEGREES) 20

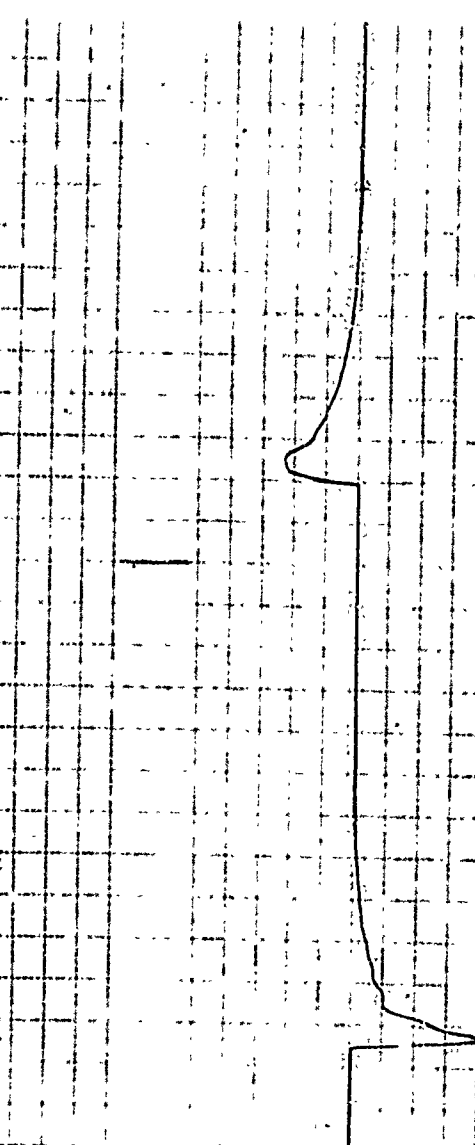
0



11.46

 $\dot{\psi}$ (DEGREES / SECOND) 5.73

0



4

2

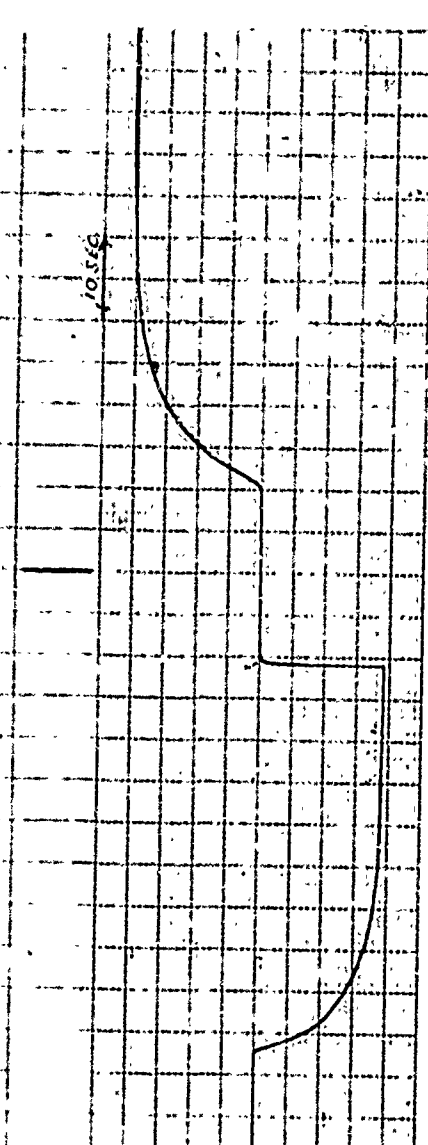
0

 $\dot{\psi}$ (DEGREES / SECOND)**B**

20

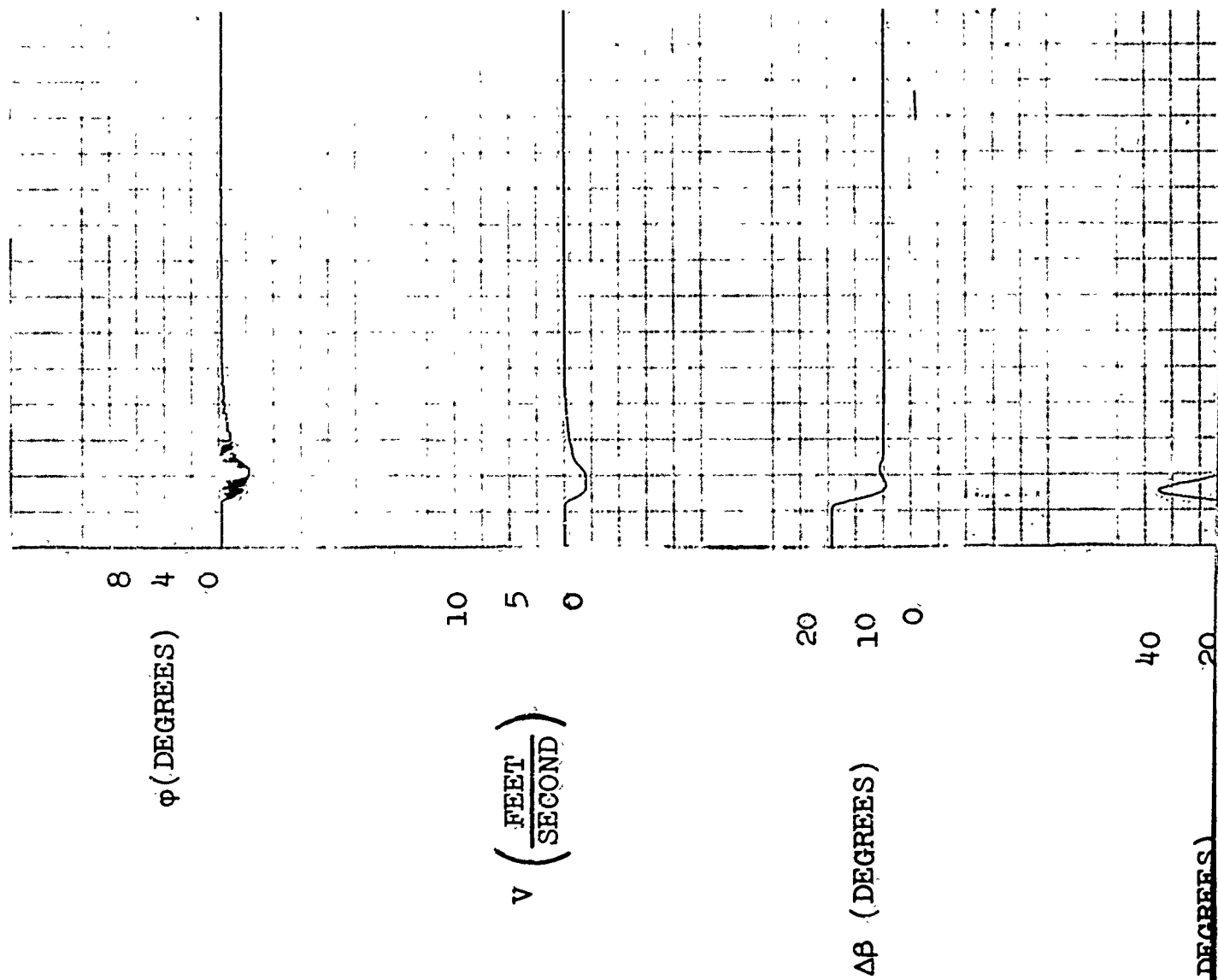
 ψ (DEGREES) 10

0



10.56

AUTOMATIC SYSTEM WITH 2 RUDDERS BEHIND THE C.G. - MANEUVER
AT 1/2 THE DESIGN VELOCITY



A

B

40
20
0
 δ_R (DEGREES)

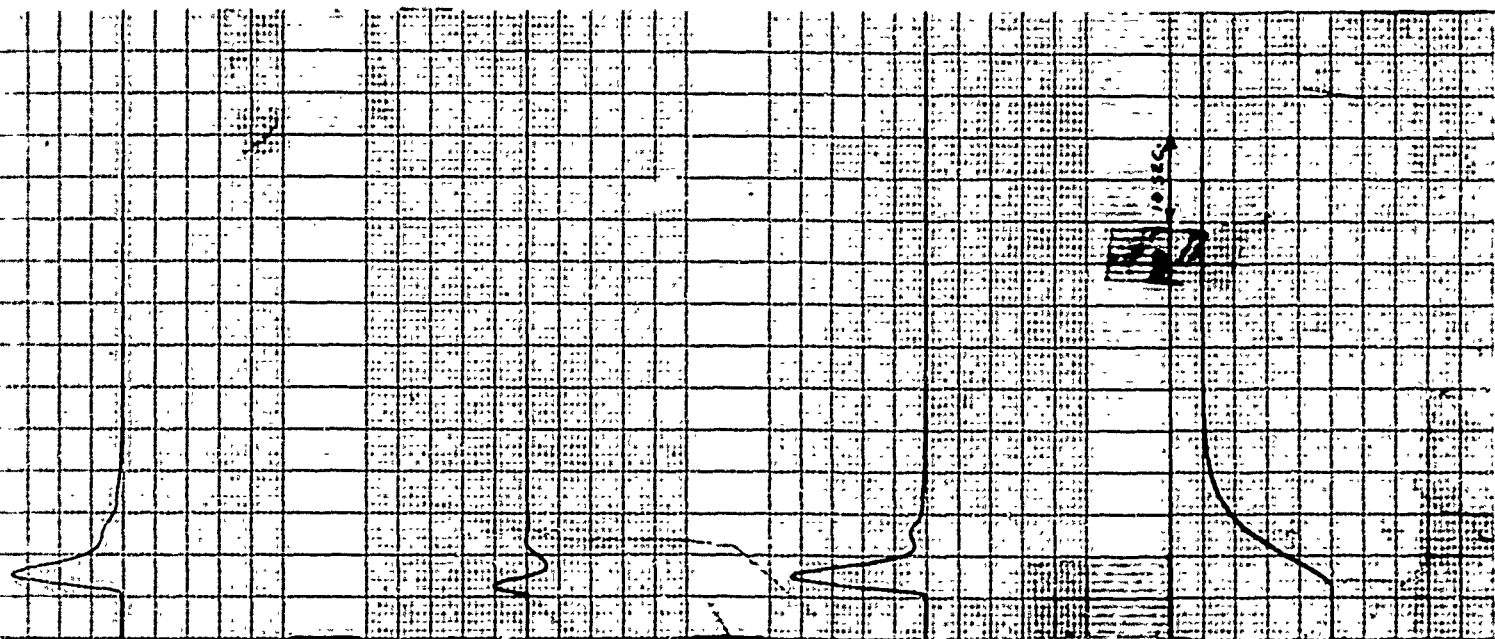
11.46

5.73
0
 $\ddot{\psi}$ $\left(\frac{\text{DEGREES}}{\text{SECOND}^2} \right)$

5.73

2.86
0
 $\dot{\psi}$ $\left(\frac{\text{DEGREES}}{\text{SECOND}} \right)$

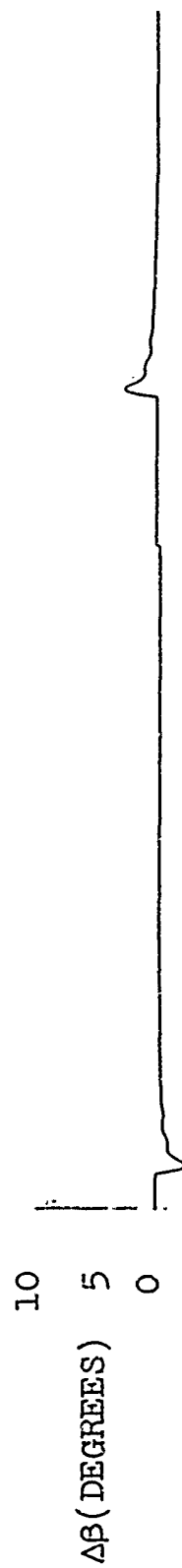
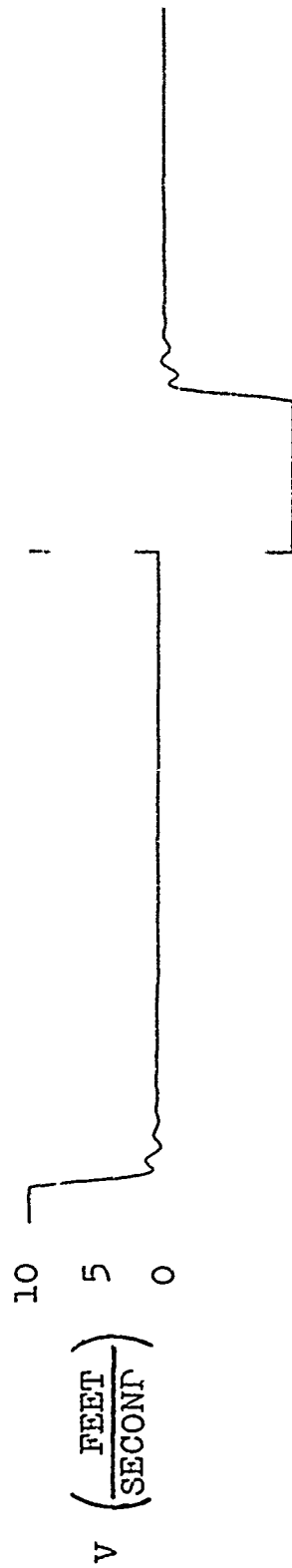
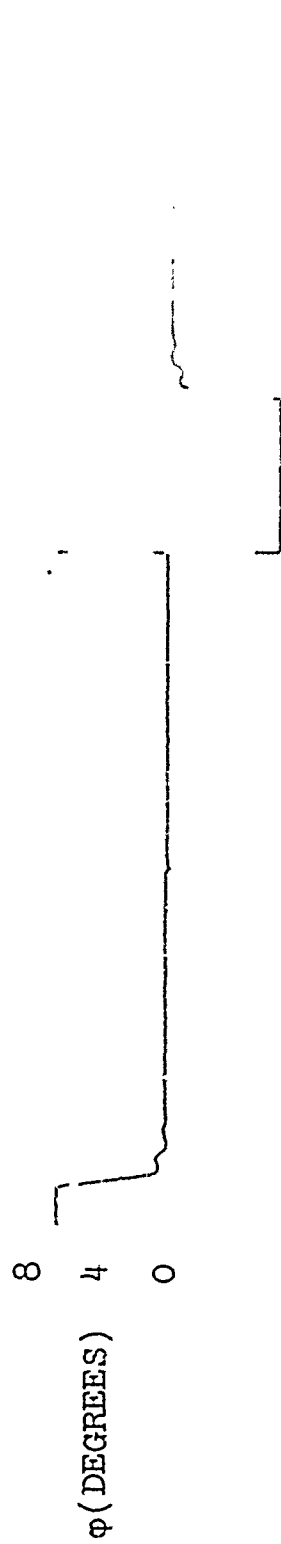
20
10
0
 ψ (DEGREES)



AUTOMATIC SYSTEM WITH RUDDERS BEHIND THE C.G. - NULLING AN INITIAL SIDE VELOCITY

RUN 1

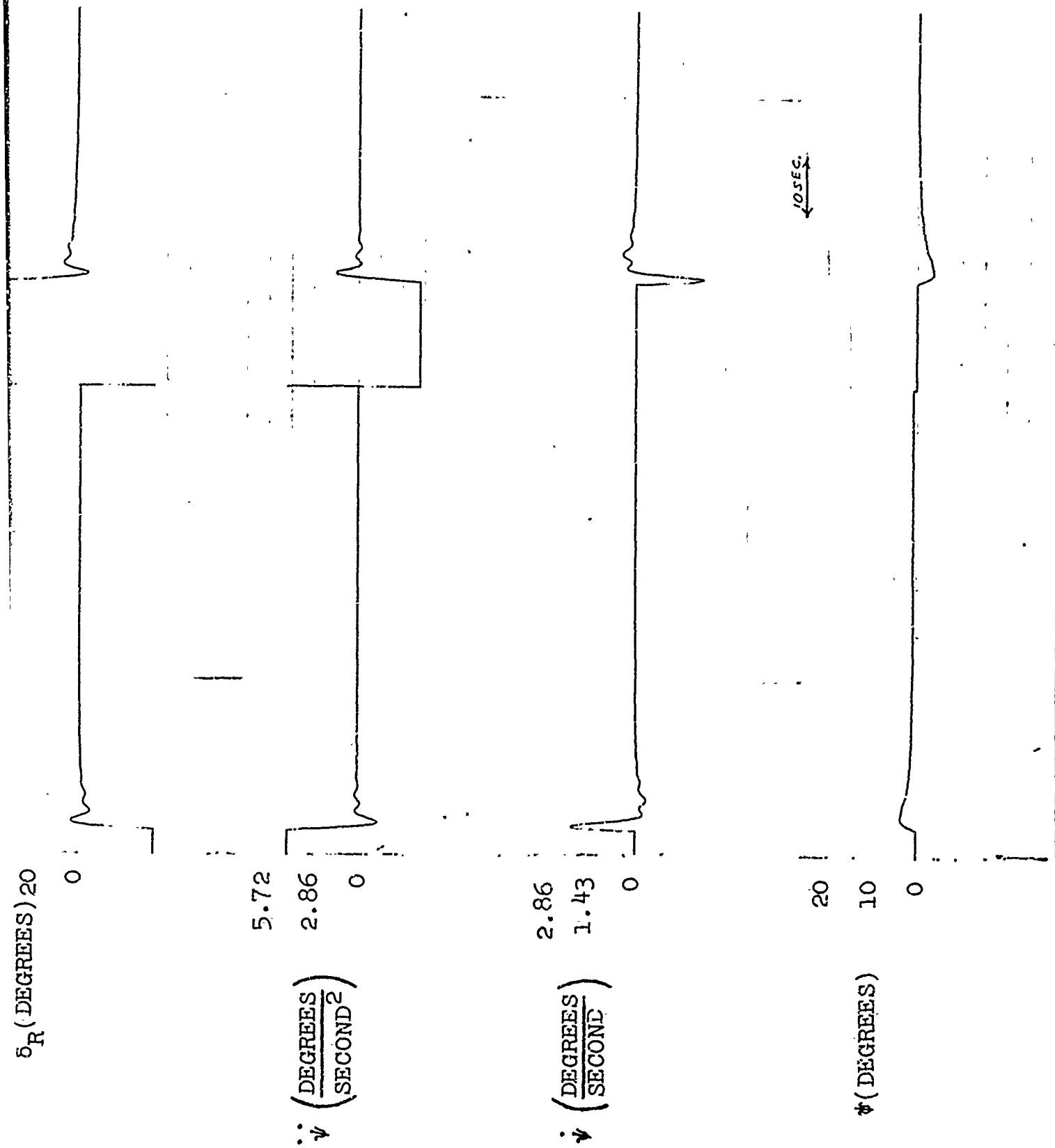
RUN 2



A

40

5 (DEGREES)



B

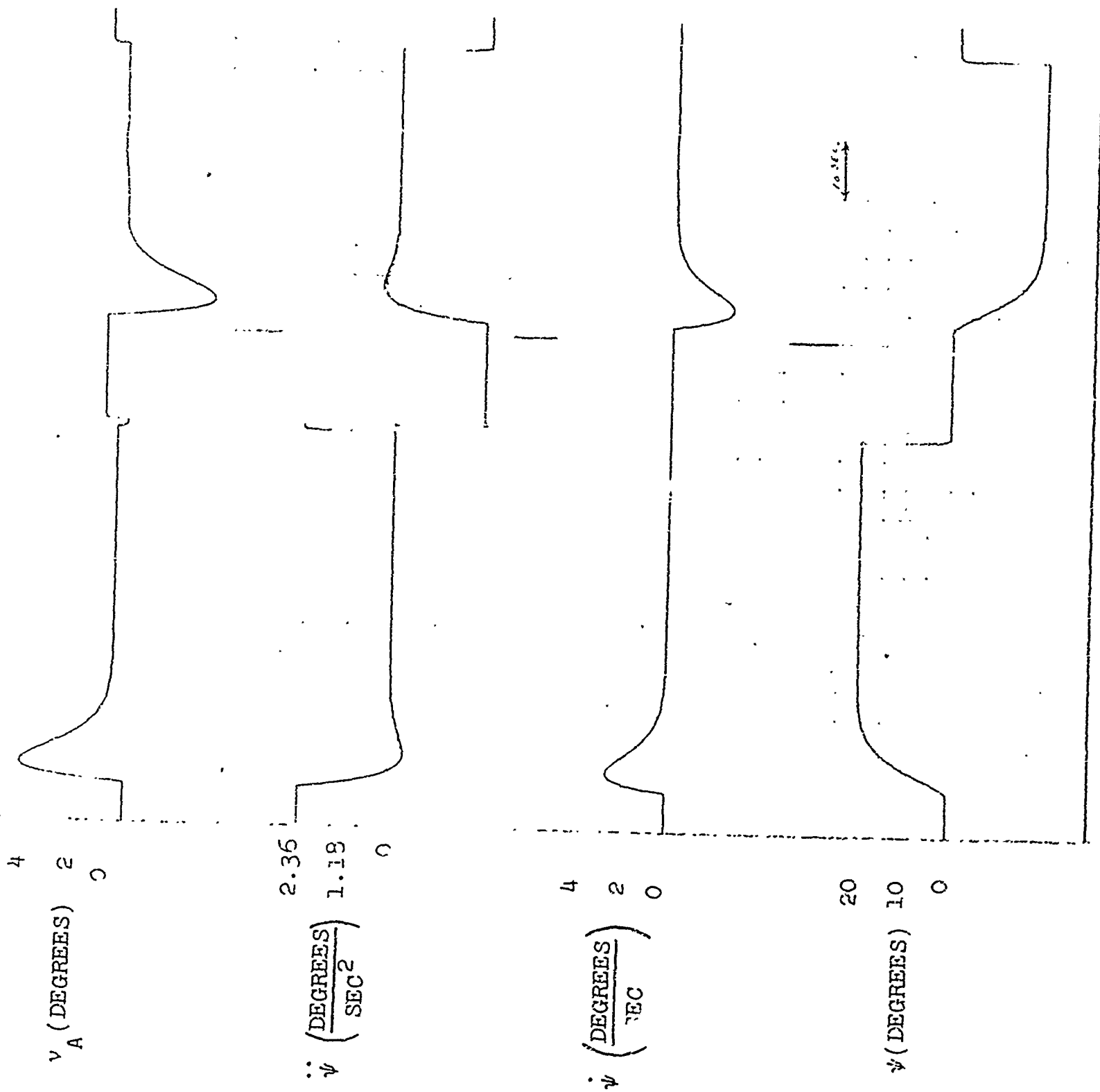
RD and AFT Normal Turn in Path of ...

A

$$\left(\frac{1}{1 + \frac{1}{2}} \right)$$

VELOCITY

B



TURNS WITH AUTOMATIC FORE AND AFT CONFIGURATION AT
1/2 FORWARD DESIGN VELOCITY

1/2 FORWARD DESIGN VELOCITY

Fore and Aft Auto with Forward Velocity = 20 knots

RUN 1

RUN 2

8

γ (DEGREES)

4

0

2

$v \left(\frac{\text{FEET}}{\text{SECOND}} \right)$

1

0

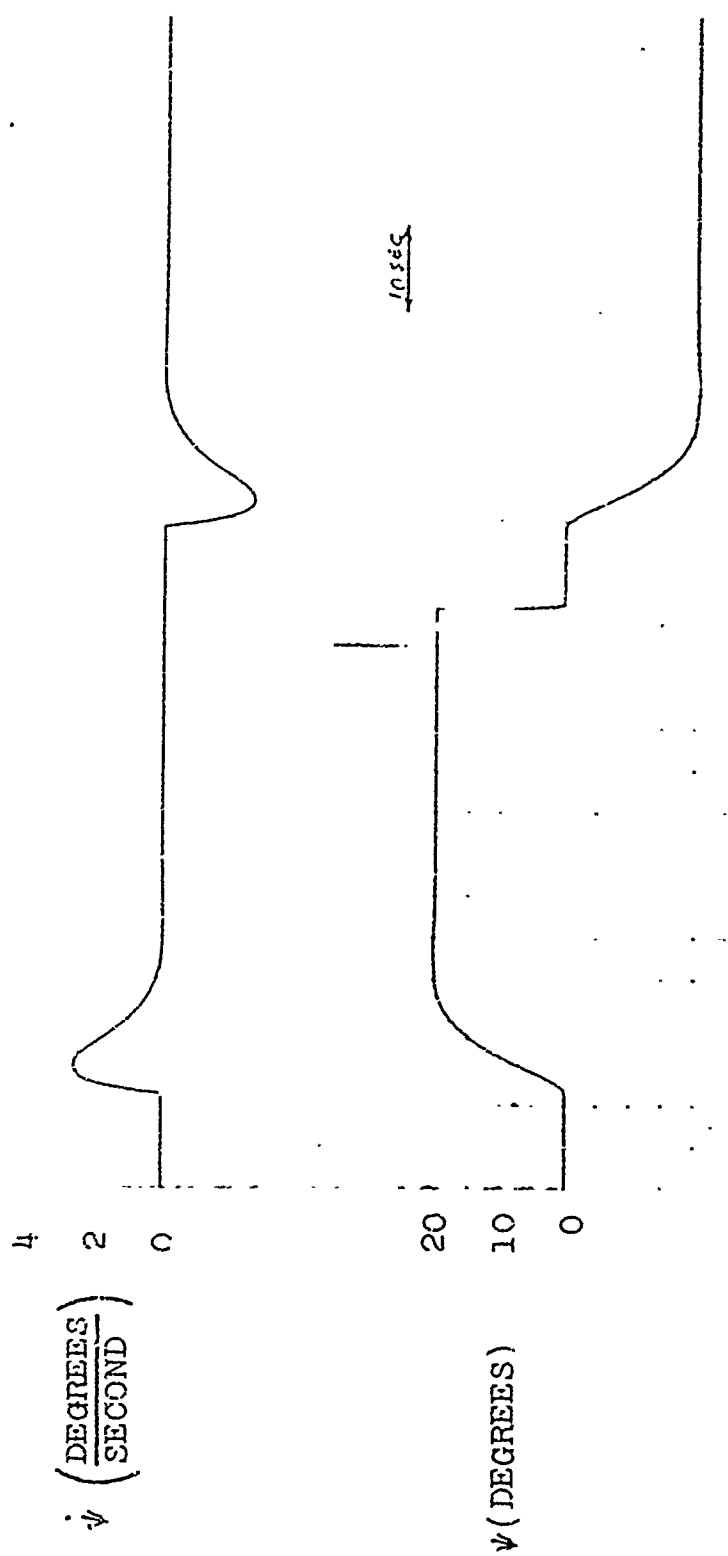
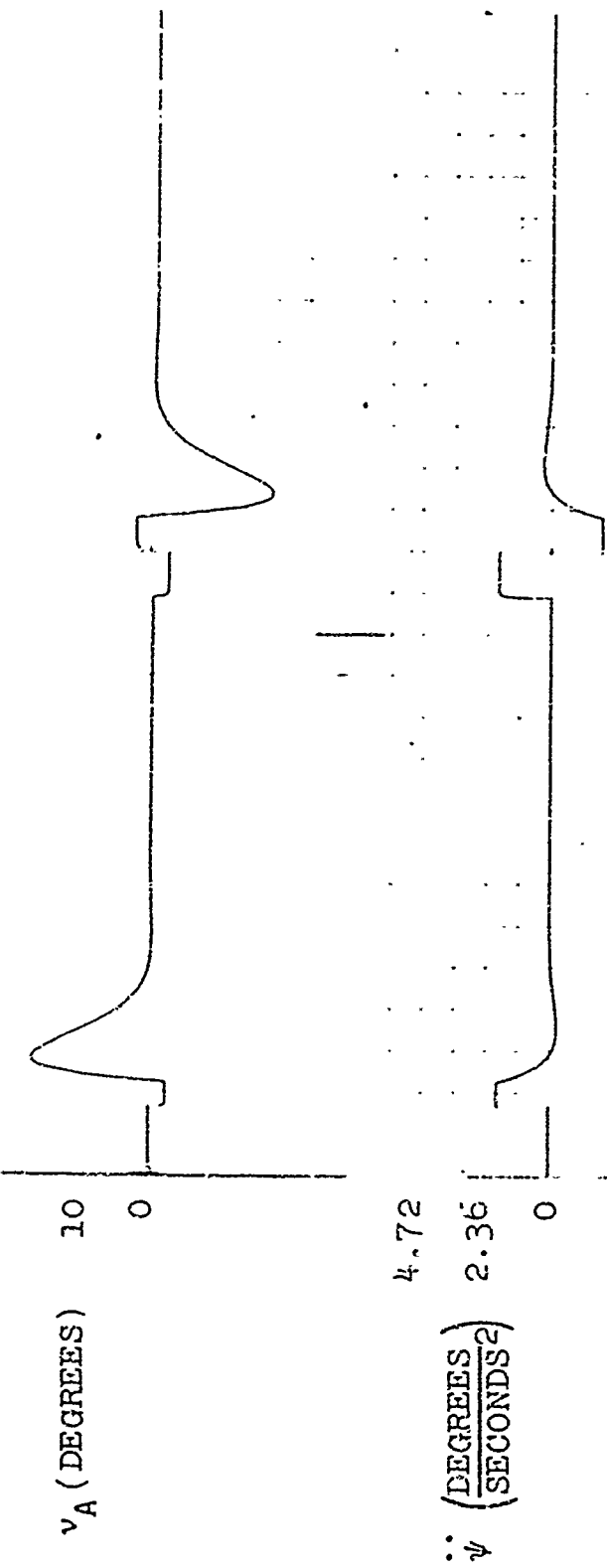
40

v_R (DEGREES)

20

0

A



B

AUTOMATIC FORE AND AFT PROPELLER CONFIGURATION NULLING AN INITIAL SIDE VELOCITY

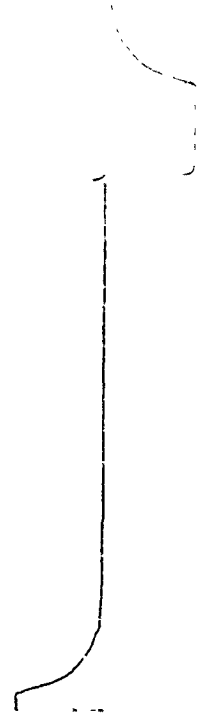
RUN 1

RUN 2

20

ψ (DEGREES) 10

0

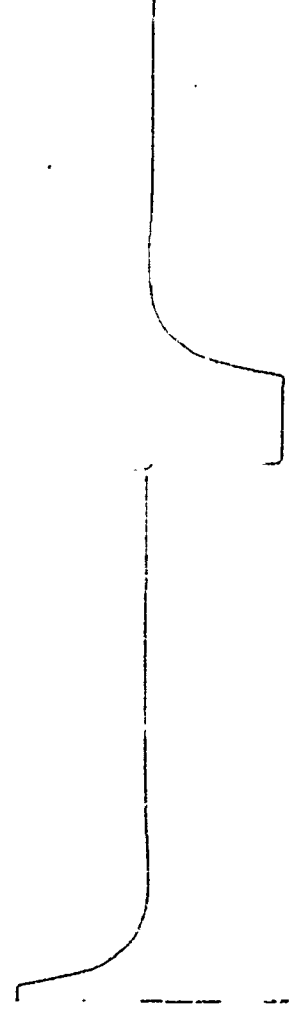


10

$v \left(\frac{\text{FEET}}{\text{SECONDS}} \right)$

5

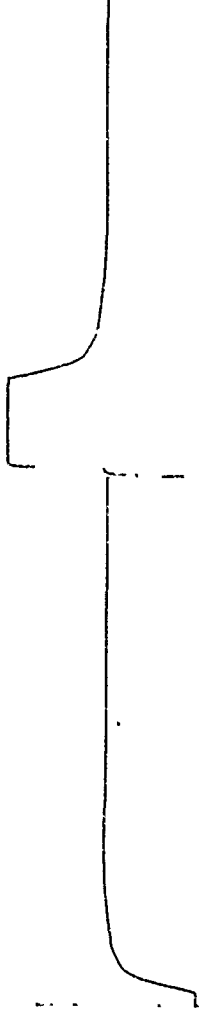
0



40

v_f (DEGREES) 20

0

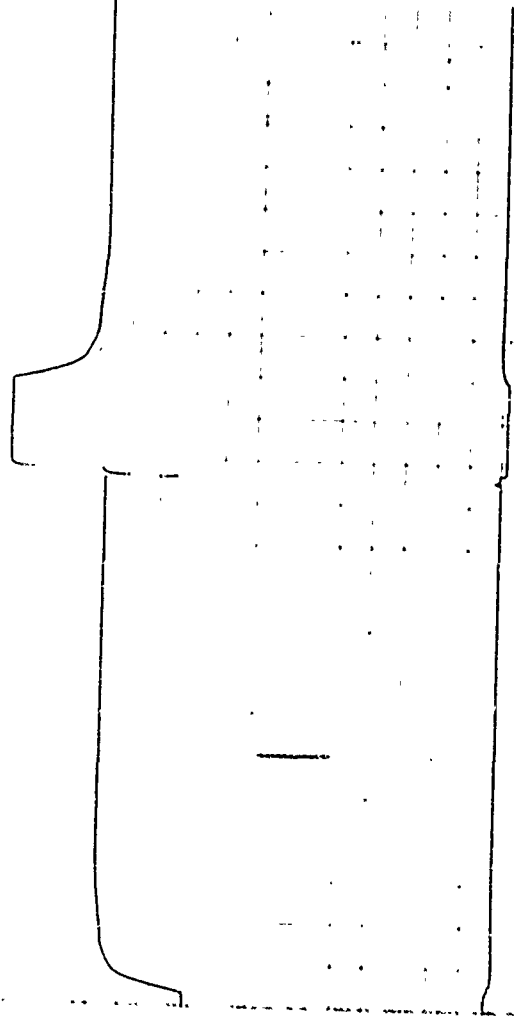


A

40

ψ_A (DEGREES) 20

0

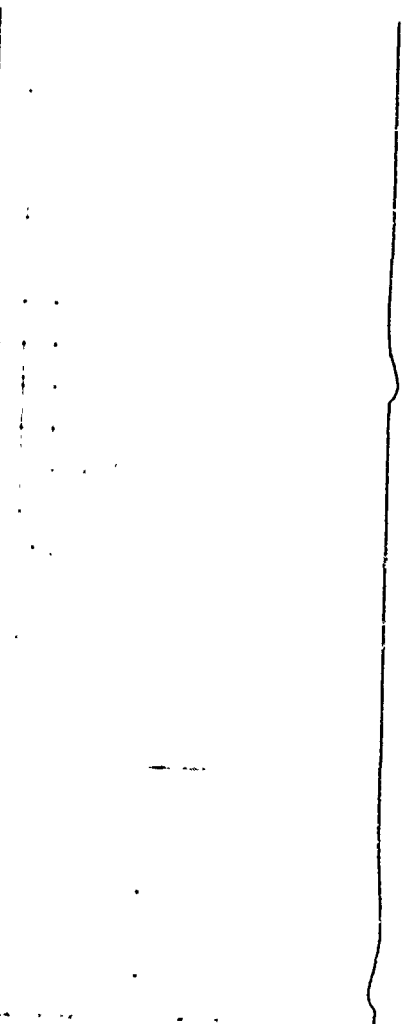


2.36

1.18

$\ddot{\psi}$ (DEGREES / SECOND²)

0



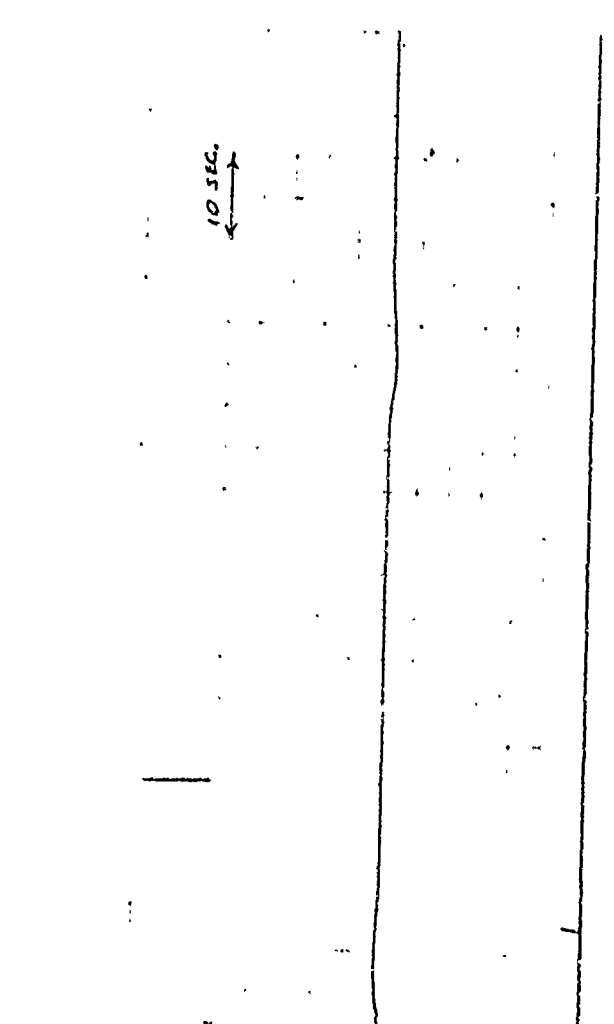
4

$\dot{\psi}$ (DEGREES / SECOND)

2

0

B

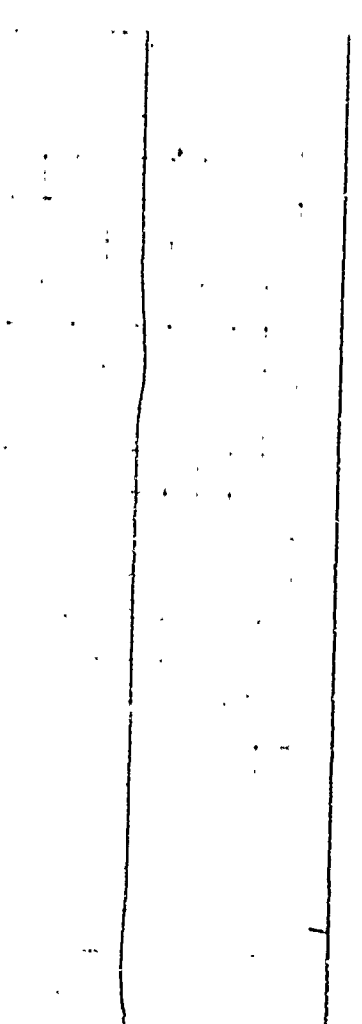


20

ψ (DEGREES) 10

0

10 SEC.



1 Experienced Operator 3 Novice Operator
 2 Experienced Operator 4 Novice Operator

1 2 3 4

2.30

1.15

$\ddot{\psi}$ (DEGREES / SECOND²)

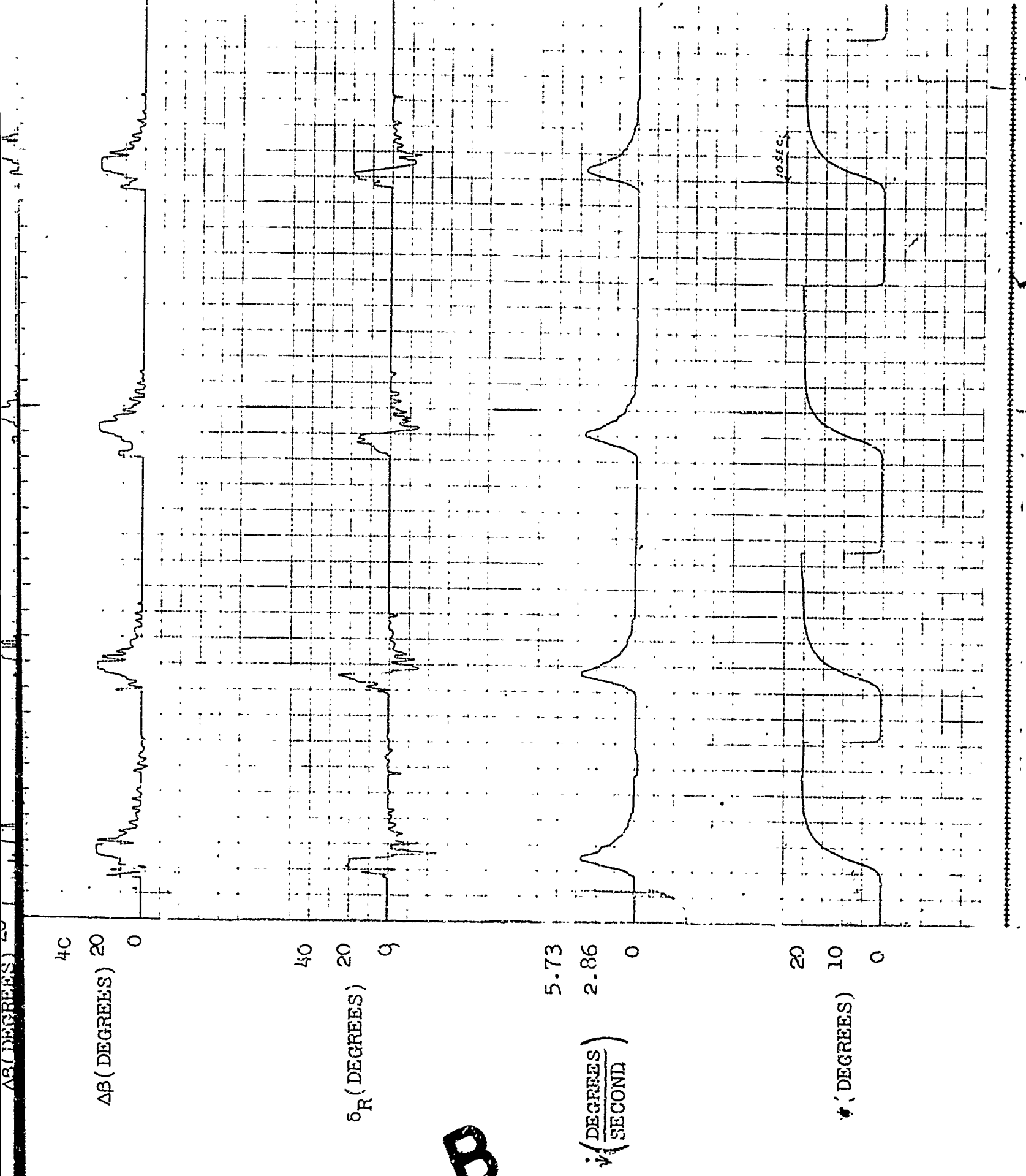
A

ϕ (DEGREES)

v (FEET / SECOND)

40

AS (DEGREES) 20

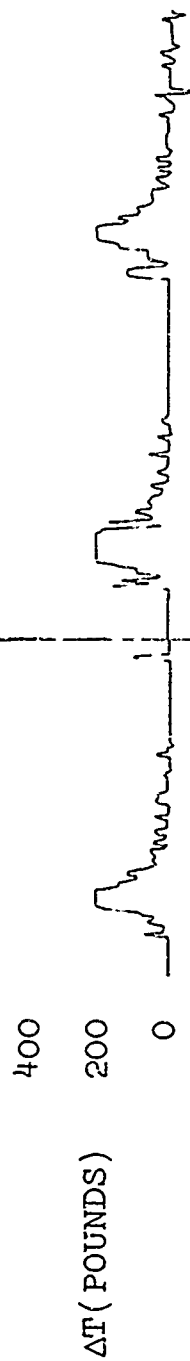
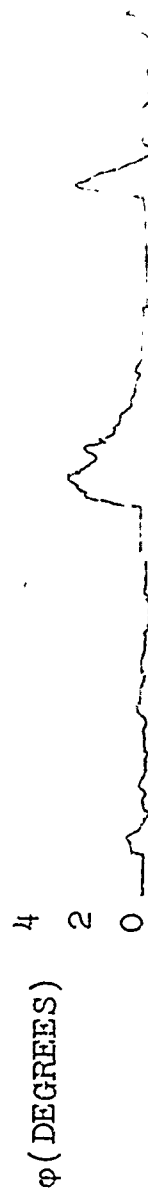


B

QUICKENED SYSTEM WITH TWO PROPELLERS

BEHIND THE C.G.

Experienced Operator | Novice Operators



ΔT (POUNDS) 200

A

